Testing a novel modeling technique for long-term coastline evolution

Master Thesis Report

L.D. Everaars

Delft University of Technology

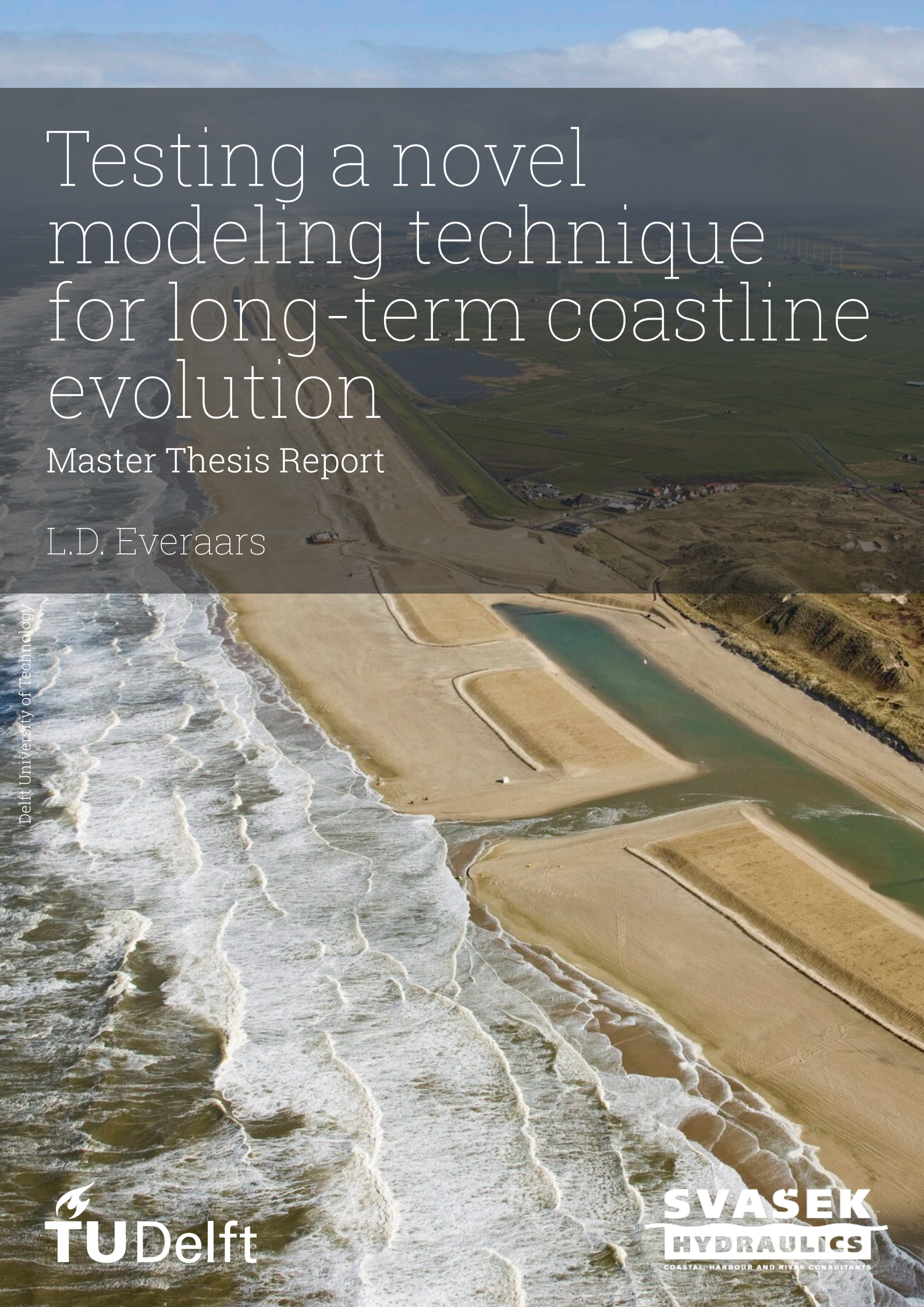

TU Delft

SVASEK HYDRAULICS

COASTAL, HARBOUR AND RIVER CONSULTANTS

Testing a novel modeling technique for long-term coastline evolution

Master Thesis Report

by

L.D. Everaars

Supervisors:	Dr. ir. M.A. De Schipper
	Dr. ir. J.A. Arriaga Garcia
	Dr. ir. A. Kroon
	MSc T.T. Kettler
Project Duration:	February, 2025 - July, 2025
Faculty:	Faculty of Civil Engineering and Geosciences, Delft
Company:	Svašek Hydraulics
Version:	Final version: 09-07-2025

Cover: Hondsbossche Dunes by EcoShape

TU Delft

SVAŠEK HYDRAULICS
COASTAL, HARBOUR AND RIVER CONSULTANTS

Preface

It is a strange experience to write an entire thesis about a coastline I have never actually stood on.

For months, the Hondsbossche Dunes was present on my screen; reduced to cross-shore profiles, bathymetric grids, volumetric cells, and lines of code. Through the data, I have got to know this stretch of the Dutch coast quite well. I have observed the beach to grow, retreat, and evolve. I followed depth contours shifting year by year, mapped sediment dispersion patterns, and evaluated model instabilities. It is like a familiar face, but yet never truly met.

To me, this is something remarkable: that you can learn so much and say so much about a physical landscape without ever physically experiencing it. It shows both the power and limitation of working behind a desk. Every model and visualization, is an abstraction of reality; it is useful and insightful, but will never show the full picture.

This thesis represents an attempt to understand real-world coastal behavior through digital lenses, and to test modelling techniques to recreate evolutional trends that align with reality. I hope it contributes, in some small insightful way, to more sustainable coastal engineering in the face of sea level rise.

I would like to thank Svašek Hydraulics for the opportunity to work on this project and be part of their team. In particular, a big thanks to dr. ir. Anna Kroon, who supervised me on a daily to weekly basis and helped with providing feedback, research directions, and discussions on the results.

Also, special thanks to PhD researcher MSc Tosca Kettler, who introduced me to the Crocodile model with great patience, helped me to set-up the coupled model configurations and provided useful feedback along the way.

Furthermore, I am also grateful to my TU Delft supervisors dr. ir. Matthieu de Schipper and dr. ir. Jaime Arriaga Garcia for their guidance, constructive feedback throughout the process, and their acceptance to evaluate my work.

L.D. Everaars
Delft, August 2025

Abstract

In times when the Dutch coastline faces pressure from coastal erosion due to the growing challenges of sea-level rise, sustainable coastal policies are essential. Increasingly large and more voluminous maintenance works are required. New sand nourishment strategies, such as mega-nourishments, are being tested along the Dutch coast. Due to the enormous quantities of sand, local safety standards increase. One example of such a project is the Hondsbossche Dunes (HBD). Although its primary function is the realization of local flood safety near the former sea dike, it also feeds nearby coast and dunes caused by natural forces like waves, currents, tides, and wind. Understanding rates and quantities of sediment dispersion to see how coastal state indicator evolve (e.g. coastal volume, beach width and depth contours) is crucial for policymaker. They must maintain the coastline as its main function of flood defense for the future, while also accommodating recreation and nature.

Literature demonstrates that one-line alongshore transport models can predict general coastline evolution trends at mega-nourishment sites well. However, their accuracy at other coastal state indicators can be limited due to, for example, the exclusion of cross-shore sediment redistribution. Recent efforts have focused on coupling such a one-line transport model (ShorelineS) with a new cross-shore redistribution model (Crocodile). Compared to other model types, the advantage of this coupling is its ability to calculate large spatial and temporal scales with minimal computational time. Additionally, the coupled model now accounts for a depth-dependent component by including this Crocodile model for the redistribution of sediment in cross-shore direction.

A data analysis of the coastal evolution at the HBD for the first 9 years was carried out. It shows that most volumetric changes occur in the initial 3 years. Furthermore, the data reveal that cross-shore activity varies over the depth. This becomes most evident from quantitative differences in volumetric changes for different vertical coastal cells (e.g. dune, beach, surfzone, shoreface). Also the differences in their correlation to the shoreline change suggest depth-dependent activity. For the models, this implies that the coupled model is likely to represent the magnitude and behavior of the volume (cells) and depth contours better.

The model comparison consist of the ShorelineS model, and ShorelineS+Crocodile (coupled model). An existing HBD ShorelineS model is extended with 4 years from 2020 to 2024, and includes a dune module, which enables the models to simulate the dunefoot and therefore provide insight in the beach-width indicator. For the coupled model, Crocodile is used as a cross-shore module within ShorelineS that is configured with a dynamic equilibrium, and a alongshore varying and curved equilibrium grid, for its best performing run (SC5).

The results of the study suggest that the SC5 simulation improves ShorelineS on the volumetric evolution indicator; it halves the error to 250 m/m^3 in 3 years time and it followings the temporal trend at the erosional zones very well. Additionally it adds new value and insight with the development of the cross-shore profile at every timestep. Although the magnitude is not yet always accurate, the SC5 simulation is able to represent independent evolution of depth contours. Despite its shown potential, the model results are constrained due to significant instabilities that appear in the model. These instabilities stem from a growing gradient-the difference in slope of the initial and equilibrium profile-which is posed by a bad translation of the equilibrium grid to a profile.

This research therefore recommends first and mostly to improve and solve the spatial and temporal stability as described above. This is necessary to make long-term predictions and contribute to future coastal maintenance strategies in the face of rising sea levels. Other relevant recommendations include creating a more realistic diffusion coefficient in Crocodile that balances subaerial and subaqueous changes better, integrating subaerial volume changes of Crocodile with ShorelineS' dunemodule in order to make a comprehensive comparison, and finally including location specific nourishments via Crocodile module and consequentially account for profile adjustment.

Contents

List of Figures

List of Tables

1

Introduction

1.1. Research Context

Across the globe, structural coastal erosion is happening [1], primarily driven by (relative) sediment deficiencies and sea level rise resulting in erosion. The rate at which coastlines retreat depends on many factors [2], with sea level change being a major contributing force. This is especially evident in the low-lying Dutch delta, where ongoing shoreline retreat poses a direct threat to coastal safety in this densely populated region. Moreover, the process of coastal squeeze [3], where natural habitats are trapped between a retreating coastline and fixed (or even expanding) human infrastructure, further limits the space for coastal systems to adapt. Recent studies show that mean sea level has already accelerated over the past century [4]. This trend is expected to continue in the coming decades. As a result, the lifetime of individual nourishments is likely to decrease.

A nourishment refers to an artificially placed volume of sand at the coast, commonly applied to mitigate coastal retreat. In the Netherlands, the Basis Kustlijn (BKL) serves as a reference level to make coastal retreat measurable and manageable [5]. However, keeping up with accelerating sea level rise requires either a significant increase in nourishment frequency and/or volume to sufficiently expand the coastal foundation area [6, 7, 8]. For example, under a extreme scenario of sea level rise rate of 32 mm/year, annual nourishment volumes may need to be up to six times larger than today [6].

A more voluminous response to this challenge is the concept of a mega-nourishment. Unlike smaller, local maintenance interventions, mega-nourishments involve the placement of large sand volumes (>500 m^3/m) that are designed to naturally distribute alongshore, feeding adjacent stretches of coastline over time. This dispersive sediment transport occurs both in alongshore and cross-shore direction. The process of cross-shore redistribution is most evident in the initial years after implementation, when the newly created coast is adapting to a more natural profile. This newly nature-based solution has been tested at different locations along the Dutch coast [9, 10]. The dispersive function of such nourishments is expected to last for decades [11], providing multiple benefits. Among these is the potential to reduce ecological nuisance in the coastal system, as the reduced frequency of interventions offers more stability for ecological development to thrive [12].

In response to the growing challenges posed by sea level rise, policymakers face increasing difficulties in selecting appropriate nourishment strategies [13]. These difficulties are expected to increase because of the uncertainties associated with long-term climate change. Yet, the voluminous mega-nourishments solution currently present a promising option to maintain the primary coastal function of flood defense while also serving recreational and ecological needs [12, 14].

Stakeholders often use key coastal state indicators, such as coastal volume, beach width, and shoreline position, to indicate the state and condition of the coast for maintenance strategies. Forecasting these coastal state indicators on bigger temporal and spatial scales is desired to develop effective policies complying with the long-term challenges of SLR and the spatial increasing needs for nourishments.

1.2. Research Problem

Coastal evolution is driven by complex interactions across multiple timescales. Currently, many models exist that try to project coastal evolution. These models differ in the timescales they cover, their level of detail, and their suitability for specific applications.

Process-based models like Delft3D [15] excel in simulating physical processes and can project a detailed and accurate shore evolution on short- to medium-long timescales (hours to decade). Mega-nourishments have been simulated before, resulting in a highly accurate representation of reality [16]. However, they are computationally demanding and often require significant calibration effort, therefore impractical forlong-term and large spatial predictions. *Data-driven models* show promising results in long-term modeling but struggle to identify underlying processes, are computationally expensive and require much data [17]. Because of their data-dependence, the model can be unreliable outside the case study limits where different coastal settings appear.

A simpler model is a *one-line* or *coastline model*. This uses empirical alongshore transport formulas to predict the evolution of the coastline position alongshore, while assuming an alongshore uniform equilibrium profile. This means that the profile change is equal to the translation of the modeled shoreline. The model only covers the wave-induced alongshore sediment transport. Generally, it is an effective way to get a first impression of the coastline evolution because of its computational efficiency. One-line models are less detailed than process-based models, but are robust predictors of general coastal evolution trends, also at spatial scales of mega-nourishment projects [18, 19, 20]. Extensive research at the Hondsbossche Dunes (HBD) [10] confirms this by showing well-correlated observations between the shoreline, volume and beach width change. This suggests that with a constant coastal profile, changes in the shoreline position represent some important coastal indicators quite well, despite the fact that the mega-nourishment brings the profile out of equilibrium. A state-of-the-art one-line (1D) model is ShorelineS [21]. Due to its free-form grid and vector-based approach it is able to simulate complex coastal shapes with large-scale changes like mega-nourishments. It has advanced capabilities compared to general one-line models, like a cross-shore interaction module that simulates dune growth and erosion. Thereby, it is easy applicable and user-friendly with low calibration effort.

Artificially maintained coastal profiles evolve toward a dynamic equilibrium, shaped by sediment transport and wave energy. The equilibrium state is based on the balance between sediment transport, wave energy, and currents. When a nourishment is applied to the coastal system, the cross-shore profile is brought out of equilibrium. When individual nourishment volumes are large or nourishment frequency is high, its return period is smaller than the adaptation time of the instantaneous profile to the equilibrium profile. This means that the coastal profile is constantly out of its natural equilibrium shape, resulting in significant cross-shore redistribution of sediment. This signifies one of the main limitations of coastline models like ShorelineS, as the distribution of volume change over the profile might be less accurate. These volumetric changes are rather important for e.g. calibration purposes. If models are calibrated on the waterline position, they might overestimate the long-term shoreline retreat when this is based on the initial years after the nourishment [10]. This limits the representation of the coastal state indicators.

To capture decadal cross-shore sediment dynamics after nourishment implementation with minimal computational efforts, the model Crocodile was developed [22]. This model follows a realistic depth-dependent dispersive and dynamic equilibrium approach for a specified cross-shore profile. Recent efforts to integrate these alongshore (ShorelineS) and cross-shore (Crocodile) models aim to enhance depth-dependent sediment dispersion, providing a better representation of coastal state indicators for long-term maintenance projects under rising sea levels. However, a knowledge gap remains on how well the coupling of these models improves this representation for a real-world case.

1.3. Research Objectives and Scope

This study hypothesizes that the inclusion of empirical cross-shore dispersive formulations to alongshore sediment transport models improves the long-term representation and evolution of coastal state indicators, like coastal volume, beach width and shoreline position (including other depth contours). While improving these indicators, it also provides additional detail on the distribution of coastal volume over the cross-shore profile.

Focus area:
The objective of this study is to provide quantitative insights into whether the interplay between longshore and cross-shore empirical formulations can improve the real-world representation of key coastal state indicators—coastal volume, beach width, and shoreline position—over decadal time scales, including additional detail on the cross-shore distribution of coastal volume.

This research motivation is captured in the context of long-term predictions in the face of sea level rise. To be able to make these predictions, in this research scope, this novel modelling technique is considered at present sea level conditions to evaluate its performance. However, for the future, the research eventually aspires to contribute to the development of more robust models and sustainable coastal management for handling erosion and maintaining space for safety, recreation and nature. Below, the exclusions are listed.

Exclusions:
To keep the study and expectations focused and manageable, it will not involve the creation of a new coupled long-term evolution model. Additionally, this project will not develop new coastal management strategies. Furthermore, making future predictions using the models is not part of this project.

1.4. Research Questions

To investigate the research objectives, the following research question is formulated:

> ”To what extent does the coupling of ShorelineS with Crocodile improve the simulation of coastal state indicators’ evolution at the Hondsbossche Dunes under present sea-level conditions, and provide additional information on bathymetric cross-shore evolution?”

The foundations for this main research question are the following sub-research questions:

1. How did the measured coastal state indicators evolve after the implementation of the mega-nourishment?
2. How well does ShorelineS simulate the evolution of the coastal state indicators at the Hondsbossche Dunes?
3. How well does the coupled model simulate the evolution of the coastal state indicators and cross-shore bathymetric change at the Hondsbossche Dunes?

1.5. Research Theory and methods

The method used to answer the stated research questions is based on a hindcast study. Hindcasting involves retrospective analysis using historical data and models to simulate past events. It is commonly applied in climate science and meteorology to recreate specific phenomena, such as weather events [23]. In scientific research, hindcasting primarily functions as a validation tool for predictive methods [24].

For this research, the methodology focuses on this hindcasting framework: Nine years of annually measured historical bathymetric and altimetric data at the Hondsbossche Dunes are analyzed to evaluate the evolution of key coastal state indicators. To demonstrate the relevance of cross-shore redistribution in this research, the analysis distinguishes different vertical and cross-shore cells based on their morphological timescale. These historical datasets provide a baseline for a model comparison between the standalone ShorelineS model and the coupled ShorelineS-Crocodile. The resulting comparisons indicate how well each simulation reconstructs the observed changes in the coastal system.

1.6. Thesis report structure

This Thesis report is organized into *nine* chapters and structured as follows. Chapter 2 provides background information on coastal management, nourishment strategies and highlights the engineering problem. Chapter 3 describes a detailed evaluation of the different coastal evolution models and emphasizes on the coupled model theory. Chapter 4 explains the methodologies utilized to assess the different research objectives and questions. Chapter 5 analyses the morphological development at the Hondsbossche Dunes from 2015 to 2024, and marks the added value of cross-shore processes

in coastal models. Chapter 6 provides the model set-up, the input variables and the different comparison runs. Chapter 7 observes the results following from the simulation runs against the historical data. Chapter 8 discusses the observed results, and the performance of the models. Chapter 9 concludes the findings of the research and offers recommendations for future model development and research.

2

Background Information

2.1. Coastal management

2.1.1. Coastal regions

Coastal areas are dynamic systems, subject to varying hydrodynamic conditions that result in alternating erosion and accretion along the coastline. Understanding these processes is crucial, especially since many coastal regions, including deltas worldwide, are densely populated and hold significant economic and cultural value. In 2020, approximately 2.15 billion people lived in near-coastal areas globally, with 898 million residing in low-lying coastal zones [25]. These numbers are expected to increase significantly under certain socio-economic scenarios, like some of the Shared Socioeconomic Pathways (SSP) [26]. This worsens the coastal squeeze [3]; the coastline is retreating while human infrastructure expands, consequently reducing the accommodation space for coastal defense, recreation, and ecological habitats. The Dutch Delta serves as a prime example of a low-lying coastal region: currently, 55% of the Netherlands is vulnerable to flooding, and 26% lies below mean sea level [27]. Given this vulnerability, the primary function of the Dutch coastline is flood defense. However, other functions—such as ecology, drinking water supply, recreation, and residential and industrial purposes—are also of great importance [3]. Therefore, understanding and managing coastal evolution is essential.

2.1.2. Nourishments and coastal policy

Since the mid-19th century, the Dutch government has annually measured the cross-shore profile (JarKus) of the Dutch coast using fixed reference poles placed every 250-500 meters. These datasets have been crucial for studying sediment budgets and predicting erosional and accretional shoreline behavior [28]. In 1990, the Dutch government introduced the coastal defense policy 'dynamic preservation of the coastline' [29], which formalized the use of nourishments as a strategy to preserve the coastline. To operationalize this policy, the coastal reference level (Basis Kustlijn; BKL) was established using the coastline position of 1990 and analysis of the coastline fluctuations between 1990 and 1980 [5]. Since then it has been revised only three times [30]. The Momentary Coastline (Momentale Kustlijn; MKL) serves as an indicator to identify the current location of the coastline. The calculation is based on a weighted average of the beach profile volume (low water line until dune foot) and the volume of the same elevation below the low water line (figure 2.1). The MKL is expressed in meters relative to the reference pole and is assessed every year in relation to the BKL position. Whether nourishments are required a comparison assessment is made by the estimation of the TKL (Te Toetsen Kustlijn) based on the MKL trend, see figure 2.1b. The coastline position is annually maintained through sand nourishments using this methodology [31].

2.1.3. Structural erosion

In 2018, research showed that 24% of coastal beaches worldwide were eroding, exceeding average rates of 0.5 meters per year over the past 33 years [1]. Structural erosion is also occurring along the Dutch coastline. To maintain the coastal profile in equilibrium with rising sea levels, the annual artificial nourishment volume has increased from 6.4 to 12 million cubic meters in 2001 [31]. Projections for

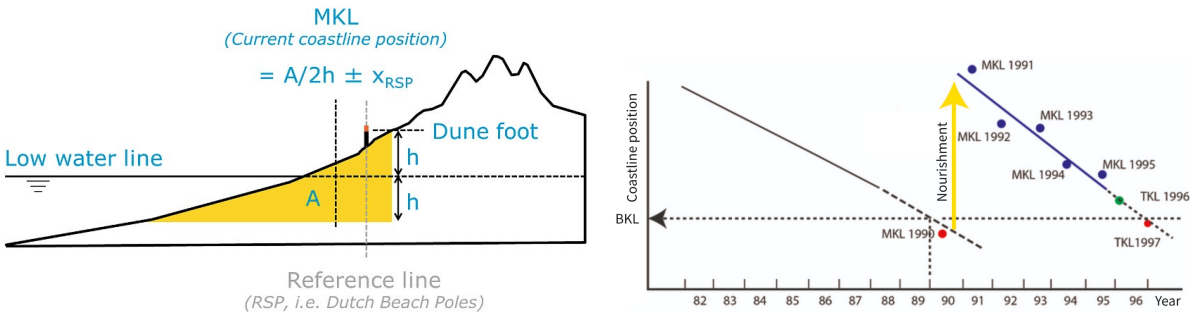

(a) Schematisation determination MKL (current shoreline position; vertical black line). The BKL is indicated in the vertical grey line ([31]).

(b) The Basis Kustlijn (BKL) and the annual Te Toetsen Kustlijn (TKL) are derived from the trend of the Momentane Kustlijn (MKL) ([32]).

Figure 2.1: Methodology visualization of MKL determination.

future sea level rise are concerning, both globally and regionally. According to the 6th Assessment Report (AR6) from the Intergovernmental Panel on Climate Change (IPCC), the Royal Netherlands Meteorological Institute (KNMI) has developed four scenarios for the Netherlands, varying in emission pathways and climate conditions. Under a high-emission scenario, the average mean sea level is projected to rise by 0.27 meters by 2050 and 0.82 meters by 2100 (50th percentile) [33]. As sea levels continue to rise, nourishments will need to become more voluminous and/or more frequent to maintain the coastal reference level [8, 6].

2.1.4. Nourishment strategies

Along the Dutch coast, nourishment strategies continuously evolved over time, also scaling the spatial scale [31] (figure 2.2). The conventional strategies are the beach and shoreface nourishments. Beach nourishments have been frequently carried out since the 1970s. Here, beach volume is increased by a placement within the range of the low waterline to the dunefoot (3 m+NAP) (figure 2.3). The average volume of a beach nourishment is about 200 m^3/m, and remains effective for about 2.5 years till it reaches the pre-nourished MKL-position [31]. In general, traditional types of nourishment involve complex and multidisciplinary implications by interaction between social, ecological and physical processes [12]. Later, it was found that nourishment placement at the foreshore had similar effectivity as the beach nourishment. Thereby, it was a generally cheaper solution and caused less nuisance for recreation and beach facilities. With the presence of offshore-sand bars, the evolution of shoreface nourishments becomes complex and is not yet fully understood. The nourishment interferes with the surfzone processes and eventually results in an accretive coastal profile. The placement only influences the bar migration if it is sufficiently large, compared to the sandbar [9]. The average volume of a shoreface nourishment is about 450 m^3/m and alongshore length of 4 km [31] (figure 2.3). Because beach nourishments are placed within the MKL zone, their effect is immediately visible, but the erosion rate increases relatively fast. Shoreface nourishments are placed outside the MKL zone, therefore the response time is delayed. Their feeding effect on the MKL-zone is between 4 and 10 years, although controlling its lifetime is not straightforward [31].

Relatively recent solutions to maintain the coast are the concepts of mega- and ebb tidal delta nourishments. These nourishments are currently still pilots and do not yet take part in the regular coastal maintenance program [31]. These innovative nourishment projects increase local flood safety levels, and by taking advantage of natural processes, like wind-driven waves and the tide, they can also feed adjacent coastlines or tidal deltas. As mentioned before, the rising sea level increases the erosive behavior of the coastal profile and MKL position. More volume and/or higher frequency in nourishments are required to match SLR. Mega nourishments are potentially a good solution to this problem (figure 2.3). The first implementation along the Dutch coast is the prominent example of the Sand Engine [9]. The Sand Engine consist of a large sand supply of 21 Mm^3. Other than the lifetime of shoreface nourishments, the Sand Engine was initially expected to last 15 to 20 years [34, 11]. However, studies suggest a good likelihood that its diffusive behavior could extend its lifespan to around 30 years [35]. Another mega-nourishment project along the Dutch coast is the Hondsbossche Dunes [10]. This project is used as the test case in this study.

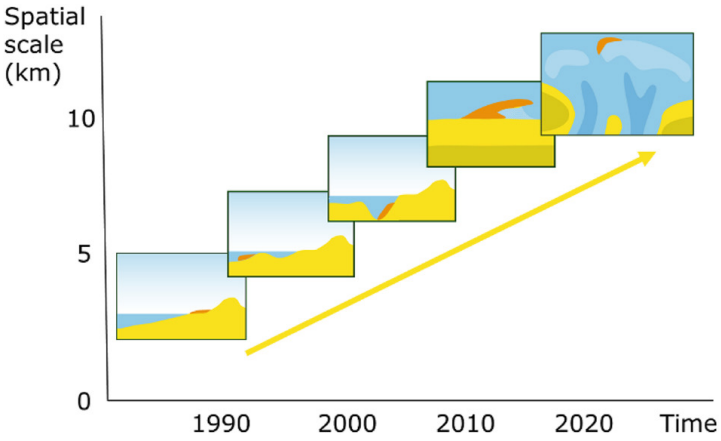

Figure 2.2: Over time nourishments have evolved from the beach, shoreface, channel wall, mega, to ebb-tidal delta nourishments. This often scales with volumetric increase ([31]).

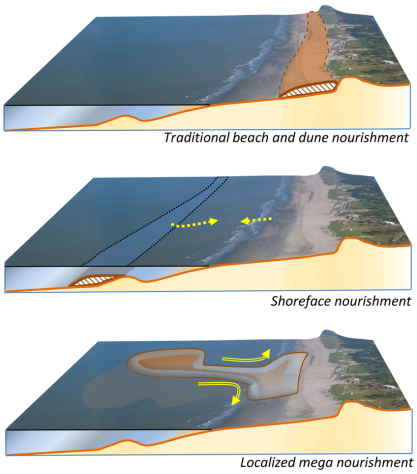

Figure 2.3: Conceptualization of different nourishment types. Ranging from the traditional beach and dune nourishment, the offshore shoreface nourishment, to the concept of a mega-nourishment ([9]).

2.2. Hondsbossche Dunes

2.2.1. Background description

The Hondsbossche Dunes are located along the Northern Noord-Holland coast in the Netherlands, between the villages of Petten and Camperduin, see Figure 2.4. Historically, a 5.5 km stretch of coastline was protected by the Hondsbossche and Pettemer Zeewering; a traditional sea dike that served as a critical flood defense of the hinterland for centuries. In the 16th century a sea wall near Petten was constructed, but was relocated several times due to coastal erosion north- and southward of the dike [36]. Groins-rigid hydraulic structures perpendicular to the coastline-were constructed in front of the dike as part of measures along the North Holland coast to prevent erosion. At the end of the 19th century, the vulnerable sand dike underwent a significant reinforcement by basalt rock. The dike has been raised and improved several times over the years. Due to its fixed position and the adjacent erosional coastlines, the dike resembled a small headland, exposed to hydrodynamic forcing [37]. With current safety standards and the increasing risks posed by sea-level rise, in 2003 the dike no longer met the critical requirements.

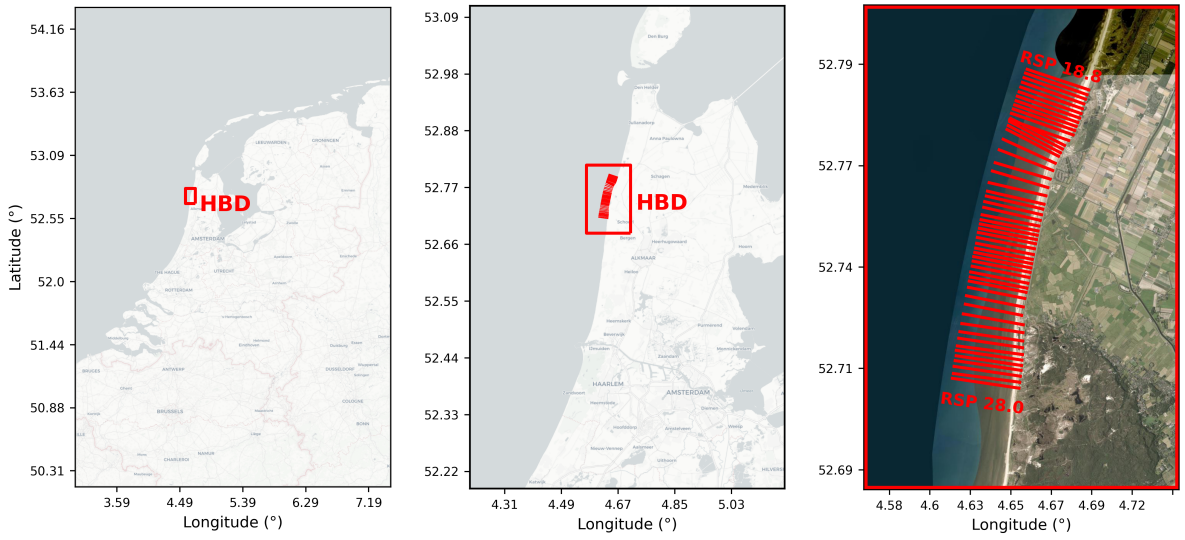

Figure 2.4: The maps indicate the location of the Hondbossche Dunes project site. The HBD are located in Northern North Holland with relevant coastal transects ranging from RSP 18.8 to 28.0.

(a) Hondsbossche Pettemer Zeewering (source: KLM Aerocarto) **(b)** Mega Nourishment in front of Sea dike (source: Trouw)

Figure 2.5: Former and new coastal protection system at Petten

2.2.2. From Hondsbossche Dike to Hondsbossche Dunes

In response, a mega-nourishment project was constructed between March 2014 and December 2015. A dynamic, nature-based solution to replace the old dike in the coastal protection system, see figure 2.5. In total, this project involved depositing over 35 million cubic meters (Mm^3) of sand on a 9-kilometer stretch, creating a wide beach and a new dune system in front of the old dike. The design allows natural processes like waves and wind to distribute the sand over time, enhancing long-term coastal resilience. The transformation not only improved flood safety standards to resist a 1/10.000 year storm for the coming 50 years, but also created opportunities for nature development and recreation. This project created a multifunctional landscape that integrates engineering, ecology, and public use.

2.2.3. Morphological evolution initial years

Because of this project's uniqueness, the site is frequently monitored to provide a better understanding of the effect, evolution, and success of the first period after the intervention. Kroon [10] evaluated the effects of the first five years following the implementation of the mega-nourishment at the Hondsbossche Dunes. To provide an initial understanding of the processes in the early years, the main findings from their research are summarized below.

Over five years, the project experienced only a 5% loss in total sediment volume, indicating significant local sediment retention and reworking. Due to the curvature introduced to the shoreline by the intervention, the central section has been eroding and the retreat rate gradually decreased toward 2020. The volume loss in this region ranged from 300 to 700 m^3/m after five years. On the contrary, the northern and southern sections near the edges of the nourishment exhibited accretive behavior.

After implementation, the steepness of the shoreline profile quickly adjusted to match adjacent coastlines, emphasizing the importance of cross-shore sediment redistribution. In the central (erosive) area, the shoreline retreated by approximately 80 meters, while in the northern and southern (accretive) sections, it advanced by around 30 meters seaward. A relatively strong correlation was observed between total volume changes and shoreline position, supporting the performance of one-line models for similar studies.

The beach width decreased to about 100 meters in the erosional center. Stabilizing trends observed in the later stages of the study suggest the beach width may begin fluctuating within ranges similar to those of adjacent coastlines. Part of the reduction in beach width is attributed to dune growth, which averaged 150 m^3/m at a relatively constant rate, independent of changes in the subaqueous volume. The study also identified a correlation between variations in dune growth and the width of the intertidal beach, suggesting that a significant portion of aeolian sediment originates from the low-lying beach, further highlighting the critical role of cross-shore redistribution.

2.3. Engineering problem

To effectively implement future strategic coastal policy, it is crucial to understand the behavior of these mega-nourishments—how the sand spreads, to where it disperses, and how quickly. This insight is vital for assessing the performance of such mega-nourishment projects as mentioned.

Coastal state indicators help to gain insight into the condition of the coast. Volumetric changes, for example, obtain understanding in sand distribution, as the dispersion can occur in both longshore and cross-shore directions. Additionally, the shoreline position and other depth contours, which are used in the calculation for the MKL-position, are also a key indicators of the coast. And lastly, an important factor is the beach width, which helps provide the basic functions of the coast, namely future safety levels and space for nature and recreation [14, 12].

Mega-nourishments are expected to last for several decades. Given this long-term prospect, model predictions on the coastline evolution, adaptation, and feeder consequences will help policymakers implementing such strategies and designs. Long-term forecast models, with minimal computational cost and with practical applicability, are desirable to cope with the evolution of key coastal state indicators under uncertain future climate scenarios.

3

Literature Review

3.1. Modeling coastal evolution

In coastal regions many dynamic processes occur, that influence the motion of fluid particles. External drivers like e.g. the tidal gravitational forces, winds and hydrostatic sea level pressures result in nearshore processes like coastal (alongshore) currents, tide and tidal currents, surface wind-driven waves, storm surges and others [38]. The physical constraints of the coastal region are the (shallow) bathymetry and the shoreline. Within this nearshore zone, many other zones are defined, like the shoaling-, breaker-, surf- and swash zone. Incident waves break at the breaker point, near the edge of the surfzone. The surfzone then becomes a highly turbulence area due to the wave collision and the interaction of waves running up and down the coast in the swashzone. The driver processes happen at different time- and spatial scales. Ranging from minutes to hours for non-oscillatory currents like tides, milliseconds to minutes for oscillatory flow in wind- and infragravity waves, and smaller time orders for turbulent flows (random) [39].

The nearshore coastal evolution occurs due to sediment transport. This transport is the complex result of the interaction across multiple time- and spatial scales of these natural drivers itself, but also with external forcing (e.g. human interventions) [40]. The upper part of the coastal profile is exposed to higher wave energy than the deeper sections. As a result, the timescales of morphodynamic changes increase with depth, ranging from hours near the shoreline to millennia on the inner shelf. These differences result in varying redistribution rates across the profile [6].

The non-linear behavior of all individual flows is quite complicated to capture in numerical coastal models. Numerous attempts have been made to model coastal evolution, leading to significant advancements in coastal evolution modeling over time.

Dealing with these complex processes can be done in different ways. Selecting appropriate models, time steps and gridsize depends on the modeling purpose. Certain processes like currents could be simplified, averaged or empirically approached. It is often a trade-off between detail and computation time.

3.1.1. Process-based models

Process-based coastal models use fundamental conservation laws in physics to solve hydrodynamics, sediment transport and the corresponding morphological change. In order to represent the hydrodynamic conditions, flow and waves use mass, momentum and energy conservation to describe fluid motion. Advection-diffusion equations are then used to describe the suspended sediment transport and empirical formulations are used to include bed load transport. The updated morphology is covered by the sediment continuity equation. Numerically, the model can be simplified into different spatial dimensions, ranging from e.g. 3D models to depth-integraded (2D) to one-dimentional models (1D).

Because these models are process-based, they are widely regarded for their physical detail. Detailed modeling hindcasting studies show an enormous detailed representation of the mega-nourishment of

the intensively researched Sand-Engine (e.g. [16, 41]). These models are normally used for short (hours to year) and medium (years to decade) timescales. Despite advancements that extend their feasibility to multiple years [42] and their accuracy on short to medium long time scales compared to one-line models [43], models like Delft3D and XBeach still demand large computational resources and require considerable expertise [21]. Additionally, to develop the model set-up and calibration efforts it takes quite some time and relies on available bathymetry datasets, making the model is location-specific. This limits its practicality for long-term (decades to centuries) and large spatial predictions (10-100km).

3.1.2. Data-driven models

With the growing availability of data from remote sensing techniques, also (partial) data-driven models have emerged as promising alternatives [17]. While these models show potential, their application for decadal predictions is also computationally expensive and requires lots of data. Moreover, they cannot directly disentangle the physical processes driving shoreline changes, relying instead on extrapolated trends from observations, which may compromise accuracy.

3.1.3. Equilibrium-based cross-shore and shoreline models

One-line models (alongshore)

Often for stable coasts, the most important cause for shoreline changes over longer timescales are the longshore effects [39]. One-line or coastline models are built upon this assumption. It also assumes an alongshore uniform cross-shore profile that does not change shape. The coastline changes are governed by the net yearly-averaged longshore transport rates (S) that follow from varying wave conditions (wave height and direction). If for a coastal cell the incoming sediment volume S_{in} equals the outgoing transport S_{out} no changes in coastline position are obtained. Alternatively, if gradients in S_{in} and S_{out} appear, the shore will either advance or retreat, moving with the model's standard profile.

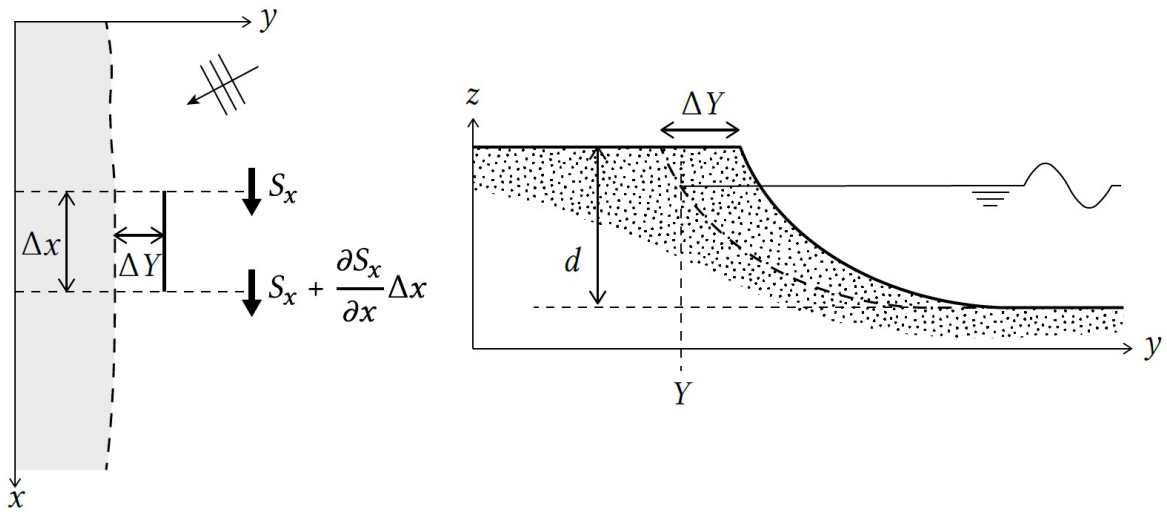

Figure 3.1: One-line model concept schematization. Under oblique incident waves, the longshore transport S_x follows. Depending on the gradient of S_{x+1} alongshore, a coastline position change ΔY appears. [39]

The first to come up with this concept was Pelnard-Considère [44]. Based on his description, many concept descriptions have been developed over time. Well-known examples of such models are GENESIS [45], LITPACK [46] and UNIBEST-CL [47]. Where the latter incorporates a more complex and detailed sediment transport formulation and description of the wave transmission, it is often assumed as the best option [48, 49]. However, the performance also depends on the application of the coastal problem and the corresponding model capabilities [49]. Thereby, UNIBEST-CL is more complex and time consuming to set up UNIBEST-CL partly due to its calibration efforts. Most evolution exploration studies of coastline models include long timescales of several decades to centuries [48, 18]. Also, on short timescales of years shoreline models do well compared to process-based models and measure-

ments [43]. Roelvink et al. [21] noted that these one-line methods simulate relatively basic coastline settings, while in reality more complex shapes occur like mega-nourishments. Also, islands, shoals, and spits, for example, affect the wave conditions at other coastal areas, or certain coastal masses may merge or separate over time. To deal with this, they proclaim that the grid should be flexibly generated at each time step. Because of its recognized potential, this new model approach ShorelineS is part of a research and development consortium (TKI Delta technology) to evaluate and innovate the model.

Equilibrium-based models (cross-shore)

Equilibrium-based models focus on the idea that coastal systems tend to evolve toward a dynamic balance (equilibrium state) over time. They ignore the profile dynamics that only affect the profile shape on timescales shorter than years. The dynamics that lead to the equilibrium state are simplified using empirical relationships or theoretical formulations to approximate coastal changes. In this way, they strike a balance between computational efficiency and reliability. By relying on equilibrium concepts rather than solving complex physical equations, they do well in predicting coastal behavior over medium to long timescales [50]. Therefore, equilibrium-based models are often used in the designing phase of shoreface nourishments. From profile measurements one can observe that they show dynamic variation, but remain within an envelope. Dynamic variation is most active in the surfzone and ends at the Depth-of-Closure (DoC) where cross-shore transport is negligible. The average of all measurements is the equilibrium profile. The difference between this (averaged) theoretical equilibrium and the instantaneous dynamical equilibrium is the exposure to the varying forcing, like water levels and waves [39].

Bruun [51] was the first to propose a simple power law equation for an equilibrium profile. Using a shape-function for the profile which includes empirically derived correlations for location-specific beaches. Other models derived over the years also incorporate formulations partly based on physical parameters like grain sizes [52]. The philosophy of such models is often used in present-day modelling projects. However, in view of nourishment operations, in these models the volume is equally distributed over the profile irrespective of the placement location. Indicating immediate adaptation of the profile to the equilibrium state after a nourishment. With this assumption, it does not simulate the short to medium timescales impact of nourishments. To bridge this gap, Kettler et al. [22] established Crocodile. This model accounts for the time depending dynamic profile response.

2D conceptual models

The equilibrium-based alongshore model fully relies on longshore transport and assumes no cross-shore interaction but an uniform profile alongshore. At many sites this has been a reasonably assumption, just like at the Hondsbossche Dunes where a data analyses study shows that the shoreline scales well with the coastal volume [10]. But as mentioned in the research problem (Ch.1.2), the coastal profile is often nourished. This constantly puts the cross-shore profile out of equilibrium, resulting in significant cross-shore sediment transport. These initial cross-shore redistributions contribute to the evolution of the shoreline position. Therefore it would be useful to combine cross-shore and alongshore interactions to obtain a conceptual 2D model.

In recent years, quite some models have been developed exploring such 2D methods [35, 53, 54, 55, 56, 57]. However, some of these models require considerable time in model set up, calibration efforts, running time and require a high level of expertise [21]. Others do not include nourished beaches or are strongly simplified.

To test the possibilities of the easy applicable model with low computational efforts on heavily nourished beaches over long time and spatial scales, the combination of ShorelineS and Crocodile has good potential.

3.2. ShorelineS

3.2.1. Model concept

The Shoreline Simulation model (ShorelineS) is a one-line model that aims to simulate coastlines on timescales of years to centuries. It has overcome several limitations of models with a fixed reference line. Existing models use a rigid grid-based approach, whereas ShorelineS uses a free-form grid. This means that the coastline is represented as a series of discrete points connected by a line segment. The

coastline consists of strings of grid points that are free to expand or shrink, of which the concatenation of the points represents the coastline. Different coastline segments can be created to have sections with complex developing features, like islands and spits. The formulation of the coastline development over time is based on the conservation of sediment:

$$\underbrace{\frac{\partial n}{\partial t}}_{\text{a}} = \underbrace{-\frac{1}{D_c}\frac{\partial Q_s}{\partial s}}_{\text{b}} + \underbrace{-\frac{RSLR}{\tan\beta}}_{\text{c}} + \underbrace{\frac{1}{D_c}\sum q_i}_{\text{d}} \tag{3.1}$$

The left-hand side of the differential equation 3.1 indicates the time derivative of a shoreline position n in cross-shore direction, which is updated every time step t. Part b of the equation is the mass conservation. It shows the amount of longshore transport Q_s m^3/yr at an alongshore coordinate point s. The longshore transport is averaged over the depth of closure D_c from where it is assumed no significant transport is happening. Term c accounts for sea level rise (SLR) limited by $tan(\beta)$, which is the average profile slope between the dune and the depth of closure D_c. The last term is the collection of the source and sink term q_i $\mathrm{m}^3/\mathrm{m/yr}$. This considers cross-shore transport, overwashing, nourishments, sand mining and exchanges with rivers and tidal inlets.

3.2.2. Desciption of model

The main structure of input variables are the initial coastline coordinates for the considered coastal stretch, the wave climate at the site, lateral boundary conditions of the simulation area and additionally supplementary data of e.g. Sand Nourishment and structures coordinates. With the input parameters and grid size, the coastline grid is initiated. Because ShorelineS has a free-form grid, it is able to add and remove grid points when a grid size exceeds plus or minus the initial grid size. A formulation is used to smoothen the grid cell transition. This free-form grid is especially useful at e.g. spit formation or shadow areas with low wave energy. Next, using Snell's law (formulation of Van Rijn (2014)), the wave angle is estimated through the wave transformation from deep offshore waters to the wave-breaking location nearshore, covering the process of refraction. Wave shadowing effect might occur. This can be due to groins, sea walls and offshore breakwaters or by other land areas. These factors can cause sediment-limiting situations, where together with updrift supply an accumulation of sediment can occur.

Transport formulations

The longshore transport at each grid point is then calculated using the wave angle and refracted wave conditions. However, how these conditions are accounted for depends on the transport formulation. Different transport formulas are implemented in ShorelineS, each handling the wave conditions differently. Table 3.1 gives an overview of the longshore transport formulations.

Formulation	Notation	Formula
USACE (1984) [58]	CERC1	$Q_s = bq_{scal}H_{S,off}^{\frac{5}{2}}sin2(\Phi_{off})$
Ashton and Murray (2006) [59]	CERC2	$Q_s = K_1 q_{scal} t_{sc} H_{S,off}^{2.4} T_P^{0.2} cos^{1.2}(\Phi_{off}) sin(\Phi_{off})$
USACE (1984) [58]	CERC3	$Q_s = K_2 q_{scal} t_{sc} H_{S,br}^{\frac{5}{2}} sin2(\Phi_{br})$
Kamphuis (1991) [60]	KAMP	$Q_s = 2.33 q_{scal} t_{sc} K_3 H_{S,br}^2 T_P^{1.5} tan_\beta^{0.75} D_{50}^{-0.25} sin^{0.6}(2\Phi_{br})$
Mil-Homens (2013) [61]	MILH	$Q_s = 0.15 q_{scal} t_{sc} K_3 H_{S,br}^{2.75} T_P^{0.89} tan_\beta^{0.86} D_{50}^{-0.69} sin^{0.5}(2\Phi_{br})$

Table 3.1: Transport formulas implemented in ShorelineS [21]

Worldwide, the most used transport formula is the CERC equation [58]. The principle of this method is that condition of the waves alongshore are proportional to the longshore transport rate. It has been calibrated using field data from sandy beaches. The CERC1 formulation from table 3.1 is the simplest form of sediment transport. CERC3 is the more common, and can be used for transformed waves to the nearshore.

CERC2 [59] includes effects of shoaling and refraction. Furthermore, it accounts for sensitivity of transport to the wave period. K_1 and K_2 are scaling parameters, where K_2 is used as the coefficient for the

wave parameters at the breaking point and K_1 is the coefficient for when off-shore wave parameters are used.

For lower calibration efforts, KAMP [60] and MILH [61] use input parameters like beach slope and grain size in their formulations. The MILH formulation re-calibrates the constants in KAMP.

Dune Interaction

One of the modules implemented in the ShorelineS simulation is the Dune module. This module requires input data of coordinates of the initial dune crest position alongshore and wind speed time series at the coast. This basic dune interaction formulation by [62] includes two main processes, namely dune erosion by wave attack and dune growth by wind-blown sand (aeolian transport). The module formulation covers equations based on the relevant physics and empirical observations. Relevant features modeled by ShorelineS are dune height (foot to crest), location of the dunefoot, beach width, and shoreline position.

The wind transport flux q_{wind} and dune erosion flux q_{wave} $(m^3/m/yr)$ contribute to the change in shoreline and dune position. In contrast to the coastline definition of equation 3.1, the sediment flux Q_s and source terms q_{wind} and q_{wave} are not only divided by the depth-of-closure D_c, but the beach (berm) D_B height as well, see formula 3.2. The flux q_{wind} and q_{wave} now also impact the position of the dunefoot n_{df}. This position is defined in formula 3.3, where the transport volume is divided over the active dune height.

$$\frac{\partial n}{\partial t} = -\frac{1}{D_B + D_c}\left(\frac{\partial Q_s}{\partial s} - q_{\text{wave}} + q_{\text{wind}}\right) \tag{3.2}$$

$$\frac{\partial n_d}{\partial t} = \frac{1}{D_h}\left(q_{\text{wind}} - q_{\text{wave}}\right) \tag{3.3}$$

As a default value the dunefoot height is defined at +3 m+NAP. The dunefoot elevation only varies when the beach slope becomes steeper than 1:15. The dunefoot then lowers in elevation, which accelerates dune erosion.

The wind-blown sand transport q_{wind} which uses the fetch length F_L. The fetch length depends on the dry beach width and wind direction. The wave-induced erosion q_{wave} is formulated such that dune erosion only takes place when the water level reaches the dunefoot. The total water level used here includes a run-up formulation.

Nourishments

Nourishments in ShorelineS are prescribed by an input file. The nourished volume is uniformly spread over the implementation area, increasing the cross-shore profile volume evenly. This instantaneous increase of volume moves the shoreline position and the complete profile seaward. The time-dependent nourishments are added as a source to term (d) in equation 3.1.

3.3. Crocodile

3.3.1. Model concept

Crocodile is a CROss-shore COstal DIffusion Long-term Evolution model which is designed to simulate cross-shore evolution of nourished beaches on decadal timescales. It can track different coastal state indicators like profile volume, beach width and coastline position. Over these long periods, such simulations have shown to be useful since the lifetime of nourishments can be predicted more realistic [6], and attributes positive to future nourishment design strategies. It bridges the gap between very detailed process-based models and simplified equilibrium theory-type models.

The basic principle of the model is that it updates the bed level at every time-step and cross-shore position $Z(x,t)$ based on how it relates to the dynamic equilibrium profile $Z_{eq}(x,t)$. The profile evolves towards a dynamic equilibrium profile, which represents the shape the coast would attain if all external forces (such as waves and wind) remained constant over long timescales. The location of this profile is defined based on a sediment balance and the mean sea level elevation. These hydraulic conditions

result in a vertical and horizontal translation of $Z_{eq}(x,t)$. The time for the actual morphology to adapt towards this instant equilibrium state varies from hours at the shoreline to millennia at the inner shelf boundary [22]. Nourishments influence the profiles morphology as well. The hydraulic conditions and the timescale ratio between nourishment implementation and the morphological response determine the resemblance between the actual profile and its equilibrium profile. The reshaping of the cross-shore profile $Z(x,t)$ depends on the profile slope and the profile curvature relative to the equilibrium profile ($Z_{eq}(x,t)$).

3.3.2. Description of model

The model is innovative in the way the model terms are described as in formula 3.2. Thereby, in present times, many observation records of nourished beaches are available, enhancing model calibration. The model is "behavior-oriented" (Kettler et al. [22]) and therefore does not solve for physical equations other than the conservation of sediments. This equation is defined in formula 3.2. The time for the instantaneous profile to realize the equilibrium morphology (term (a)) is reflected by the different model terms that describe the cross-shore behavior.

$$\underbrace{\frac{d(Z-Z_{eq})}{dt}}_{\text{a}} = \underbrace{\frac{d}{dx}\{D(z')\frac{d(Z-Z_{eq})}{dx}\}+\epsilon_D(Z)}_{\text{b}} + \underbrace{E(z')}_{\text{c}} + \underbrace{F(Z-Z_{ini})}_{\text{d}} + \underbrace{W(Z-Z_{eq})}_{\text{e}} + \underbrace{Source(z,t}_{\text{f}} \tag{3.2}$$

Diffusion-behavior term

Term (b) is the diffusion term that redistributes perturbations of the actual morphology from the equilibrium state. Here, the term includes a depth-dependent coefficient $D(z')$ (m^2/day), being the diffusivity profile. The coefficient varies vertically over the profile. In this way it accounts for the different morphological timescales. It represents how easily sediment moves (redistributes) at a certain depth. It controls the speed of the morphological response. Originally, the formulation $D(z')$-shape in literature was derived by fitting it to results of process-based model runs by resimulating nourished and unnourished beaches. Crocodile, however, connects the diffusion coefficient to the local wave and water level climate. Above the low water line (figure 3.2(a)), the cumulative distribution function (CDF) represents the chance of water level rise above a certain level. In the subaqueous part (figure 3.2(b)) the CDF is represented by the chance that waves are broken using the breaker parameter $\gamma = 0.44$.

This approach results in greater robustness, as it is easier to apply to other coasts with different hydraulic settings. Using this wave and water level data, it estimates the frequency with which different parts of the profile are active. Four profile zones are distinguished based on their morphological timescale and response, see figure 3.2(c):

(Z1) The upper part of the active zone reaches from the low water line up to the maximum elevation, which is reached by the runup of the waves. No further transport is considered exceeding this runup elevation.

(Z2) Near the waterline, maximum transport rates are reached. This rate extends in the surfzone, between the low waterline and the surfzone boundary, and is assumed to be constant.

(Z3) From the surfzone to the depth-of-closure.

(Z4) At lower depths of the shoreface, the transport activity is active on decadal to century timescales. This is mainly due to wave shoaling and tidal currents.

* To assure mass-conservation of sediments over the profile, the term ϵ_D is introduced in the equation. As the dispersion varies in depth, this ϵ_D redistributes the loss of sediment over the profile by the weight of relative change.

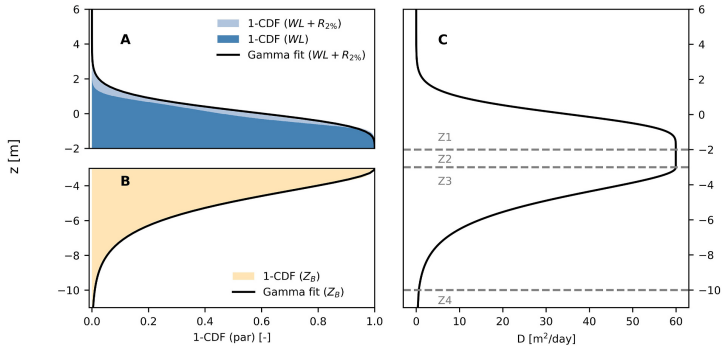

Figure 3.2: Example of the diffusion coefficient definition $D(z')$. Shape in (A) is calculated using the CDF of exceeding water levels. The curve in (B) is based on a survival function of breaking waves. (C) shows the resulting diffusion formulation. [22]

Background erosion term (longshore transport)

In formula 3.2 term (c) refers to the background erosion. This term accounts for the long-shore transport gradients that pass the cross-shore profile. The representation of sediment supply and losses ($m^3/m/yr$) to the profile shape is redistributed by the shape of the diffusion term $D(z)$. The input quantity of calculated alongshore gradients E_{tot} of this model term could be based on morphological observations or potentially by using long-shore transport models.

Nourishment loss

The third term on the RHS, term (d), represents the sediment losses after a nourishment implementation due to increased exposure to waves and currents. Initially, sediment volume is rapidly eroded, but slows down using an exponential decay function. Also, at different depths the profile lose sediment at various speeds. For extreme cases, as for mega nourishments, the planform shape of the coast significantly changes. Crocodile can account for wave transformations that occur for the notable coastline orientation for the new coastline shape. In the coupled model (Ch. 3.4), nourishments are configured via the ShorelineS model. In the Crocodile formulation, this comes apparent in the term (c), which induces the alongshore transport by ShorelineS. Therefore, this nourishment term becomes irrelevant.

Sediment exchange with the dune area

Term (e) accounts for the interaction with the dune area. This is done by a simplified aeolian transport formulation, only depending on beach width (BW). Studies have shown that wider beaches may lead to higher sediment supply. So, aeolian transport linearly scales with the fetch length. The dune area is not part of the equilibrium profile and, therefore, acts as a source or sink. This term is also not used in the coupled model (Ch. 3.4), as it is already accounted for by ShorelineS' dune module.

Nourishment implementation

The last term, term (f), indicates the changes due to a nourishment implementation. The volume was added as a spatial and time depended source term (z, t). Crocodile matches the predefined input parameters like design height and seaward slope.

3.4. Coupling ShorelineS and Crocodile

A coupling of the models ShorelineS and Crocodile would mean that both model formulations update each other at, for instance, every step in time and space. So, for every Crocodile profile (transect) that is defined alongshore and at every time step, a longshore transport flux (E_{tot}) is provided by ShorelineS in the background erosion term (c) (formula 3.2). The depth-depended diffusive formulation $D(z)$ then distributes the flux over the cross-shore profile. If all other terms (b-f) are being reworked for the same timestep, the new vertical positions $Z(x_i, t)$ are calculated accordingly. This influences the shoreline position, which then updates the coastal gridpoint in the ShorelineS model (s_i, n_j). This coastline feedback that Crocodile uses is transmitted via the source term (b) in formula 3.1. The coupling model technique is still in the testing phase. Therefore, comparing the performance of this coupled model to a standalone ShorelineS model provides understanding of depth-dependent formulations in models and helpful information for research development purposes.

4

Methodology

This chapter outlines the methodologies to address the research questions and objectives presented in Chapter 1. To structure this research, it is divided into two different phases. The essence and primary focus of the research are concentrated on the first two phases, wherein a hindcast study is performed. As explained in section 1.5, this approach can be used to simulate and analyze historical phenomenal evolutions of sediment transport.

4.1. Phase 1 - Data Analyses

4.1.1. Morphological JarKus Data

In order to assess the performance of sediment transport models, a real-life case is used to set a reference level to these models. The function of this first phase is to construct and analyze this reference level utilizing a nine-year JarKus observation data-set at the Hondsbossche Dunes. This data analysis is conducted over the years following the placement of the mega nourishment in 2015, up until April 2024.

From this period, 10 measured datasets are available, see figure 4.1. The JarKus dataset consists of cross-shore altimetric and bathymetric profiles for the Dutch coast. These annually transect measurements are collected by Rijkswaterstaat since 1965. The profiles are spaced approximately every 250m and aligned perpendicular to the coast. This open-source dataset is processed by Deltares to the standardized format of NetCDF.

For a single profile the observations are composed of two different measurement sets: subaqueous (blue) and subaerial (green). The bathymetric data below the waterline is measured using a single-beam echo-sounder instrument from a survey vessel, whereas the topographic data is obtained using GPS/GNSS and lidar measurement devices. From this timeline, it can be seen that datasets are not necessarily measured on the same day; also, subsequent years do not have a fixed interval. It is important to be aware of these differences when analyzing the datasets.

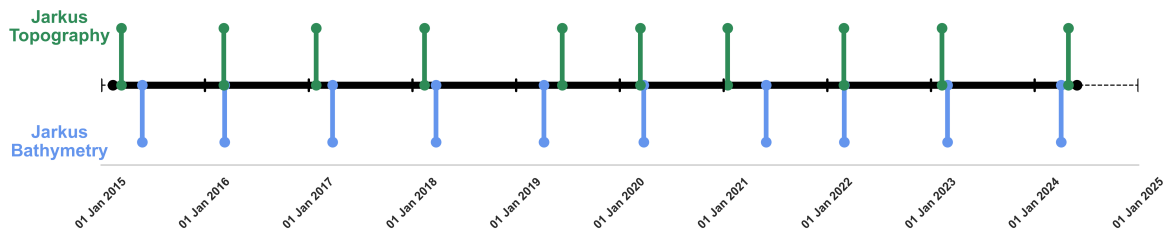

Figure 4.1: Timeline of measured data: blue indicates the bathymetry measurements underwater, and green indicates the topography measurements on land

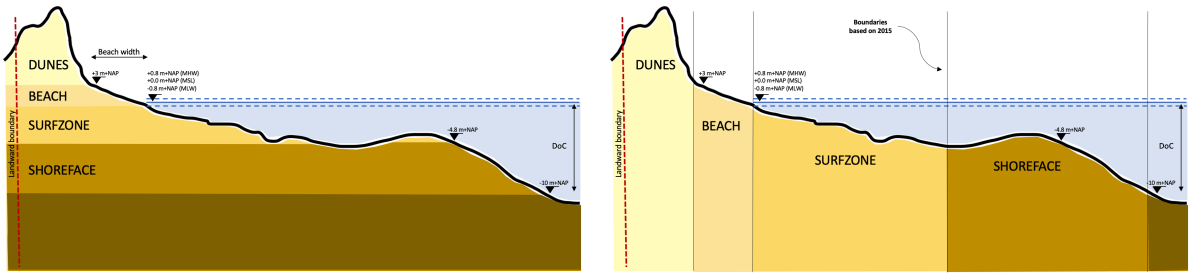

(a) Vertical volume cells schematic sketch

(b) Cross-shore volume cells schematic sketch

Figure 4.2: Definitions of coastal cells used in data analysis. The vertical cells (figure a) are used to access the basic volumetric changes, the cross-shore cells (figure b) are used to get a better insight into cross-shore subaqueous behavior.

The JarKus data is analyzed using Python to quantify the different coastal state indicators. The trends of the coastal indicators can be traced over time to create a measure for the models and to identify patterns that reveal the potential added value of cross-shore redistribution to longshore transport. Or more concrete for this research, where Crocodile could theoretically improve ShorelineS.

4.1.2. Depth Contours and Beach Width Definition

To better assess the significance of depth-dependent cross-shore transport formulations, the cross-shore profile is first defined to obtain a clear and useful representation of the data. Based on differences in morphodynamic behavior and timescales, the following areas are distinguished: upper shore-face, surfzone, beach and dunes, ranging from -10,0 m+NAP at the seaward depth-of-closure to the landward boundary which reaches up into the dunes such that all transport is captured. Waves start breaking at a depth of -4.8 m+NAP, indicating the surfzone's edge [10, 63]. The shoreline position is assumed to be equal to the average of the cross-shore positions of the MHW (+0.8 m+NAP) and MLW (-0.8 m+NAP) levels to avoid disturbances in the coastline representation. This aligns with the definition used by [10, 64]. In literature, the dunefoot is widely assumed at +3,0 m+NAP along the Dutch coast [64]. The beach width is defined as the difference between the shoreline and dunefoot position. Lastly, the landward boundary (red line in Figure 4.2) is specified until the dune area ends or up to where dune growth is perceived. Because often further landward, less sand is transported.

4.1.3. Coastal Volumetric Cells Definition

Figure 4.2a shows the different vertical cells between the seaward and landward boundaries. With the definition of the depth contours as described above, these cells follow previous research conducted at HBD [10, 63]. The volume is then obtained by the area of the cell times a meter width.

A challenge with this vertical cell definition is that the significant dynamics of the outer sandbar complicates the delineation and description of the surf zone and shoreface based on fixed depth contours. As can be seen in figure 4.2a, the tip of the outer bar can also contribute to the volume cell of the surfzone. To account for these volumetric changes, cross-shore cells are introduced (Figure 4.2b). Here, the separation between the surf zone and shoreface is positioned at the midpoint between the cross-shore locations of the waterline and shoreface boundary (-10 m+NAP). It turns out that this approach provides a reasonable estimate of the location of the trough landward of the bar. However, a limitation of this approach is that the cell widths vary slightly between transects, making it less suitable for direct quantitative analysis alongshore. Nonetheless, it remains effective for assessing relative changes.

4.1.4. Model implications

In the data analysis the combination of both vertical and cross-shore cell definitions are used to get a more complete indication of the morphological evolution. The output of this method are visualizations of the data. This indicates trends and emphasizes the relevance of the depth-dependency contributions of transport alongshore.

4.2. Phase 2 - Model Simulations

The second phase builds on the data analysis. Different model simulations are used to hindcast the same nine years that were analyzed from the JarKus data. In this way the performance of the models can be qualified and quantified for the models ShorelineS and the coupled model (ShorelineS & Crocodile).

The models (ShorelineS and ShorelineS+Crocodile) are configured using input data of wave climate, wind, and water levels. Also the initial geometry of the shoreline is specified, and a file with additional nourishments since 2015. Svašek Hydraulics has a working and calibrated ShorelineS model, that was tested on the first 5 years after implementation. This model is extended with 4 years of wave data from 2020 and 2024. The wave climate data of the remaining years are retrieved through the North Sea transformation matrix by Deltares [65] for the whole North Holland coast. Furthermore, data on additional nourishments over the nine-year simulation period were received from the operator company Boskalis [63].

For the coupled model Crocodile is added as a module to ShorelineS. A few important inputs for this Crocodile are the diffusion shape file (Ch.3.3, and the initial and equilibrium bathymetry grid definitions (Ch.6).

The models are compared to observations (phase 1 output data) to evaluate how effectively they represent coastal state indicators: coastal volume, beach width, and depth contours. Furthermore, the analysis in phase 1 emphasizes the behavior of specific aspects within the data. This highlights the potential of depth-dependent cross-shore contributors to one-line models.

The volume definition in the comparison represents volume changes due to net alongshore sediment flux (Q), illustrated in Figure 4.3. As described in Ch.3.1.3, in the ShorelineS model, changes in volume directly correlate with shoreline changes. In contrast, Crocodile distributes net alongshore sediment flux across the profile with the diffusion coefficient, as exemplified in Figure 3.2.

Note that volume changes from the dune module (beach and dunes) in ShorelineS are not included in the comparison since Crocodile lacks integration with this module, which would lead to overlapping accounting of subaerial volume changes.

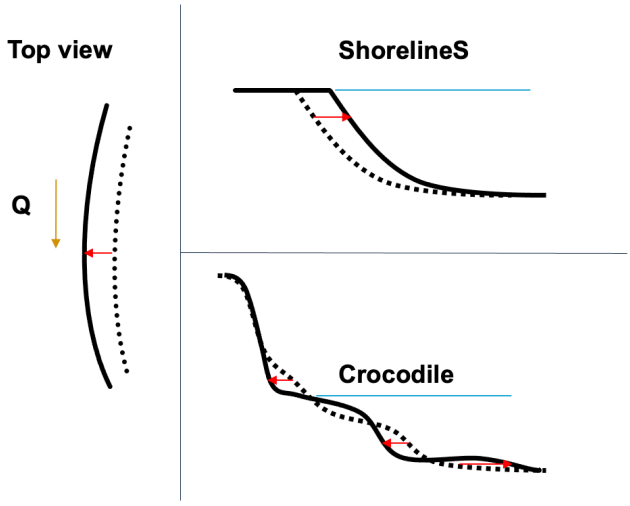

Figure 4.3: Illustrative sketch of volume comparison definition. The figures on the right-hand side show the difference in volume evolution due to the net alongshore sediment flux.

5

Results Data Analysis of Hondsbossche Dunes Case Study

5.1. Area description and coastal conditions

As indicated in Figure 5.1, the Hondsbossche Dunes are located along the North North-Holland (NNH) wave-dominated sandy coast. It experiences a semi-diurnal microtidal climate where, on average, spring and neap tidal ranges are around 1.6m (±0.8 m+NAP, MLW and MHW). Given the relatively shallow North Sea, the Total Water Level (TWL) is mainly dominated by water level set-up and wave run-up [39]. Between 2015 and 2024 waves are observed coming from WSW to NW direction, see figure 5.1. These waves were translated nearshore using wave transformation matrix [65] based on observation stations in the North Sea. The figure depicts the spectral significant wave height (H_{m0}) at -6 m+NAP offshore. Mostly, waves come from 285 - 315°N, under both energetic and calm wave conditions. Also, from the specific wave direction 250 - 260°N many waves comefor 21% of the time, with mainly H_s between 0.0-2.0m The mean spectral significant wave height over this period is 0.92 m with a corresponding peak wave period (T_p) of 5.42 s. Similar conditions are found in literature that considers longer timeseries [66, 10]. In these sources, the mean annual wave height H_s is around 1.0 m, during northwestern storms however, H_s can get about 4.7 m high at a depth of -10 m+NAP.

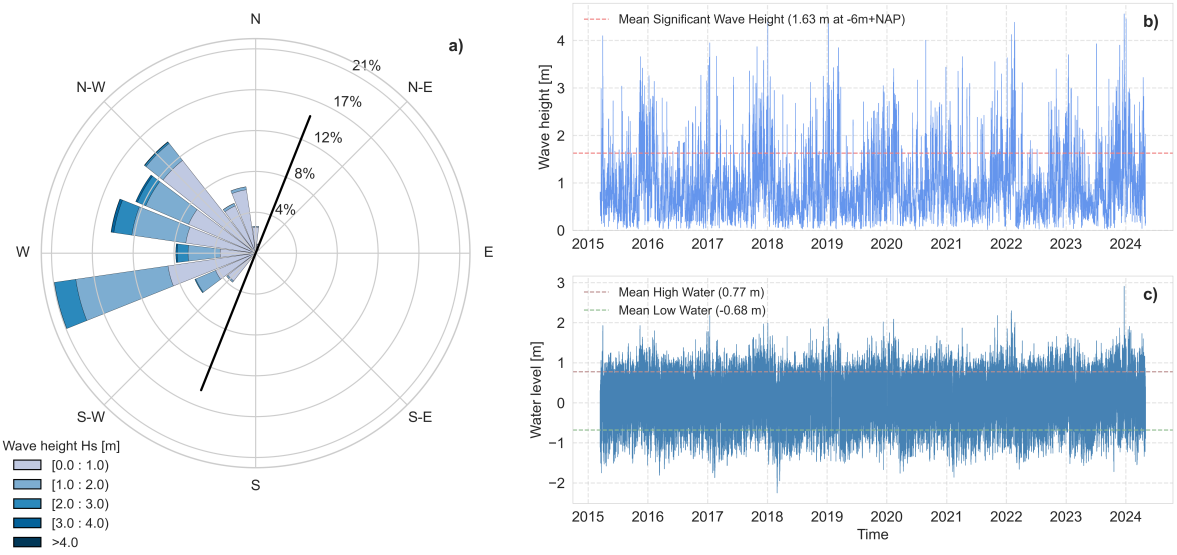

Figure 5.1: Figure a) shows the offshore wave climate near HBD (52.74578, 4.63320) at -6m+NAP between 2015-2024, with average coastline in black b) indicates wave timeseries of the wave climate, with the mean Hs of about 1.63 meter. c) illustrates the time series of the Mean Water Level, with a Mean High Water of 0.77 m+NAP and Mean Low Water of -0.68 m+NAP.

The sediment size that is native to this coast varies over the cross-section profile. Close to the waterline grain sizes between 250 to 325μ are common [67]. Finer materials are found in the dune system (220 to 280μ) and more seaward at the shoreface (170 to 200μ) [10].

Since the HBD project was completed in 2015, five additional nourishments have been executed at this site. The location, start and end date, and nourished volume are provided in table 5.1. Three beach and two shoreface nourishments come to a total added volume of almost 3.6 Mm^3 of sediments.

Nr.	Kp start	Kp end	Length [m]	RSP start	RSP end	Type	Date start	Date end	m^3	m^3/m
1	8500	10000	1500	25.10	26.65	Beach	3/1/2018	4/30/2018	1,070,932	714
2	8500	10000	1500	25.10	26.65	Shoreface	9/1/2020	11/30/2020	506,118	337
2	4250	6000	1750	21.10	22.80	Shoreface	9/1/2020	11/30/2020	632,045	361
3	8350	10300	1950	25.32	26.37	Beach	11/1/2022	12/31/2022	805,924	413
3	4400	5950	1550	20.90	22.45	Beach	1/1/2023	2/28/2023	575,453	371

Table 5.1: Executed nourishments in the period 2015-2024. The data specifications are provided by Boskalis. [63]

5.2. Data Analyses Results

5.2.1. General Morphodynamics of Nine Years

The coastal profiles alongshore have undergone significant changes. In Figure 5.2, the cross-shore profiles from 2015 (light brown) to 2024 (dark blue) are plotted for five representative transects. The vertical red line marks the landward boundary, whose spatial location is indicated on the aerial map.

The evolution of profile RSP 18.8 (north) shows a significant seaward advancement of the shoreline, together with a seaward movement of the dune foot. A similar pattern is observed at profile RSP 28.0 (south), although the shoreline advance is less pronounced. Here, embryonic dune developments are visible. During the construction of the HBD artificial dunes were constructed, of which a large part in the central section (RSP 20.71 – 25.31). The figure illustrates the gradual and significant growth of approximately 5 meters that this dune system experienced. The shoreline, however, shows a strong retreating movement.

The dynamics of sandbars below the waterline are clearly illustrated in the figure. This 3D behavior stems from both past and present wave forcing conditions. Although sandbars tend to fluctuate around a mean position, long-term trends spanning several years reveal variations in their locations. A cyclic pattern of onshore or offshore migration becomes evident, where sandbars increase in size as they move seaward before eventually dissipating. This phenomenon is still not fully understood in existing literature. The long-term mean migration of these sandbars is captured in the cross-shore profiles by the multi-year measurement intervals.

The cycle duration of sandbars varies along the Holland coast. The direction, size, and number of sandbars differ alongshore. Visualizations of the JarKus data up to 2019 [39] indicate that the northern section of the Hondsbossche Dunes has exhibited stationary and undisturbed sandbar movement since 1970. In contrast, the southern section displayed a 15-year bar cycle before stabilizing around 2000.

Since the construction of the Hondsbossche Dunes, clear movements of bar migration are visible in Figure 5.2. Because their morphological timescales are long, additional years of data are required to establish significant trends. Due to the complexity of offshore bar migration, this aspect falls outside the scope of this project.

The recognizable shape of the Hondsbossche Dunes location (RSP 18.8 - 28.0) results in a coastline that protrudes into the sea more than it did before 2015. In theory, this planform shape gradually disperses over time due to hydrodynamic forces such as wave action and tidal transport. The coast is maintained by additional nourishments (Table 5.1). Previous studies after the mega-nourishment implementation [10, 63] indicate a general trend in which the central section of the nourishment (RSP 22.0 – 26.3) experiences erosion, while the northern and southern sections exhibit accretion. This pattern is also reflected in data from 2015 to 2024, as illustrated in Figure 5.3a. The figure shows the total volume change of the integrated profile relative to the initial state after project completion in March 2015.

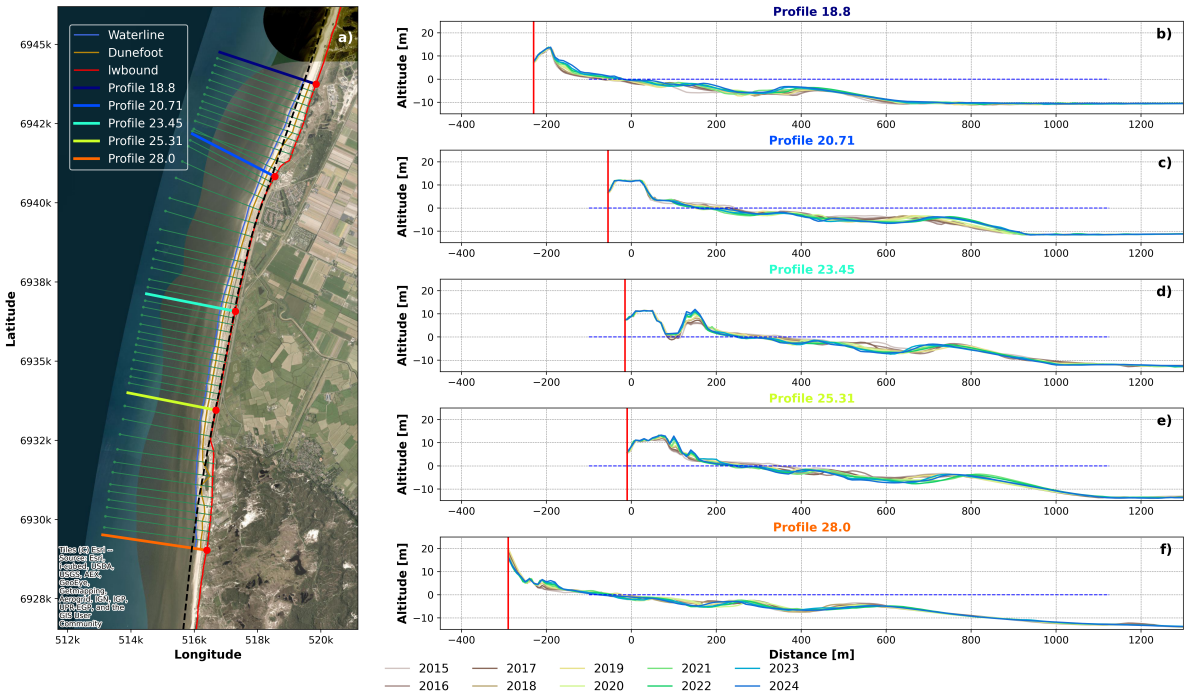

Figure 5.2: Overview of a variety of transects. Left figure shows an aerial overview map of the transect locations shown on the right. The profile evolution over the period 2015-2024 (brown to blue) are shown for transects RSP 18.8, 20.71, 23.45, 25.31, 28.0. The red vertical line indicates the landward boundary used in the volume definition.

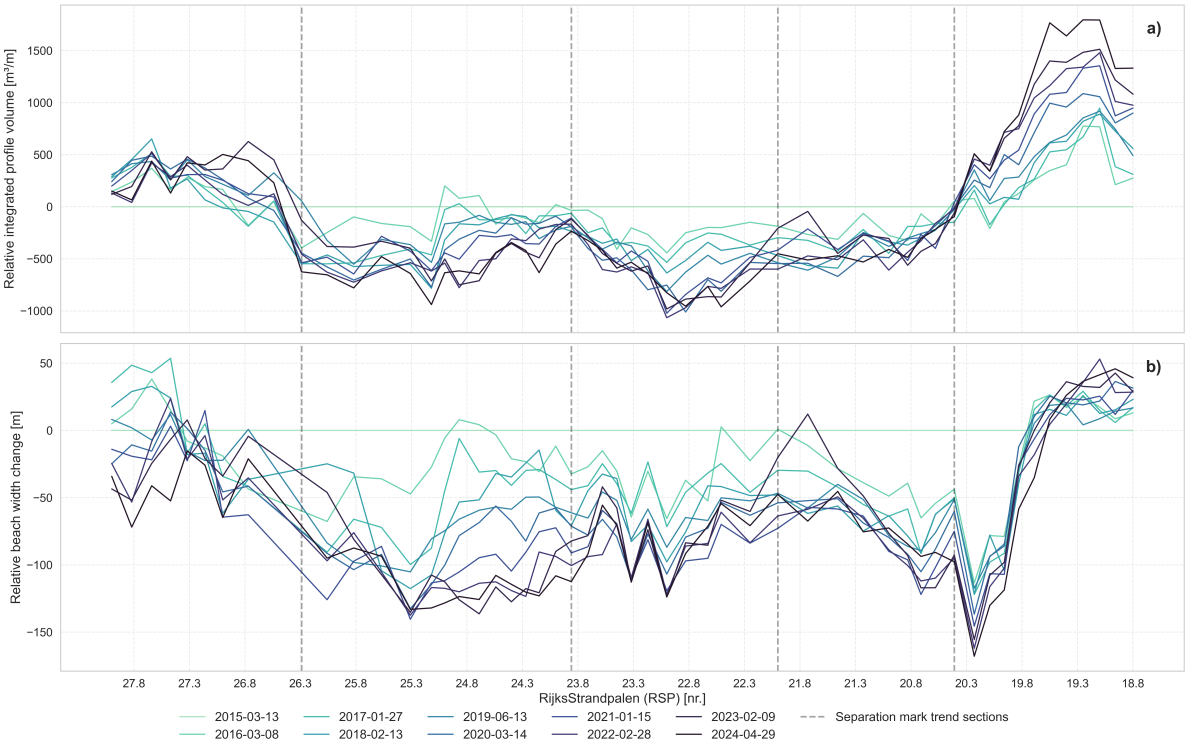

Figure 5.3: Figure a) shows the alongshore view of the integrated cross-shore profile volume change relative to initial state (implementation nourishment 2015). Figure b) shows the alongshore view of the beach width change relative to initial state. Both coastal indicators project the data over the period of 2015 till 2024. The vertical dashed lines separate sections of transects along the coast with similar behavior.

The alongshore volumetric change is categorized into three main trends: northern, southern, and central sections. Within the central part, three sub-patterns emerge. The northernmost section shows the most significant sediment accumulation, with gains of up to 2000 m^3/m over nine years. The southern section experienced also volume increases, but to a lesser amount. Also, most of its volume is gained in the initial years following the mega-nourishment. Recent trends indicates a stagnated tendency.

The section between the accreting areas is predominantly erosive, with the middle part losing up to 1000 m^3/m in profile volume since mega-nourishment's implementation. The mid-northern area shows no clear trend, while the mid-southern area gradually losses volume over time.

Similar to volumetric changes, beach width exhibits significant fluctuations alongshore over time, see Figure 5.3b. The large fluctuations are partly caused by the opposing evolution of the shoreline and dunefoot. The shape of the changing indicator deviates slightly from the integrated volumetric observation as the beach width change varies more in gradualness and quantity. Nevertheless, it generally aligns with the accretive and erosive patterns reflected in volume changes.

Over the course of nine years, the mid-northern section experienced a substantial reduction in beach width, with some locations retreating by over 150 meters. On average, the beach width in this area has retreated by approximately 100 meters. In contrast, the northern segment is the only region where the beach has expanded. In the southern segment, the beach initially advanced seaward but in later years started to reduce.

According to an analysis of the coastline observation of the complete North North-Holland (NNH) coast of the years 2015-2020 [10], the profile steepness of the HBD decreased to similar proportions of adjacent coastline in the first two winters on average. This indicates a fast cross-shore adaptation. Also the beach width seems to have reached similar magnitudes to those of nearby coasts for most transects, varying between 80 and 140m in 2020.

5.2.2. Volumetric Evolution by Coastal cells

Vertical Volumetric Cells

Two approaches outlined in the Methodology (Ch. 4), are employed to assess depth-dependent volumetric evolution behaviors and timescales. The first approach involves analyzing vertical coastal cells. Figure 5.4 illustrates how these vertical coastal cells—dune, beach, surf zone, and shoreface—evolve over time, showing relative volume changes compared to the initial state in 2015. Each line represents the section averaged volume change (sections indicated in Figure 5.3a). The gray shading indicates periods when additional nourishments were implemented, mentioned in Table 5.1.

The figures reveal that for the beach, surf zone, and shoreface (<3 m+NAP), two groups emerge: the northern and southern segments (blue and yellow) display accretion, while the central segment (purple, violet, and pink) exhibits significant erosion. This aligns with trends in Figure 5.3a.

The most significant volume changes occur in the surfzone for the central section. Here, an average negative rate of -200 m^3/m in three years time was observed. Since 2021, however, annual volume changes have stabilized as there has been little net change on an annual basis. In contrast, the northern and southern segments remain relatively stable over time, but the south segments eventually lose up to 200 m^3/m. At first glance, the evolution of the surf zone does not appear to be directly influenced by additional nourishments.

In contrast, the evolution of beach volume clearly responds to nourishment interventions. Following the completion of the Hondsbossche Dunes project in 2015, the additional beach nourishment in 2018 targeted the orange zone (RSP 23.86 – 26.29) but was completely eroded within a year. The two subsequent beach nourishments, carried out in the winter of 2022-2023, were located in the same zone as in 2018 and within the purple zone (RSP 20.41 – 22.0), influencing all segments. Overall, the annual volumetric changes are significantly smaller than those in the surf zone.

Initially, shoreface volume across all segments experienced erosion for the first four years. However, a notable increase in volume of about 50 m^3/m occurred in 2020, attributed to two shoreface nourishments in 2020 (zones 23.86 – 26.29 and 20.41 – 22.0). After this, the northern segment stabilized, while others experienced some volume loss. The northern middle section (purple) showed volume

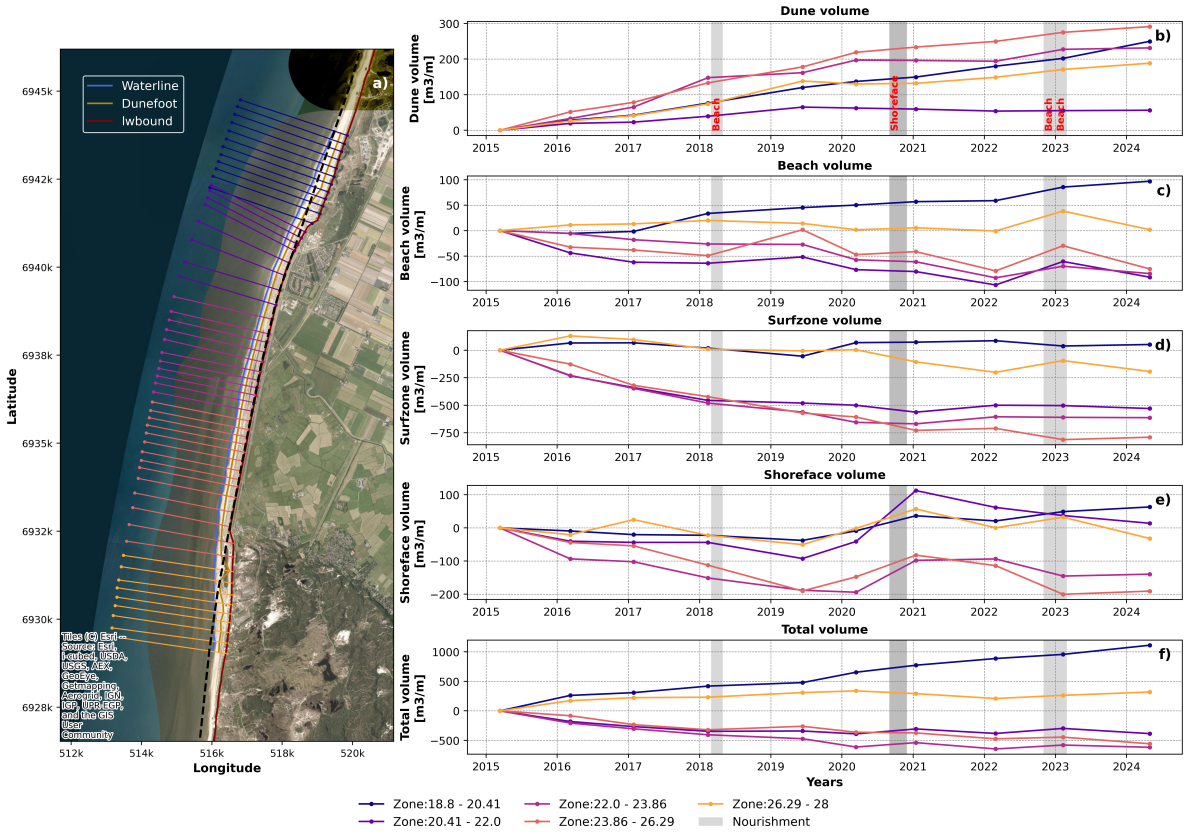

Figure 5.4: Figure a) shows an aerial overview map of the different alongshore zones, with transects RSP 18.8 (north) to RSP 28.0 (south). The plots show the average volume changes over time for different vertical coastal cells grouped by the different zones (colored lines). The four vertical cells—dune b), beach c), surf zone d), and shoreface e)—are plotted individually, with total volume evolution at the bottom in Figure f).

changes comparable to the blue (north) and yellow (south) segments, though the underlying causes remain unclear.

In the middle segment, all coastal volume cells below +3 m NAP exhibit the fastest response within the first years after the mega-nourishment implementation. Later, volume change appears to stabilize. Dune growth, however, seems independent of the dynamics in the lower coastal cells. Dunes continue to grow consistently across all segments, with the mid-center () and mid-south (pink) sections experiencing the most substantial dune growth—up to 300 m^3/m on average in orange zone (RSP 23.86 – 26.29). The artificially constructed dunes in the middle segment have gained significant height and volume over time. In contrast, the mid-north section (purple) is the only area where dune growth has stopped, with no further increase observed since 2019.

Overall, the northern segment (blue) accumulated the most sediment, doubling the loss experienced by the mid-sections. The southern segment (yellow) gained about one-third of the northern increase, while mid-sections faced a net loss of up to 500 m^3/m, but stabilizing after 2020.

Cross-shore Volumetric Cells

To gain an alternative insight into the developments in the cross-shore direction, the cross-shore cell method was used. Figure 5.5 shows the accumulative volumetric change for all transects (x-axis) plotted against time (y-axis). This was done for all cross-shore cells: dune zone, beach zone, surf zone, and sandbar/shoreface zone.

From this figure, the alongshore distinctions previously observed in Figure 5.3a become visible once more. The most intense colors are found in the surf zone, indicating that the largest annual changes occur in this area. The central part of the surf zone shows sediment changes on the order of 800 m^3/m, which aligns with the mid-section trend in Figure 5.4. In contrast, the northern part of the surf

zone reveals large accumulations that were not apparent in Figure 5.4, likely due to differences in cell definitions between the two analyses.

The beach zone shows a similar spatial pattern to the surf zone but with smaller annual volumetric changes. The shoreface zone does exhibit a different trend. Volumetric changes fluctuate across the northern, central, and southern segments, which is also reflected in the trendline of Figure 5.4. A potential explanation for this irregularity could be the shoreface nourishments carried out during the winter of 2020.

Dune growth appears to gradually increase in the southern-central and mid-central regions that also show the most pronounced increases in Figure 5.4. Meanwhile, the northern-central section remains relatively stable, and the northernmost part shows a slight decrease in dune volume. This is possible because the dunes are able to grow vertically as horizontally, but horizontal growth is not really captured because of the fixed 2015 vertical boundary.

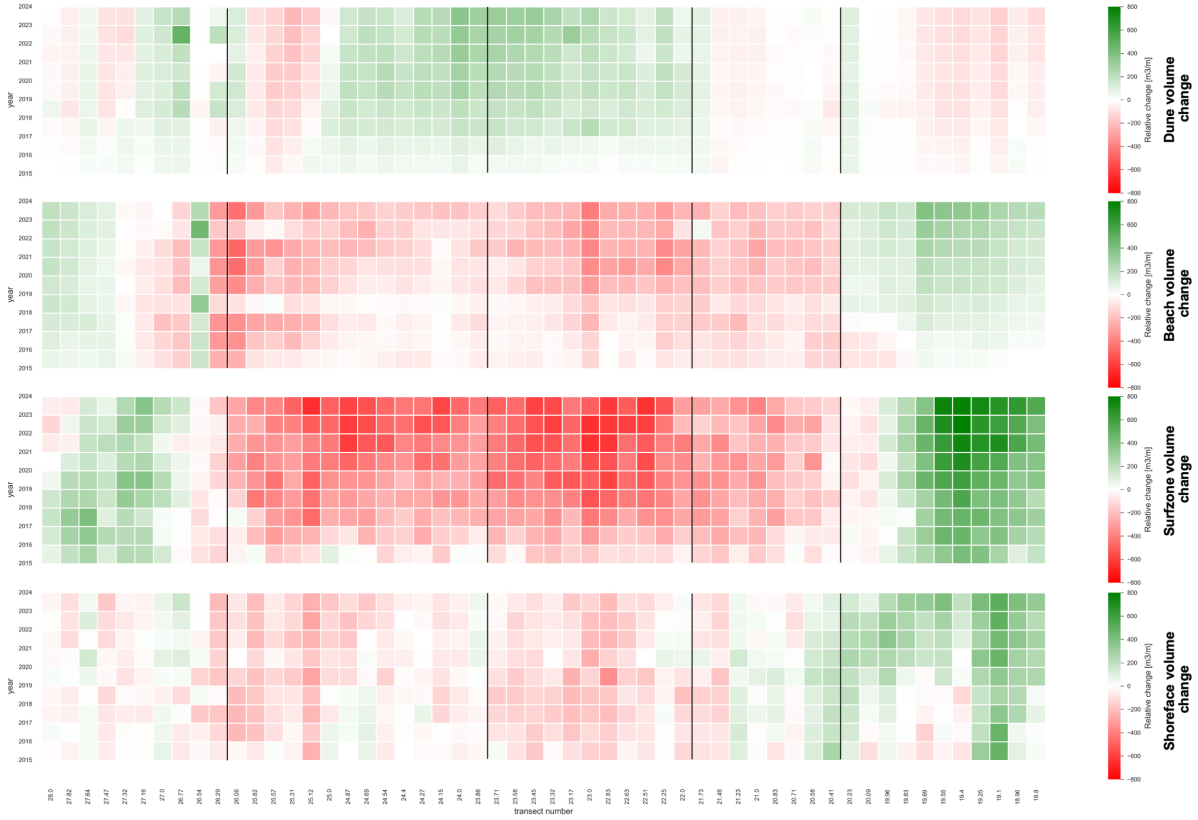

Figure 5.5: Cumulative volume evolution per transect for cross-shore defined cells. Red indicates loss of sediment, and green resembles accumulation. From top to bottom: dune zone, beach zone, surfzone, sandbar/shoreface zone.

5.2.3. Shoreline Correlations

To assess how well changes in the waterline reflect coastal changes in terms of volume and beach width, correlations with specific cross-shore cells provide insight into depth dependency. Existing literature indicates that shoreline position and beach width are strongly correlated with profile volume [10]. Using Jarkus data, these correlations have been extended by an additional four years, as shown in Figure 5.6. The data points in the plot represent the alongshore-averaged volume change over nine years.

For the period extension for 2015–2020 to 2015-2024, the correlation between the change in integrated profile volume and beach width decreased from $r^2 = 0.75$ to $r^2 = 0.68$ (representing the coefficient of determination for linear regression), see Figure 5.6. However, the shoreline position change related to the integrated profile change shows a small improvement from $r^2 = 0.84$ to $r^2 = 0.89$, Figure 5.6. The found correlations indicate that coastal volume changes scale well with variations in shoreline and beach width.

Further analysis of sub-volumes within the coastal profile reveals correlations between the waterline and cross-shore cells as well. Figure 5.7 shows that dune volume changes are very weakly correlated with shoreline changes. However, the beach and surf zone volume changes are strongly correlated ($r^2 = 0.78$ and $r^2 = 0.90$, respectively). In contrast, the correlation between shoreline position and shoreface volume changes is much weaker than that observed for the beach and surf zone.

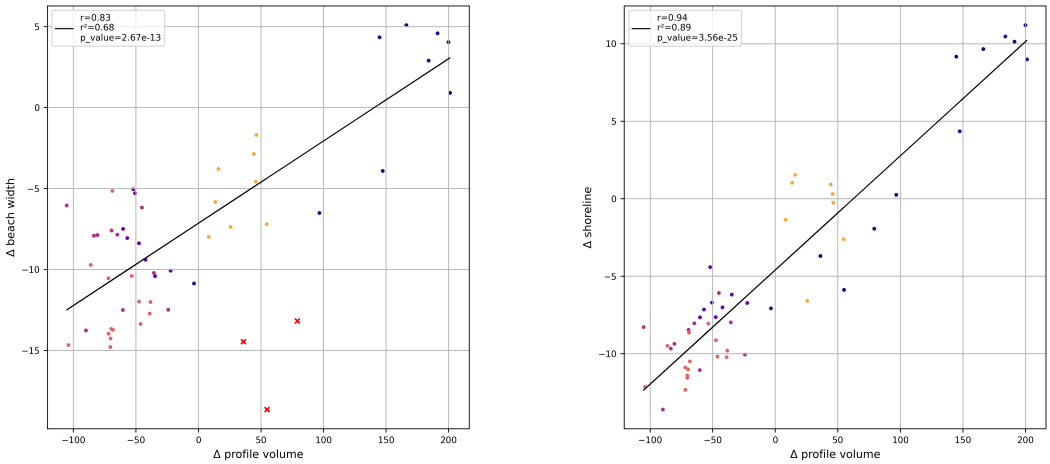

Figure 5.6: Extention of 4 years of correlation plot literature: a data point in the figure indicate the change of a [parameter] compared to the year before at a certain transect, averaged over 9 years. The colors represent the different coastal segments. Observations with a red cross are marked as outliers. This are datapoints where the artificially created lake just south of the middle section complicates the beachwidth definition.

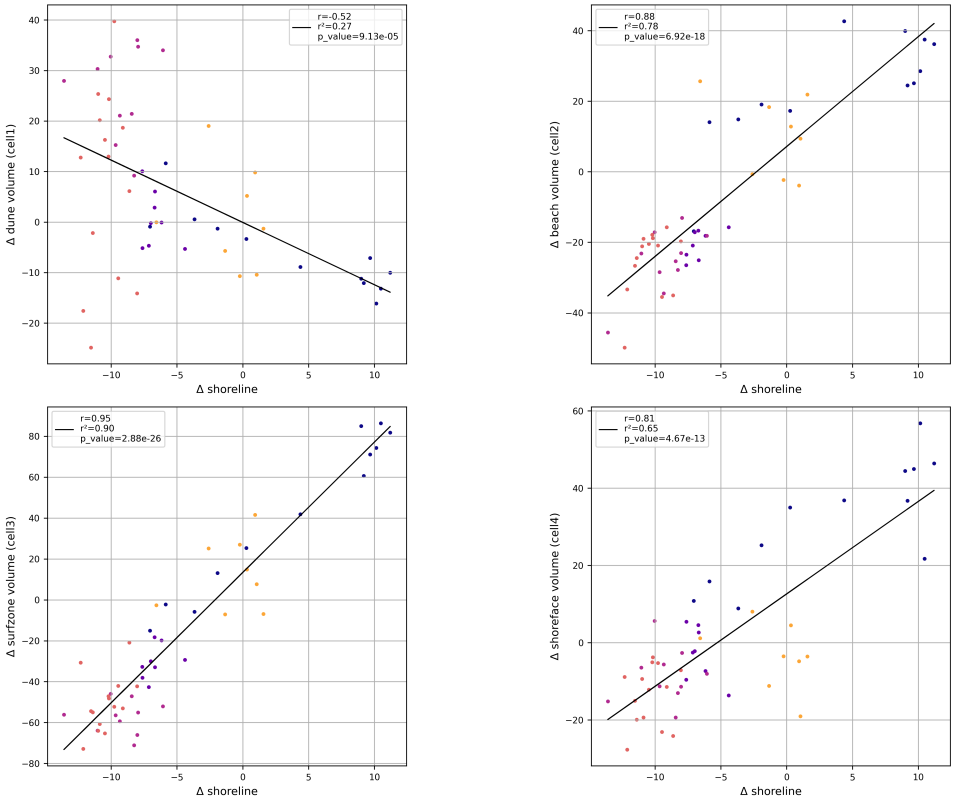

Figure 5.7: Correlation plots of different cross-shore cells to the shoreline change: a data point in the figure indicates the change of a [parameter] compared to the year before at a certain transect, averaged over 9 years. The colors represent the different coastal segments as defined in Figure 5.3a.

5.3. Discussion and Implications Evolution Models

5.3.1. Discussion Data Analyses

The results from the data analysis highlight clear differences among the northern, southern, and central zones in terms of both changes in sediment volume and beach width. The central zone is experiencing ongoing erosion, particularly in the surf zone, while the northern zone shows a consistent pattern of sediment accumulation. The most significant changes in the cross-shore profile occur in the first period after the mega-nourishment project. These changes stabilize in the following years. The initial changes differ in magnitude for the different vertical cells. This indicates that depth-dependent processes play a crucial role immediately following the mega-nourishment.

This comes clear from, for example, in the most central zone, the surfzone experiences up to four times more erosion in 2018 than other vertical cells (Figure 5.4). Suggests that there is less morphodynamic activity with depth. Likewise, when an additional nourishment is added to the system, the volume change does not distribute evenly across the profile, and shows location-specific response across vertical cells.

In addition, the vertical volumetric cells differ in their correlation to shoreline changes. Meaning that volumetric change activity is not uniform over the depth. The volume change in the surfzone shows a well-correlated relation to the shoreline changes ($r^2_{surf} = 0.90$), shown in Figure 5.5. However, the shoreface and dune volume changes are (much) more weakly correlated with the waterline ($r^2_{shore} = 0.65$ and $r^2_{dune} = 0.27$). Stronger correlations to the waterline position are found closer to the waterline. Meaning that the depth-dependent activity of these cross-shore processes is important in comprehending coastal dynamics. For the dunes, the dune growth is largely independent of the shoreline change. Suggesting that different subaerial processes, like aeolian transport, dominate over subaqueous interactions.

Nourishments are constructed with a steeper slope than the former and adjacent coastal profiles. The time for the profile to adjust towards its equilibrium slope usually takes months to years (sources). In the period for a coastal profile to adjust its slope, stronger cross-shore processes are expected. As an attempt to explore the presence of initial cross-shore activity, a ratio is defined—inspired by Dean [68]—between the nourished volume change within a profile (ΔV_{net}) and the volumetric planform change based on a one-line principle ($\Delta S_{shoreline} \cdot D_{DoC}$). In the initial years after nourishment, this ratio is expected to be relatively low, suggesting that most of the nourished volume is retained and redistributed within the profile while the shoreline (platform) retreats. Over time, the ratio gradually increases towards an asymptotic value, where the profile is adjusted to the longshore-dominated coastal equilibrium state.

However, such a trend is not observed at the HBD, as shown in Figure 5.8; instead of a gradual increase towards an asymptote, the ratio remains highly variable over time. The figure presents the average ratio for each coastal zone, as defined earlier. Although no consistent trend is apparent, the fluctuations in the ratio suggest that cross-shore processes are present in the morphological evolution of the area, but that cross-shore dominance due to slope adjustments are not captured.

A reason that there is no clear initial cross-shore dominance might be because the profiles are already adjusted to the slope of the adjacent coastal profiles. Research of Kroon [10] at the HBD showed that between 2015 and 2016, all profile slopes adjusted to ranges of nearby stable coastal profiles. This analysis was made with additional measurements from the construction company. JarKus data, used in this research, are measured annually and might therefore not have captured this adjustment. Also other research [69, 70] showed that profile adjustments happen within small time ranges of months to 1.5 years.

This suggests that the expected cross-shore dominance in the initial years may have been less significant at the HBD site or not have been covered by the data. The current study provides only a limited investigation into cross-shore and longshore transport dominance. As such, this topic is identified as a key area for future research and is included in the recommendations.

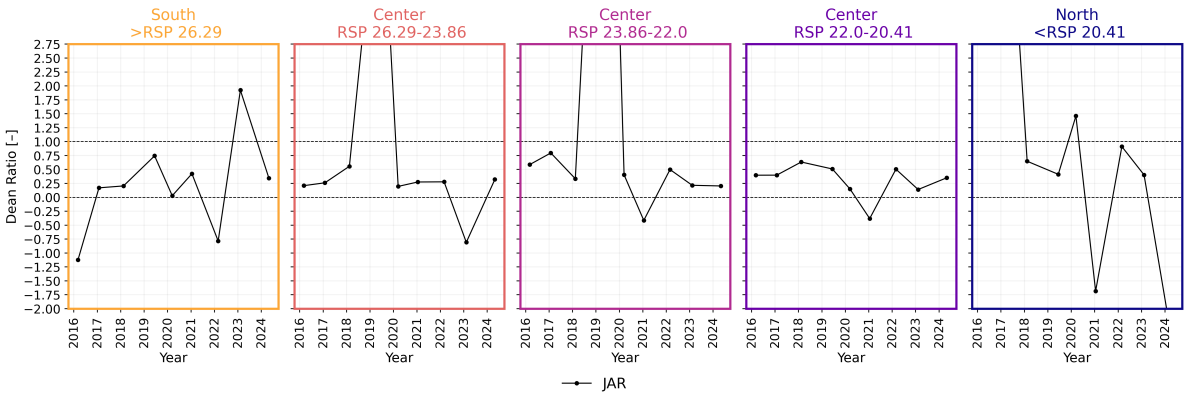

Figure 5.8: Average dean ratio of the different coastal zones. The black line represents the JarKus data.

5.3.2. Implications Evolution models

The discussion of the data analysis results highlighted several essential points that have implications for the performance of the coastal evolution models used in this research. One such implication is that the non-uniformity of volume changes across the profile does not align with the ShorelineS assumption of a constant profile in the cross-shore. Crocodile, however, is able to make cross-shore redistributions. Therefore it is expected that the coupled model, ShorelineS+Crocodile, is able to better represent the magnitude and trend in the vertical subaqueous volumetric cells. This also highlights the importance of a good cross-shore diffusion coefficient, as is seen that the morphological activity decreases with depth.

Furthermore, because the correlations of the volume cells are better correlated near the waterline, the contour lines further offshore are less affected by the coastline change. In the erosive middle section, even a shoreface expansion is observed at some transects. The coupled model diffuses sediment along the profile. Therefore it is expected that the coupled model could better represent the offshore contour behavior. However, whether the coupled model will perform better in the initial years is not known as no clear trend was observed in the dean ratio (Figure 5.8).

The inclusion of Crocodile does not affect the dune module of ShorelineS, used to model dune evolution. But as the dune module is dependent on the dry beach width, it is influenced by Crocodile. The dry beach is defined by, among others, the high-water line. In the coupled model this parameter follows from crocodile.

In the coupled model, nourishments are uniformly implemented using ShorelineS. This means that location specific nourishment trends in the different volumetric cells will not be modeled accordingly.

These implications highlight the theoretical improvements that may be possible with the use of a coupled model. In the simulation results of Chapter 7, the focus will be on the aspects mentioned above.

6

Model set-up

To carry out a hindcast study that aligns with the same time frame used in the data analysis, the models must first be set up. This setup consists of two parts: initially, the configuration of ShorelineS, followed by the setup of the coupled model that has been integrated with it.

6.1. ShorelineS input and configuration

The ShorelineS model was already largely set-up for this case-study. For previous research purposes, Svasek Hydraulics set up this model for the period 2015-2020. An extensive Generalized Likelihood Uncertainty Estimation (GLUE) analysis was performed by [20]. This GLUE analysis exhibits over 7000 simulations with varying combination of parameters. These parameters include: the median grain size ($D_{50} = 234.95\mu m$), breaker index ($\gamma = 0.705$), scaling factor of longshore transport parameter ($q_{scale} = 1.1427$), offshore depth of wave input ($d_{deep} = -6.0m + NAP$), active profile height ($d = 10.462m$). This best fit used a CERC longshore transport formulation. The volume-based calibration input parameters were adopted for this analysis. In recent years, the additional modules have been released. For the Hondsbossche Dunes the new dune module is a relevant addition to the ShorelineS model. The inclusion of this module showed a significant improvement of the shoreline [71]. The initial shoreline input that was used for the calibration was smoothened to avoid instabilities in the extensive GLUE calibration. But now that there are no extreme parameter combinations involved, a non-smoothed JarKus 2015 measured coastline is used.

This calibrated ShorelineS model spans the time frame of 2015 to 2020. To extend this period to 2024, additional hydrodynamic conditions are added.

6.1.1. Hydraulic Conditions

The wave conditions are prescribed at 59 locations along the North-Holland coast, stretching about 55 km. As mentioned and analyzed in Chapter 5, the wave conditions are were translated from offshore observation stations to nearshore ($d_{deep} = -6.0$m+NAP) from a wave transformation matrix [65]. The wave data consists of the spectral significant wave height H_{m0}, with the corresponding peak wave period T_p and wave direction.

6.1.2. Dune and Nourishment Implementation

Wind and initial dune data are specified to utilize the dune module. The wind data is necessary to enable the dune to grow, using an aeolian transport flux q_{wind} (formula 3.2). This flux formulation is based on the wind speed and direction as described in paragraph 3.2.2. Besides the wind data, the details about the dune is also prescribed. ShorelineS uses this information to create an initial dune system reference. Based on this data, the dunes can grow and erode as explained in Chapter 3.2.2.

Also the realized nourishments over the period 2015-2024 at the Hondsbossche Dunes (Table 5.1) are listed in .nor file. There are two different ways to specify nourishments in ShorelineS. Restricted to a set of lines, or via a selected polygon in the shape of the nourishment location. For this research

we only have the specified information as in Table 5.1. Therefore the noruishemtns only cover the details between what alongshore transects (RSP's) the nourishments where implemented, and the nourishment type. The latter matters, because as described in Section 2.1.4 beach and shoreface nourishments differ in the speed and duration they feed the coast.

6.2. Coupled model input and configuration

The coupled model uses ShorelineS as the main driver of the model, while Crocodile functions as a module to redistribute sediment in the cross-shore direction at a set of selected profiles. The initial bathymetry of these designated profiles is seeking an equilibrium. To provide this, an equilibrium profile is needed as input.

Since equilibrium conditions may vary spatially along the coastline—and because the orientation of the coastline can shift during the simulation—an equilibrium grid is constructed. This grid enables the selection of profiles alongshore for insight into the cross-shore redistribution at that location.

6.2.1. Equilibrium Profile

To construct the equilibrium grid, a representative equilibrium profile is required that reflects the local coastal conditions. This profile is derived by fitting an mean cross-shore profile to over 50 years of JarKus measurements (1970–2025) at a relatively stable section of the coast.

The selected location should not be too close to the altered coastline influenced by the mega-nourishment, as this could falsely affect the representation of the equilibrium. At the same time, it should not be too far away, to avoid differences in coastal orientation and hydrodynamic conditions.

Initially, for this model, a standard equilibrium profile was selected approximately 6 kilometers south of the Hondsbossche Dunes (see Grey transect in Figure 6.1). The average beach width, volume, and shoreline position at this location have remained relatively stable over time. Additionally, there are no hard coastal structures such as groynes in this area that might disturb the natural equilibrium.

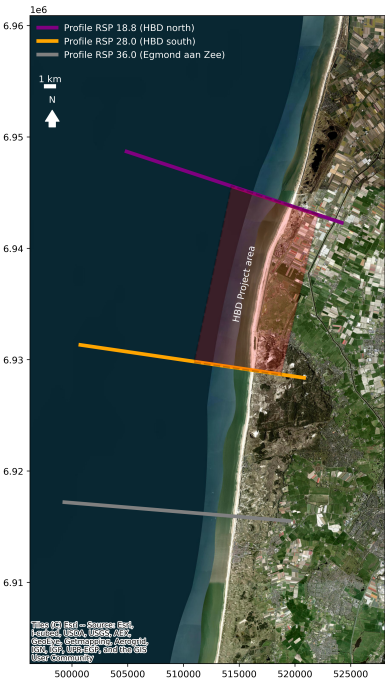

Figure 6.1: Aerial map with an overview of the equilibrium profile definition location.

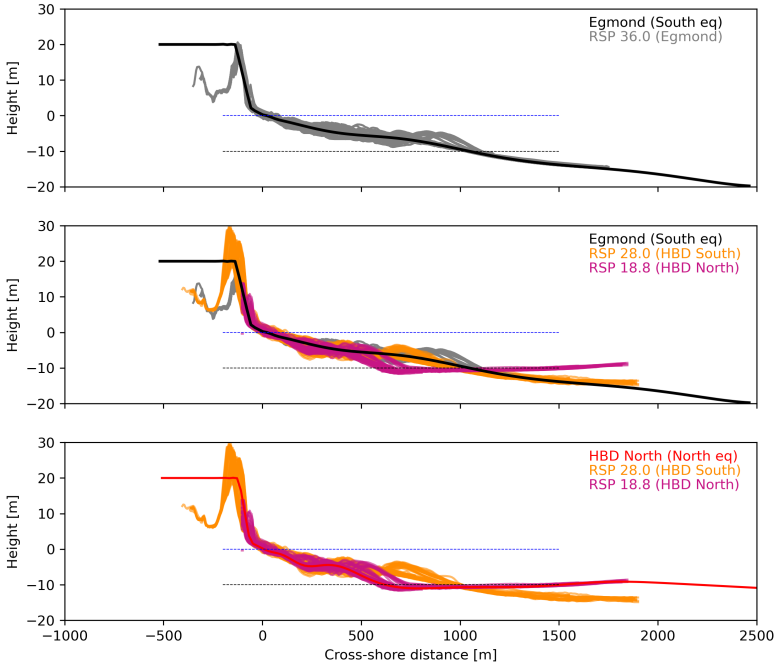

Figure 6.2: Cross-shore plot of Egmond equilibrium profile fit (top), Egmond profile comparison to HBD north and south (middle), and HBD noord profile comparison to HBD north and south.

Figure 6.2a shows how the equilibrium profile (Black line) at the location of Egmond fits the historical JarKus data (Grey lines). The southernmost profile at the Hondsbossche Dunes (Orange line) aligns

well with this equilibrium profile, as shown in Figure 6.2b. This indicates that the historical cross-shore profile near the southern end of the Hondsbossche Dunes closely resembles the equilibrium conditions derived from the adjacent coast south of the nourishment.

In contrast, the purple profile in the exact figure displays a noticeably different shape. In the lower shoreface region (around -6 m+NAP), the slope is steeper, followed by a relatively flat section near -10 m+NAP, and even a shallow area appears just offshore.

Figure 6.2c illustrates an alternative approach in which the equilibrium profile is fitted to historical data at the northernmost location of the Hondsbossche Dunes project, instead of a location at a respectable distance north of the project site. This is done because here the coast is affected by a shift in orientation, also the profiles do not represent the shallow area in front of the northern HBD area well, and because of the presence of groynes. These factors complicate the definition of a true equilibrium state in this area.

Therefore, the equilibrium profile at the northern end of the Hondsbossche Dunes is defined based on the profile derived from this exact location (purple transect RSP 18.8 in Figure 6.1). The equilibrium profile here is indicated with the red line in Figure 6.2c.

6.2.2. Initial and equilibrium Grid

With the equilibrium profile selected, an equilibrium grid can be constructed. This grid spans from RSP 18.8 to 30.0 and is defined based on spatial coordinates, as illustrated in Figure 6.3b.

To visualize how the observed coastal profiles relate to the equilibrium condition, JarKus measurements are superimposed on this grid. The 2015 JarKus dataset is used to define the initial grid, representing the coastal bathymetry at the start of the simulation. The hypothesis is that, over time, this initial grid will evolve towards the shape of the equilibrium profile.

To suppress sharp local variations in the JarKus data while preserving underlying trends in coastal morphology, a Gaussian smoothing filter is applied. This method calculates a weighted average, where points closer to the target location have a higher influence than those further away. A standard deviation of 20 is used, meaning that the elevation values of 20 neighboring grid points contribute to the smoothing. Based on several test runs, this setting provides a good balance between preserving sufficient detail and filtering out strong edges in the data.

In areas where the JarKus data lies landward of the equilibrium grid or where no data points are available, elevation values are supplemented using the corresponding points from the equilibrium grid. Additionally, since JarKus data only extends to a limited depth, but the Crocodile model requires bathymetry to reach sufficient depth for numerical stability, the equilibrium profile is also used to fill in the deeper parts of the initial grid where the measurements stop. An example of the resulting initial grid is shown in Figure 6.3a.

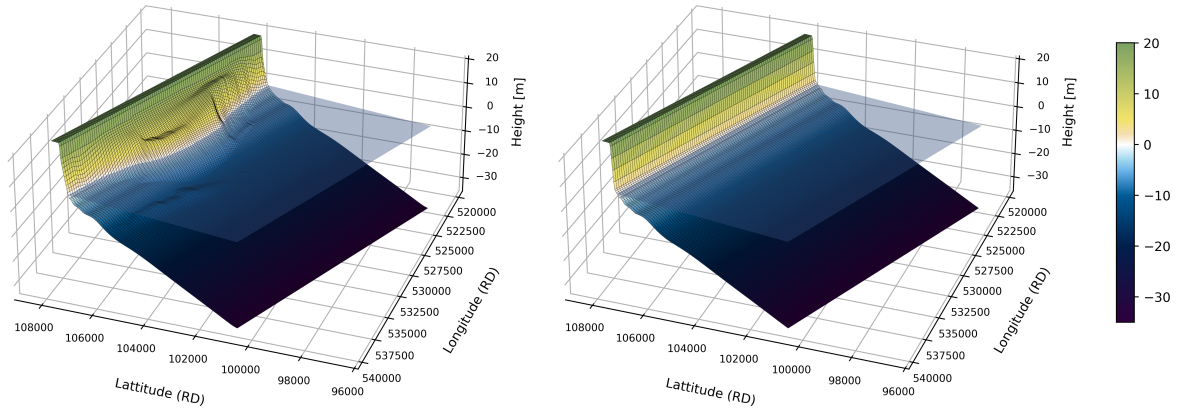

Figure 6.3: Initial grid configuration of a straight equilibrium coastline (left) and Equilibrium grid (right).

6.2.3. Crocodile Configuration

In Crocodile, cross-shore profiles can be assigned alongshore. To enable comparison between the profile evolution produced by the coupled model and the measurements from the data analysis, these cross-shore profiles are aligned with the JarKus transects. The profiles are constructed on the ShorelineS grid points, with the closest grid point to each JarKus transect selected as the reference location.

These cross-shore profiles are oriented perpendicular to the local shoreline. As the coastline evolves during the simulation, this results in a rotation of the profiles due to changes in coastal orientation. Any volumetric changes in the initial profile resulting from this rotation are accounted for in the volumetric model analysis presented in Chapter 7.

6.3. Simulation Setting Table

Several simulation runs were performed using different input variables. Simulation Table 6.1 shows which components were included in each run.

The first run that includes the Crocodile module represents a very basic setup of the coupled model. It assumes that the coastline is in a static equilibrium, that the initial coastal bathymetry settles to a straight shoreline, and that the equilibrium profile is uniform along the entire alongshore direction. These conservative assumptions can be gradually improved to physically better reflect real-world coastal behavior. Run SC1 to SC5 systematically explore and enhance the physical processes represented in the models. Beneath is explained why and how these components could improve the model results.

Run ID	Model	Period	Components ShorelineS	Components Crocodile
S0	ShorelineS	15-03-2015 / 30-04-2024	Dune module + Nourishments	-
SC0	ShorelineS+Crocodile	15-03-2015 / 30-04-2024	Dune module + Nourishments	Basic (straight) equilibrium grid (RSP 16.88-30) + Static Equilibrium
SC1	ShorelineS+Crocodile	15-03-2015 / 30-04-2024	Dune module + Nourishments	Basic (straight) equilibrium grid (RSP 16.88-30) + Dynamic Equilibrium
SC2	ShorelineS+Crocodile	15-03-2015 / 30-04-2024	Dune module + Nourishments	Curved equilibrium grid (RSP 16.88-30) + Static Equilibrium
SC3	ShorelineS+Crocodile	15-03-2015 / 30-04-2024	Dune module + Nourishments	Curved equilibrium grid (RSP 16.88-30) + Dynamic Equilibrium
SC4	ShorelineS+Crocodile	15-03-2015 / 30-04-2024	Dune module + Nourishments	Curved equilibrium grid (RSP 16.88-30) + Static Equilibrium + Gradual varying eq profile
SC5	ShorelineS+Crocodile	15-03-2015 / 30-04-2024	Dune module + Nourishments	Curved equilibrium grid (RSP 16.88-30) + Dynamic Equilibrium + Gradual varying eq profile

Table 6.1: Simulation Table overview. Run S0 only consist of the ShorelineS model, whereas SC0-5 add Crocodile. These runs add different components, that could effect the simulation output.

6.3.1. Dynamic Equilibrium

In contrast to static equilibrium, dynamic equilibrium assumes that the position of the equilibrium profile or grid shifts in response to changing conditions. These conditions influencing the development of the equilibrium profile are illustrated in Figure 6.4. Translation of the profile (a) can be driven by gradients in longshore sediment transport (b), sea level rise (c), and the addition of nourishments (d).

The latter aspect is particularly relevant in the case of a mega nourishment. Due to the large volume of sand added to the coastal system, there is a significant increase in sediment volume within a cross-shore profile. This excess volume cannot simply disappear, except through gradual erosion. A more realistic representation of the equilibrium profile would therefore assume that this added volume is evenly redistributed across the profile, resulting in a seaward shift of the equilibrium profile.

Over time, as the nourishment volume decreases due to natural processes, the equilibrium profile gradually returns towards its static equilibrium position. However, it will never fully return to the pre-nourishment state, as the profile now contains additional sediment volume introduced by the nourishment.

Sea level rise is not very relevant for this small period of 9 years. Nevertheless, this will be a very important factor when simulating over decades to centuries.

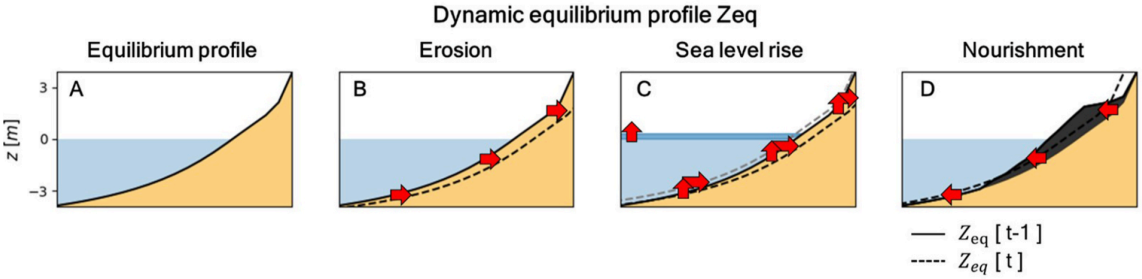

Figure 6.4: Dynamic equilibrium option in Crocodile model [22]: Erosive behavior, Sea level rise and additional sediment by nourishments.

6.3.2. Curved Equilibrium Coastline Shape

When zooming out from the location of the Hondsbossche Dunes, it becomes evident that, on a larger spatial scale, this area is situated within a bend along the coastline. The coastal stretch to the north and south of the Hondsbossche Dunes differ in coastline orientation. This also comes clear from the top graph in Figure 6.5. The graph shows the mean orientation of the mean high waterline along the North-Holland coast throughout 2015-2024. We see that the orientation to the south has an orientation of about 277°. The north varies between 290°and 285 °. The linear increase in orientation of at the Hondsbossche Dunes confirms that the coast has a bended nature. This makes the assumption of a straight equilibrium coastline shape less accurate and physically incorrect, see the blue grid in Figure 6.5. The impact of this assumption becomes more significant as the simulation domain is expanded. In such cases, the equilibrium profile increasingly deviates horizontally from the initial profile, which can lead to a higher rate of adjustment toward equilibrium and, consequently, an overprediction of erosion.

One way to address this issue is to introduce a curved equilibrium coastline that aligns with the coastal orientations to the north and south of the Hondsbossche Dunes, see red grid in Figure 6.5. The connection or intersection points of this optimally fitted curve lie at the locations where the coastline positions before and after the mega nourishment implementation begin to diverge (i.e., between 2013 and 2015). The newly defined equilibrium and initial grid shape that represent this component improvement are shown in Figure 6.7.

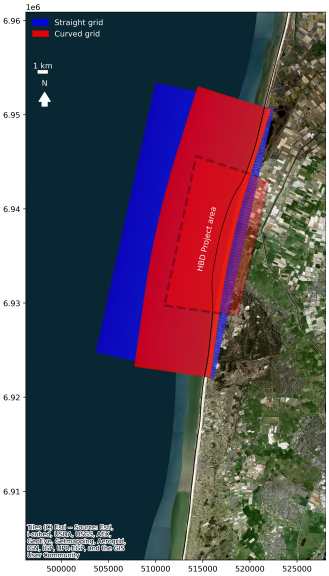

Figure 6.5: Equilibrium grid configuration: The blue grid shows the straight equilibrium grid that hooks the coastal shape. The red grid shows the curved equilibrium grid that aligns with the nature of the coast.

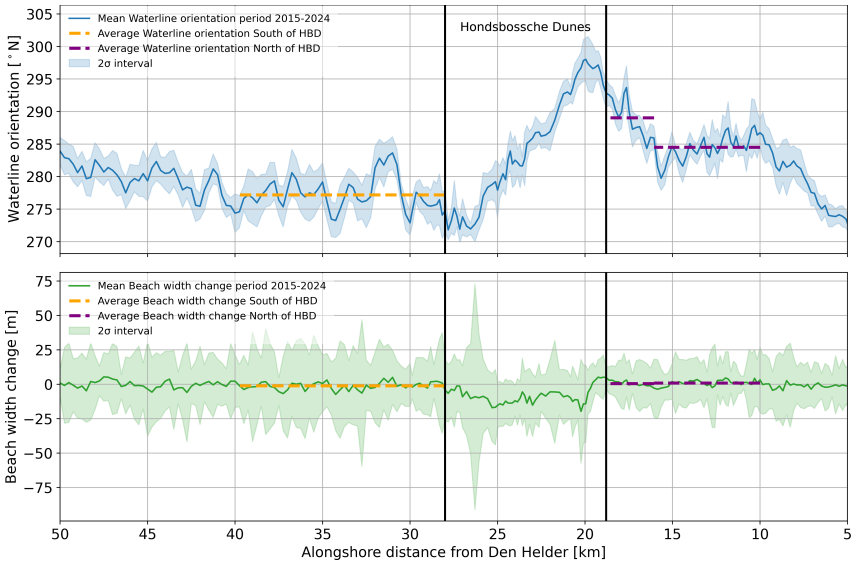

Figure 6.6: The upper graph shows the north holland mean high waterline orientation averaged over the period 2015-2024. South to the Hondsbossche Dunes the orientation is relatively stable around 277°, as to the north, it changes from 289° to 285°. This figure illustrates that the Hondsbossche Dunes are situated in a bend. The lower figure shows the beach width change over the same period. From this figure can be seen that the beachwidth is relatively stable for locations north and south of the HBD, but that the beach width at the HBD has been declining.

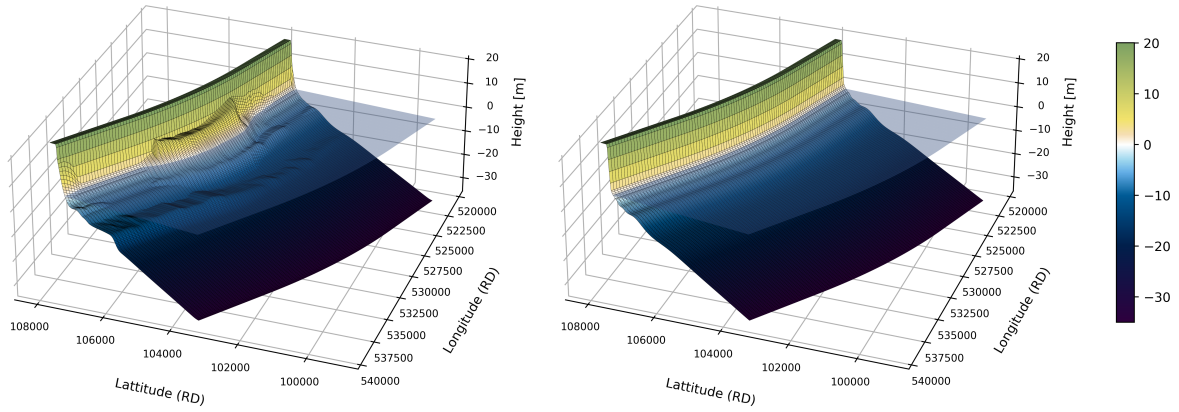

Figure 6.7: Initial grid configuration of a curved equilibrium coastline (left) and Equilibrium grid (right).

6.3.3. Alongshore Varying Equilibrium Profile

The assumption that the equilibrium profile is uniform alongshore is a conservative simplification. Over longer coastal stretches, the coastal system and its conditions can vary significantly. An example is the changing coastline orientation, which affects longshore sediment transport and determines whether a particular section of the coast lies within a wave shadow zone for a certain wave direction.

In addition, human interventions can also significantly impact the coastal equilibrium. For many years, a sea dike flanked by groynes existed at this location. The North Holland coast, north of the Hondsbossche Dunes, is still completely characterized by numerous groynes. These structures disrupt the natural wave-driven processes along the coast and interfere with the longshore transport, resulting in

a distorted representation of the cross-shore profile. It is then debatable what the actual equilibrium profile is. As described in Paragraph 6.2.1 , the equilibrium profile at the north is taken equal to the most northern part of the Hondsbossche Dunes.

The newly grid in Figure 6.8 now contains a gradual variation between the profile south and north (black and red line respectively in Figure 6.2).

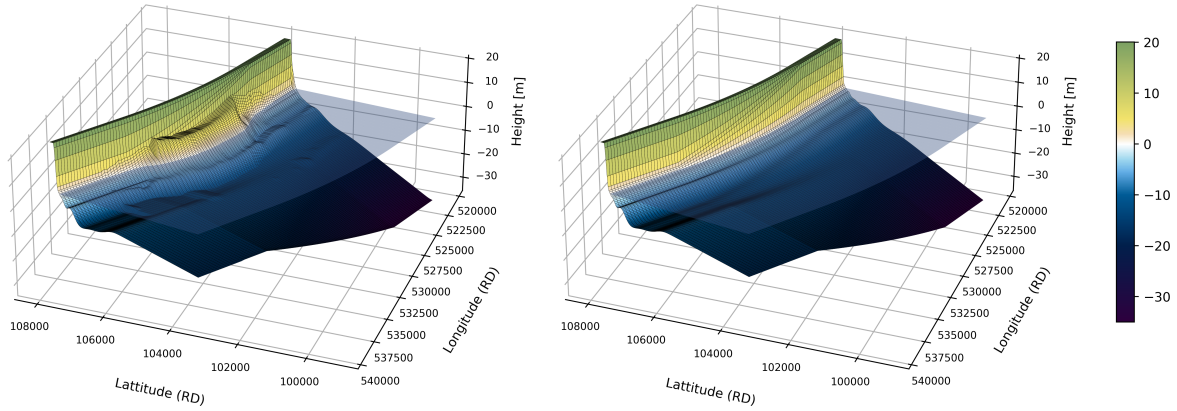

Figure 6.8: Initial grid configuration of a curved and alongshore-varying equilibrium grid (left) and Equilibrium grid (right).

7

Model Results

This chapter provides an overview of the hindcasting simulation results detailed in Simulation Table 6.1. It begins with an assessment of coastal evolution by analyzing volumetric changes to understand morphological development. Additionally, changes in volume across vertical cross-shore cells are examined to clarify overall volume dynamics. Then the beach width results are presented, which are derived from the evolution of shoreline and dune foot positions. Finally, additional benefits of the coupled model are evaluated through the development of selected cross-shore profiles and their depth contours.

7.1. Results of Volumetric Evolution

7.1.1. Volume definition, limitations and instabilities

Coastal volume is an important measure as it is directly linked with the primary flood defense function of the coast. The total volume gives an indication of the general behavior of this indicator. The total volume change after the first three years (2016, 2017, 2018), after five years (2020), seven years (2022), and nine years (2024) is shown in Figure 7.1. Here, the simulated alongshore volume change at a certain time step is plotted against the black dotted measurements. The volume definition is explained in the Methodology (Ch.4.1), where the volume is based on the net alongshore sediment transport flux. The volume change of ShorelineS is calculated as the shoreline change times the depth of closure (subaqueous volume). The coupled model computes this by the profile integral change. However, the measurements (black) indicate the complete total volume change (including beach and dunes).

During the setup of the coupled model, certain Crocodile profile locations were found to be repeatably unstable across different simulations. This instability resulted in unrealistic values for the volume changes of these profiles and had a negative impact on both the results and the stability of adjacent profiles. To avoid distorting the outcomes, in the coupled model, specific outlier Crocodile profiles were deliberately excluded in advance. This approach helps minimize non-representative behavior in the model and preserves the reliability of nearby sections. At the locations where the Crocodile profiles are not defined in the coupled model set-up, an expression for the shoreline evolution is simulated by ShorelineS.

Despite these adjustments, major wiggles and outliers still emerged in all coupled simulations (SC0-SC5), see Figure 7.1. The instability varies per simulation in initiation time and intensity. The instabilities that occurred within the first three simulation years used a static equilibrium (dotted lines). In contrast, all three simulations with dynamic equilibrium remained stable over this same period. Among them, simulation run SC5—the model using a curved grid with alongshore-varying equilibrium—which remained stable for the longest period and performed best of all coupled model simulations. However, from 2020 onward, an instability began to develop at transect RSP 26.5. To make a clear and meaningful analysis, ShorelineS is primarily compared to the SC5 run, mainly within the stable first 3 years.

Furthermore, a few transects showed consistent performance throughout the simulation period. There-

fore, a few stable transects are used in a profile and contour analysis in Paragraph 7.3.2.

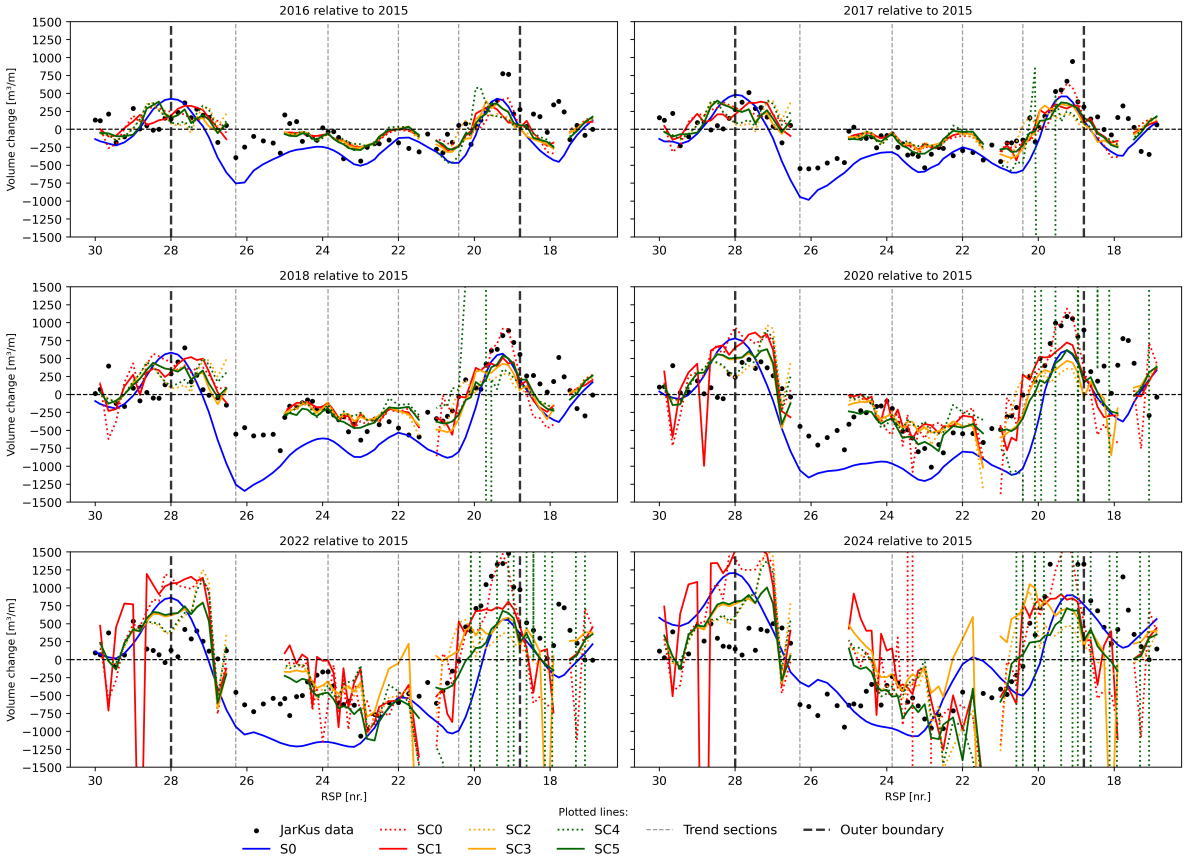

Figure 7.1: Model output results of volumetric change over the period 2015-2024. An overview of all simulation years can be found in Appendix A.1.

7.1.2. Alongshore Volumetric Change

Figure 7.1 shows the spatial distribution of the major volume changes per simulated year. All simulations broadly reproduce the erosion and accretion patterns observed in the measurements: significant erosion occurs in the central segment (RSP 20.42–25.82), while accretion peaks are found to the north and south of this zone, which is also noticed in the Data Analysis (Ch.5) in Figure.

In this Paragraph, first general trends are described of all simulation models, after which the analysis focuses on a comparison between the ShorelineS (S0) simulation and the best-performing coupled simulation (SC5).

Simulation results all models

The coupled models (SC0-SC5) provide more detailed and accurate representations compared to ShorelineS over at least the first three years. The ShorelineS run (S0, blue) shows a smooth pattern, resembling the shoreline position shape. The coupled models, on the other hand, exhibit more localized variation. The increased peakiness of these curves confirms this, suggesting that each Crocodile profile experiences an individual cross-shore redistribution.

For the different coupled simulation runs, volumetric changes are comparable throughout the initial years. This, while there are differences in horizontal offset between the initial and equilibrium grid. The offset in grid configuration varies between the straight (red) and curved grids (orange and green). But also between static and dynamic equilibrium configurations (dotted vs. solid lines). A larger offset could mean a bigger difference in slope between the profile and its equilibrium, which influences the rate of adaptation towards the equilibrium profile.

Another notable comparison is between SC3 (solid orange) and SC5 (solid green). Both use a curved grid and dynamic equilibrium, but SC5 also incorporates an alongshore-varying equilibrium profile. In the southern region where the profiles are yet the same, results are nearly identical. Moving northward for SC5 the equilibrium profile changes, and so the simulations diverge. This is reflected in the RMS error plot (Figure 7.3), where SC5 shows smaller increases in RMS error towards the north and remains stable for a longer period, whereas SC3 becomes unstable more quickly. This is likely due to the significant deviation of the equilibrium profile from the initial profile, where large slope differences occur. This makes the profile more sensitive to instabilities.

General Results Erosive zone

In the erosive central area (RSP 20.42-25.82), the SC5 simulation consistently shows less erosion than ShorelineS, which is in line with the measurements. During the first two years, the difference is approximately 250 m³/m. In the subsequent three years, this difference increases to about 550 m³/m around RSP 24. Accordingly, the Root Mean Square (RMS) error in this central zone is significantly lower for the coupled model compared to ShorelineS (Figure 7.3). However, the S0 simulation is still defined as a subaqueous volume change.

General Results Accretive zone

ShorelineS and the coupled model show accretion in the north and south area of the HBD. The JarKus measurements indicate that the north and south areas of the HBD have an accretive asymmetry; more volume accumulation of sand in the northern zone (<RSP 20.42) than south (>RSP 26.82). Both models do not show such an asymmetry, and consequently underpredict accretion in the north, and underpredict in the south. The RMS error for the north and south zones is of similar magnitude in the early simulation years (Figure 7.3).

Volume Evolution over Time

Using the volume definition as described in Section 7.1.1, the simulation SC5 provides a better representation of the volume change over time. This holds true not only for the total quantity but also for the shape and temporal behavior of the change, as shown in Figure 7.2. The figure shows the average volume changes per alongshore zone (colors defined as in Figure 7.9).

Notably, in the erosive central section (the middle three plots), the SC5 scenario closely follows the solid line. During the first three years, there is a more pronounced volume loss, after which the trend stabilizes over the following years. This pattern is particularly clear in the central section RSP 22.0–20.41. In contrast, the northern section (blue) and the southern section (yellow) show an under- and overestimation of the total volume, respectively. In the central sections, ShorelineS illustrates that the subaqueous volume changes predicted by a one-line model—as represented by S0—do not fully scale with the measured total volume. This indicates that additional processes play a significant role, some of which are accounted for in SC5.

Figure 7.3 compliments this, by showing that ShorelineS collects RMS error more rapidly in the early years compared to SC5. Over time, the RMS error flattens across all five segments. SC5 also shows a steep but smaller rise in error, which stabilizes within the first four years. At its peak in 2019, the best-performing simulation (SC5) reached an average error of 250 m^3/m, which ShorelineS almost doubles. However, unlike ShorelineS, the error for the coupled model continues to grow in the following years, mainly due to extreme values caused by model instabilities. It is good to mention that in these comparison plots, S0 still represents the subaerial volume change.

To place the S0 subaqueous volume in perspective, the blue dashed line in Figure 7.2 adds beach and dune volumes. As a result, the trend line more accurately reflects the actual volume evolution compared to the subaerial volume alone (blue solid). This highlights the significant positive impact of including beach and dune volumes in the simulation, particularly in the northern zone. Although the accuracy of the simulated evolution in the central zones remains variable, this line shows that the ShorelineS simulation is a good estimate of reality, especially in the first 3 years.

Furthermore, the data analysis in Chapter 5 shows that, based on the JarKus measurements, there is no clear indication that initial transport is cross-shore dominated (Figure 5.8). The same holds for the SC5 simulation, which at times exhibits similar variability in the Dean Ratio (See Appendix A.7). This

might suggest that cross-shore dominance in the initial years was less significant at the HBD site. So, this may indicate a growing potential for applying one-line shoreline models at the HBD site.

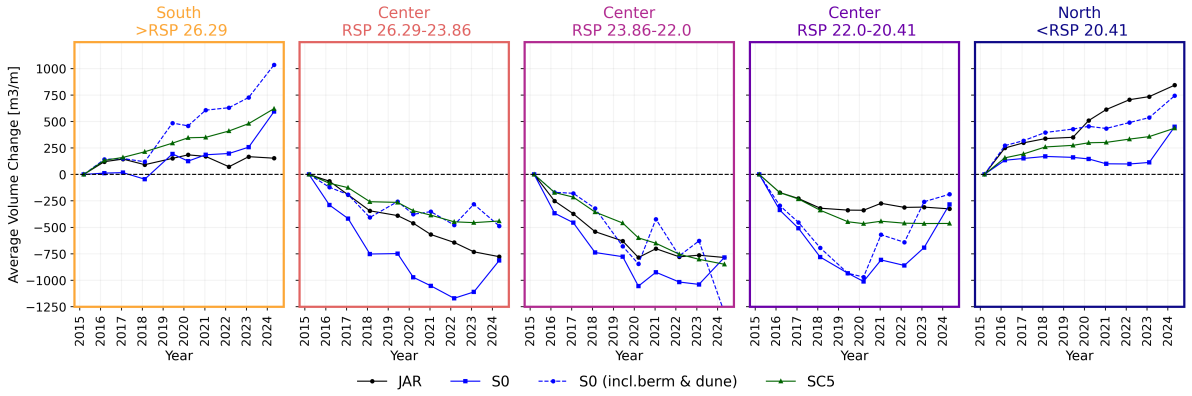

Figure 7.2: Volumetric change simulations over time in the period 2015-2024. From left to right indicate the South to North subsections defined in 5.

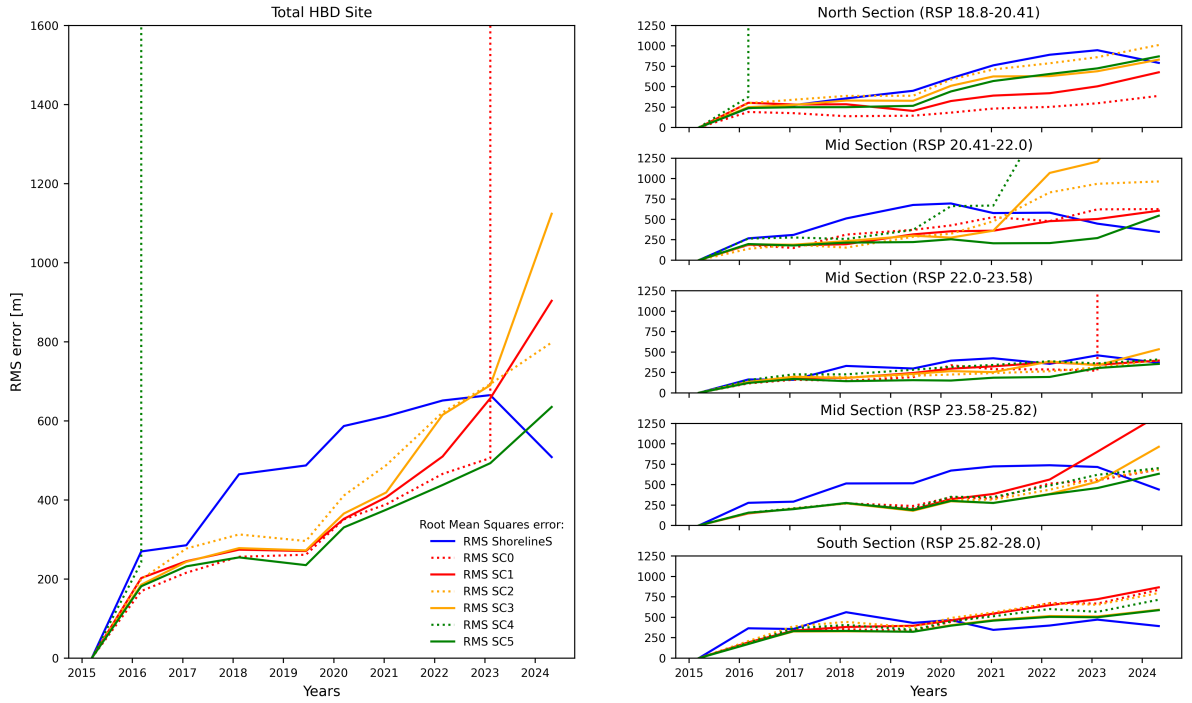

Figure 7.3: Root Mean Squares (RMS) Error evolution Volumetric change simulations over the period 2015-2024. On the right, the error development for the different zones is shown.

7.1.3. Volumetric Evolution of Vertical Cells

To gain better insight into the volumetric changes, the evolution of different subaqueous cells are examined. The results are presented in Figure 7.4, which shows the volumetric changes over the first three years for the surfzone (left) and the shoreface (right).

Surfzone Volume

The evolution of volume changes in the surfzone closely follows the pattern of the total volume shown in Figure 7.1. Both ShorelineS and the coupled model exhibit similar patterns that align well with the measured data, but the magnitude of morphological activity for SC5 is lower than the measurements. In contrast, the ShorelineS results correspond closely to the observed data. This is what was expected

based on the data analysis results (Figure 5.7), the shoreline changes and surfzone volume changes have shown to be strongly correlated ($r^2 = 0.90$).

Shoreface Volume

In contrast with the surfzone, the shoreface volume changes in the right-hand panel show a different trend, both in magnitude and alongshore variation. Although the total volume change identifies the region between RSP 23.88 and 26.2 as the most erosive area (Figure 7.1), the JarKus data indicate that in this zone, even shoreface accretion sometimes occurs. Consequently, ShorelineS aligns less accurately with the measurements in this region. This is also what was found in the data analysis in Chapter 5, where the correlation between the shoreline change and shoreface volume change is also shown weaker ($r^2 = 0.65$).

Differing from contrast to ShorelineS, the coupled model displays a different shoreface volume change pattern compared to its the surf zone representation. The coupled simulations show a more evenly distributed pattern along the coast, with a tendency toward accretion. While the magnitude of this volume change appears realistic, the JarKus measurements indicate erosion rather than accretion, implying a mismatch in the modeled volume behavior.

Implications of different simulations for Volumecells

The different coupled model simulations (SC0-SC5) reveal notable mutual differences that depend on the grid configuration that is used. A straight grid (red lines) has a larger horizontal offset between the initial and equilibrium grid in the central region of the Hondsbossche Dunes. This grid setting produces the least erosive behavior in the central area for the surfzone, and the most accretion at the shoreface. This denotes that the grid and model set-up adjustments towards SC5 have shown clear improvements.

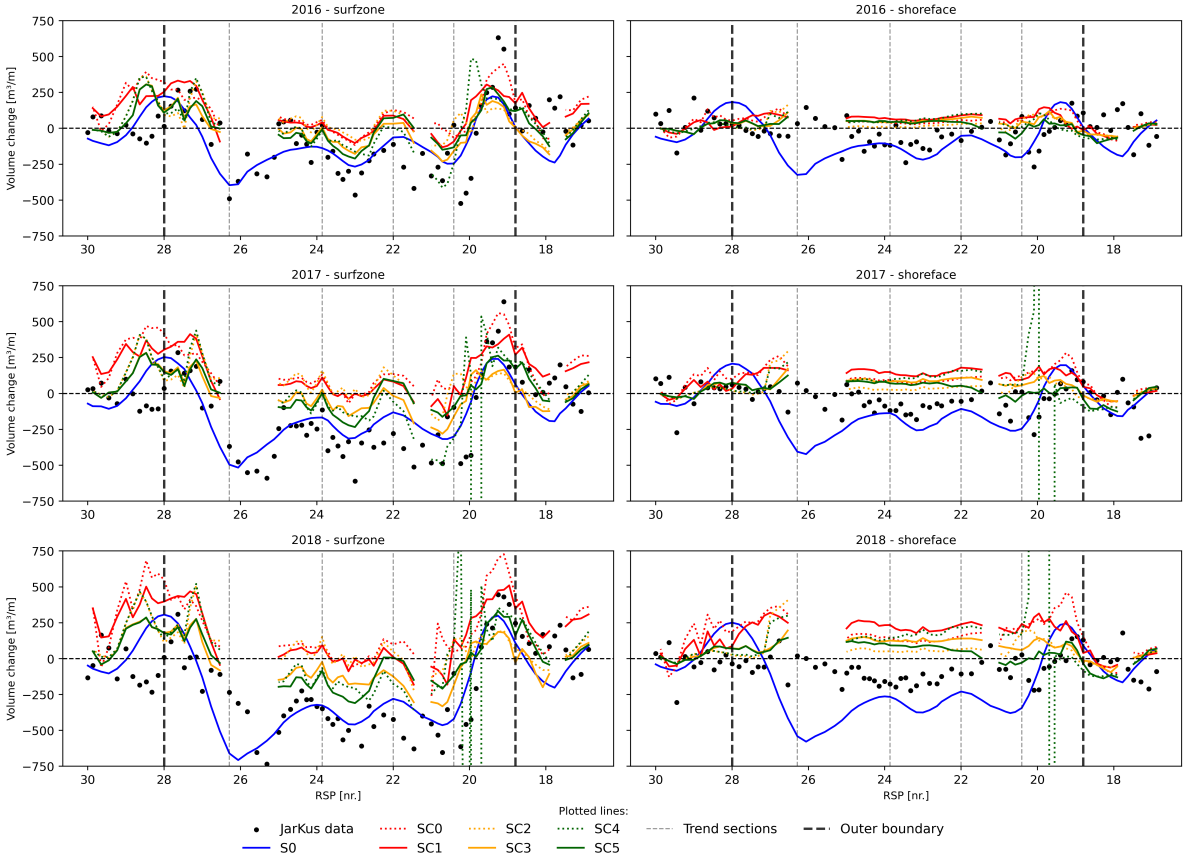

Figure 7.4: Model output results of vertical volumetric cell change over the period 2015-2018; the left figure shows the surfzone volume change and the right figure shows the shoreface volume change. An overview of all simulation years can be found in Appendix A.2 (surfzone) and Appendix A.3 (Shoreface).

Discussion on Subaerial Volume Changes

The SC5 simulation also changes subaerial areas of cross-shore profiles. The subaqueous and subaerial changes add up to the total volume change of SC5. The subaqueous changes are underpredicted consistently; however, the total SC5 volume is shown to be quite accurate. This means that the subaerial volume changes are likely an overestimation of reality. It suggests that the model possibly compensates for the lack of subaqueous erosion (Figure 7.4) by accounting for sediment erosion above the waterline.

This alongshore sediment balance is demonstrated in Figure 7.5. The green solid line presents the total volume change of SC5, just as shown in Figure 7.1. The striped green line indicates the subaqueous volume changes (surfzone and shoreface). The difference between these lines is covered by the subaerial changes shown in the green dotted line. It shows that the subaqueous changes are relatively small and the subaerial changes relatively large, and that this balance is not in the right proportion yet.

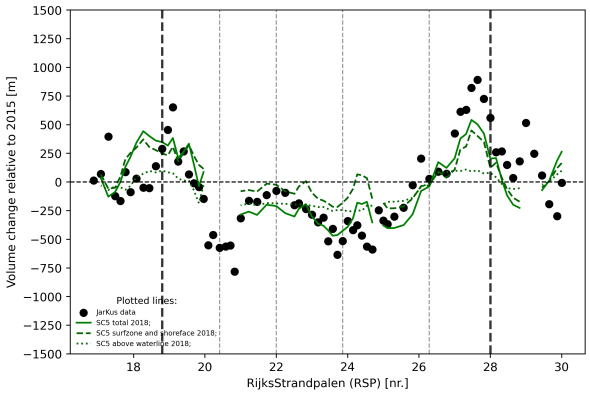

Figure 7.5: Subaerial and subaqueous volume elements of the model simulation SC5 compared to the total volume.

7.2. Results of Beach Width Evolution

Beach width is a key coastal indicator, important for both ecological development and recreation. It is defined as the distance between the shoreline and the dune foot, which can each change independently. To better understand beach width, first, the separate developments of the shoreline and dune foot are examined.

7.2.1. Shoreline and Dunefoot Evolution

Shoreline Evolution

Figure 7.6 shows that ShorelineS run (S0) produces the most accurate changes in shoreline position compared to the JarKus measurements. This is also reflected in the RMS error shown below in Figure 7.6. After the first 3 years, the average error of the coupled model is nearly 50 meters, whereas the error of ShorelineS is only about 30 meters. In the years following 2019, the average error for S0 and SC5 became more equal. In the first year, the coupled model SC5 lies 30 to 50 meters below the S0 simulation, which is conserved for the following years. This means that within the first 3 to 5 years, the erosive center section has a larger coastline retreat, but north and south show a smaller coastline extent than S0.

So both models show a fairly accurate shoreline evolution with an average error of about 50 meters after 8 years of simulation, but the ShorelineS model better grasps the description of the measurements, as it exhibits a lower degree of shoreline retreat.

Dune Evolution

The dune foot development during the initial years shows very similar results for ShorelineS and SC5 (Figure 7.6). In years beyond 2020, the dune foot retreat in SC5 is slightly less pronounced than in ShorelineS, bringing it closer to the measurements. This is also reflected in the development of the RMS error shown below in Figure 7.6. In the center section, both models overestimate the dune foot progradation observed in the measurements, varying between 20 to 50 meters in the first 3 years.

This also occurs in the north and south in the southern zone (RSP 26.0 and 27.0), where the model predicts substantial dune growth. A similar peak is visible in the north (RSP 20.0), but here the dunefoot expansion is underpredicted. Both locations lie in the transition zones from the former sea defense dam to the adjacent coast.

The dunefoot expansion of SC5 is a little lower than ShorelineS from 2018 onward. The reason for this might be that the shoreline position of SC5 is further landward, resulting in a smaller dry beach width than S0. This dry beach width works as a driver for the dune growth formulation in the dune module (Ch. 3.2.2).

So the dunefoot migration is very simular for both simulations, but over time the small difference becomes more pronounced, resulting in a lower error for SC5.

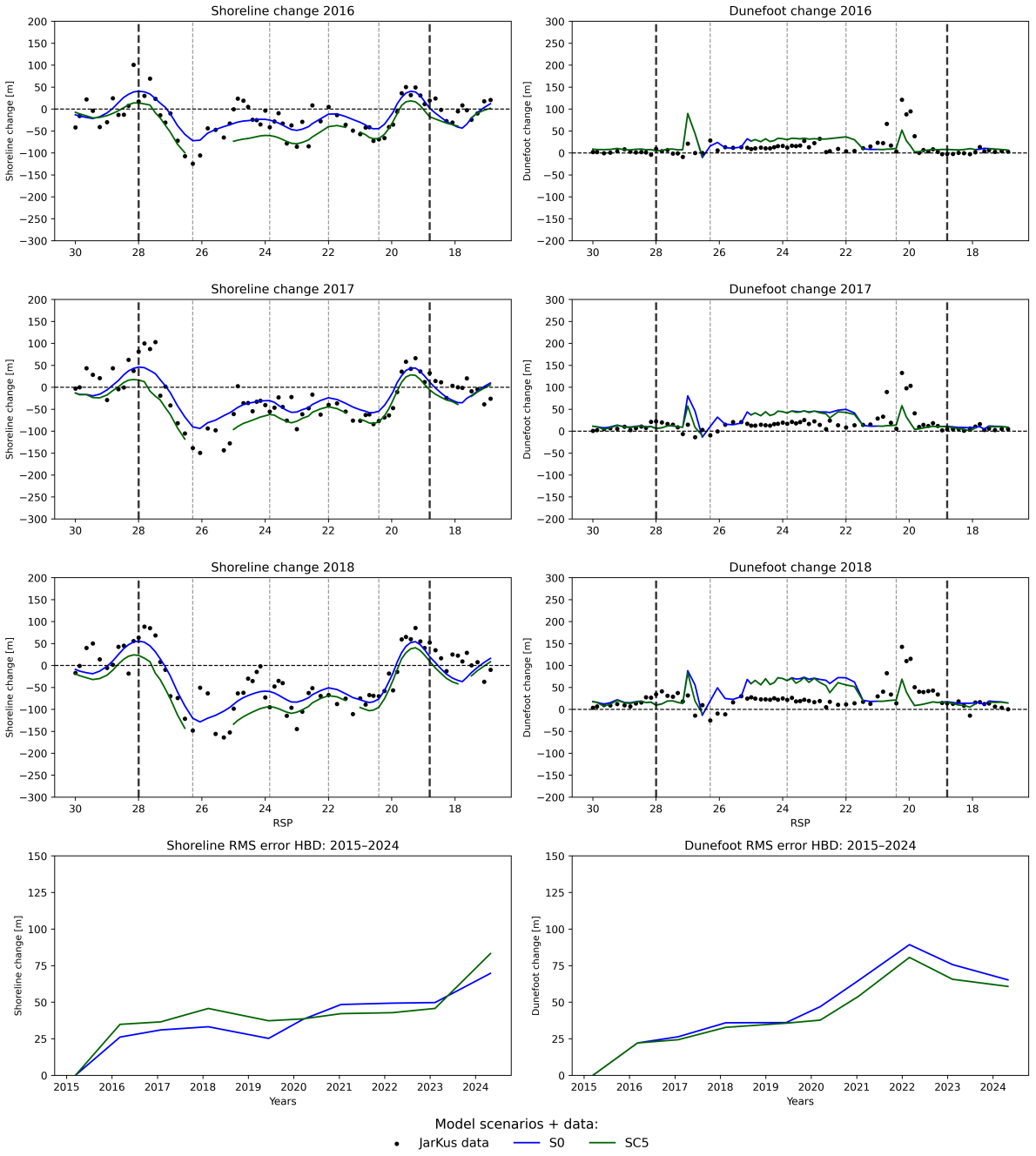

Figure 7.6: Model output results of shoreline and dune foot change over the period 2015-2024. An overview of all simulation years can be found in Appendix A.4 (shoreline) and Appendix A.5 (dunefoot).

7.2.2. Beach Width Evolution

Beach width is a key indicator that is intended to be fully modeled. Therefore, the absolute quantitative evolution of beach width is considered here, rather than its relative change as done previously. As shown in Figure 7.7, beach width varies significantly along the coast. In particular, large widths are found in transition zones between the old sea dike and the existing beach, as well as in the southern central segment (RSP 20.0, 25.0, 27.0), where beach widths exceed 400 meters in some locations. The peaks between RSP 26 and 27 are the result of artificial dune segments with spacing, located in front of the newly constructed freshwater source in the south.

The ShorelineS simulation provides a very accurate representation of the beach width, outperforming the coupled model. Only in the southern central segment (RSP 24–26) does it underestimate the width, as the shoreline position is more landward in this area, see Figure 7.6.

The coupled model also provides a good indication of beach width but is less accurate during the first three years. This is mainly due to the shoreline position of SC5, which lies 30-50 meters landward relative to S0 (Figure 7.6). After this period, as the beach width becomes more stable and adjusts to the surrounding beach segments, the error decreases and SC5 becomes nearly identical to S0.

In 2022, the simulations and measurements indicate an almost stable beach, with widths ranging between 100 and 150 meters. However, in 2024, the simulations show diverging results, with an irregular increase in beach width alongshore. This may suggest a model instability, or it could be the result of extreme events. Figure 7.8 also shows an increased error for all simulations in the final two years.

So, the beach width is well simulated for both models. The ShorelineS model output is slightly more accurate due to the precise shoreline simulation (Figure 7.6), especially in the region from RSP 28.0 and 22.0. This is also reflected in the RMS error development for the different zones in Figure 7.8.

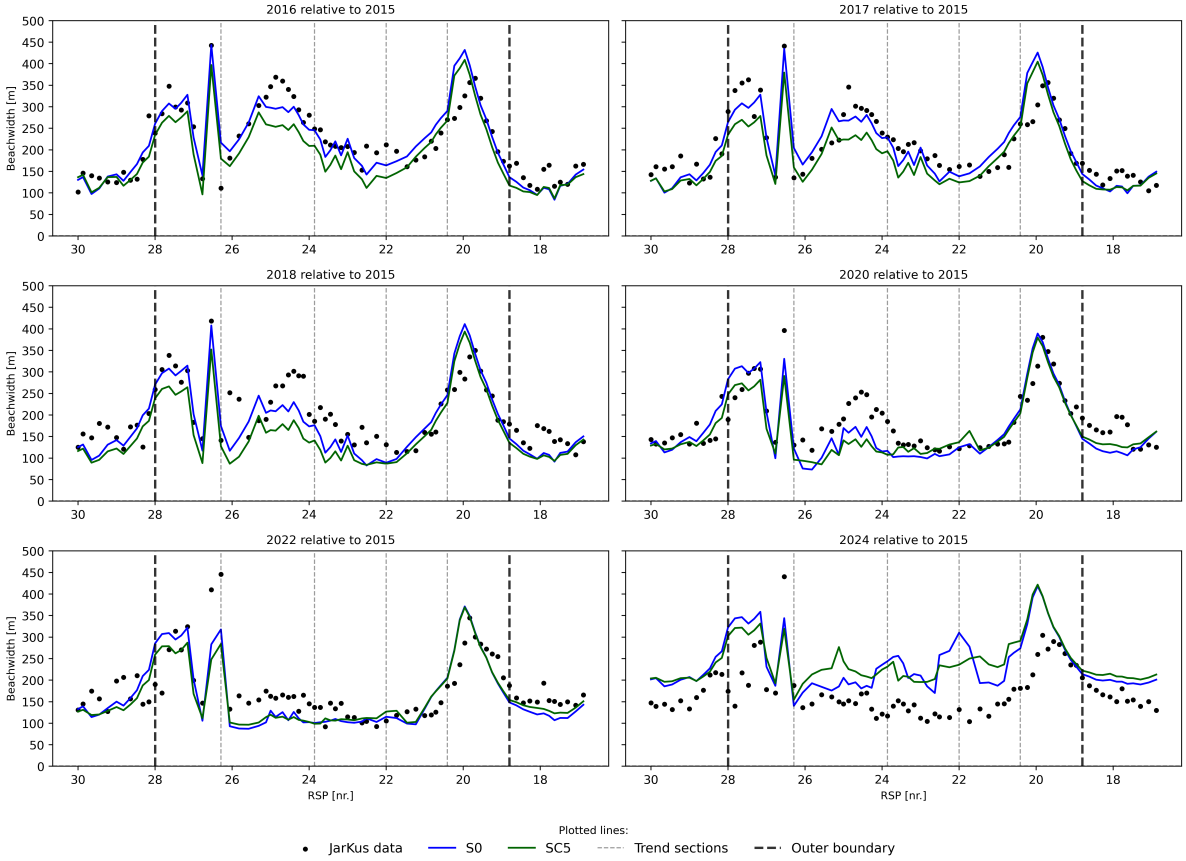

Figure 7.7: Model output results of beachwidth over the period 2015-2024. An overview of all simulation years can be found in Appendix A.6.

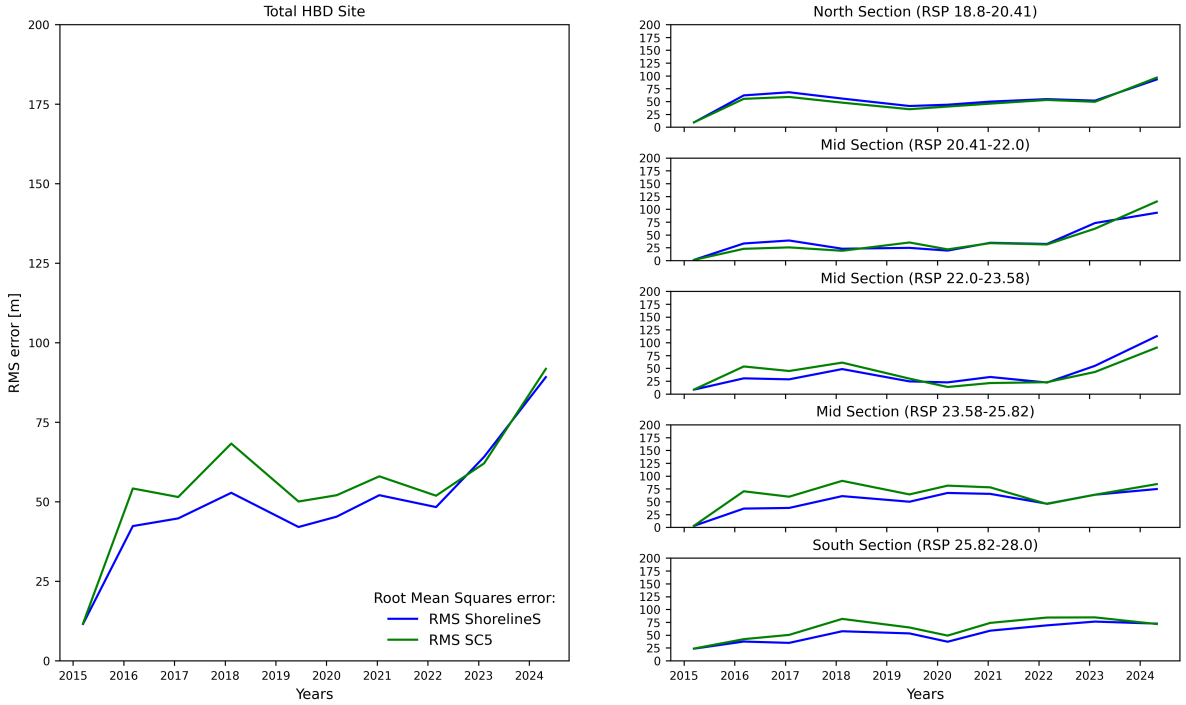

Figure 7.8: Root Mean Squares (RMS) Error evolution Beach Width simulations. On the richt, the error development for the different zones are shown.

7.3. Profile Development Results

Building on the analysis of volume and beach width, this section examines how depth contours and cross-shore profiles evolve over time. Unlike ShorelineS, which assumes a fixed profile shape, the SC5 simulation with Crocodile adds depth-dependent dynamics. Comparing these helps assess the added value of the coupled model.

7.3.1. Development of depth contours

Five stable transects were selected across the nourishment zones (Figure 7.9), with the evolution of several depth contours shown in Figure 7.10. These include the dunefoot (+3 m+NAP), shoreline (0 m+NAP), breaker zone (-4 m and -5.5 m+NAP), and the lower shoreface (-8.5 m+NAP) near the depth of closure. The y-axis represents the cross-shore position relative to the shoreline, and the x-axis spans the years 2015 to 2024. The Markers indicate the measurements from the JarKus dataset, while the blue and green lines represent corresponding simulations of ShorelineS (S0) and the coupled model (SC5), respectively.

Subaerial Contour Results

Both models generally reproduce the measured dunefoot and shoreline evolution well. In the central zone (RSP 25.0, 23.17, 20.71), however, a contrasting trend is observed: while the dunefoot progrades, the shoreline retreats—indicating beach narrowing. This was also observed in paragraph 7.2.2 and the data analysis in Ch. 5 where it was shown that dunevolume increased indepenently of shoreline changes.

In the northern and southern transects (RSP 28.0 and 19.1), a clear progradational trend is present. ShorelineS tends to slightly over- (RSP 28.0, 20.71, and 19.1) or underestimate (RSP 25.0 and 23.17) dunefoot progradation. Also signs of dune erosion are captured in both models. Notably at transect RSP 23.17 and 25.0 around 2022 a discrete-like landward shift of the dune foot is visible, which indicates dune erosion during a storm event.

Subaqueous Contour Results

A key difference appears in the shoreface dynamics. ShorelineS links all depth contours directly to shoreline movement, which results in significant errors in shoreface contours, especially where the shoreline retreats but deeper contours remain stable or even prograde. The coupled model, on the other hand, shows a progradational trend for the shoreface. Although not always completely accurate, the model better represents shoreface behavior in general sense, particularly at RSP 20.71.

The assumption of a uniform cross-shore distribution in ShorelineS appears more representative in the northern and southern transects, where almost all depth contours show a progradational trend similar in magnitude to the shoreline. However, in erosive areas, where the shoreline often retreats, a one-line assumption is less evident, and the benefits of Crocodile become visible.

Both models struggle to represent conditions in dynamic areas, especially near wave breaking at -4 m and -5.5 m+NAP. However, these equilibrium-based models are not designed to capture such features.

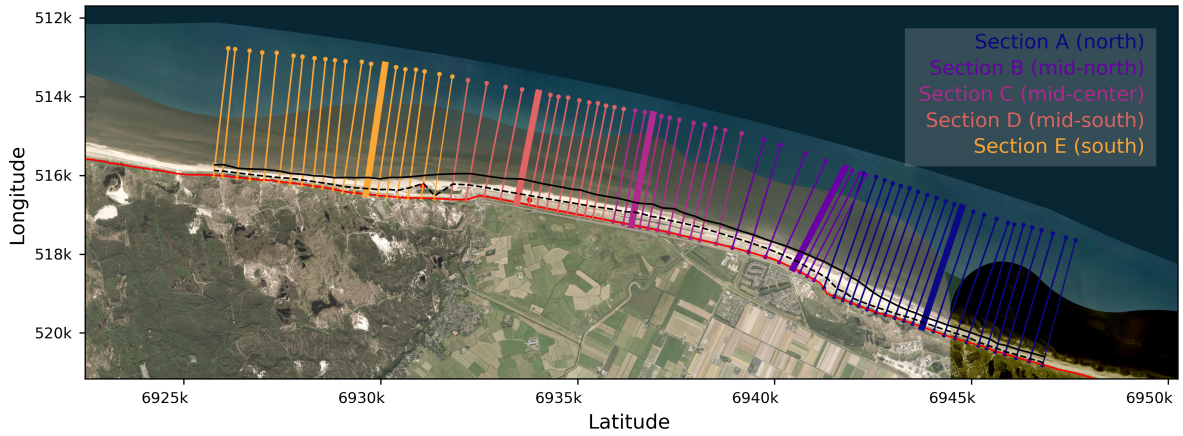

Figure 7.9: Aerial map of the selected profiles for the model analysis. In every zone a transect is selected.

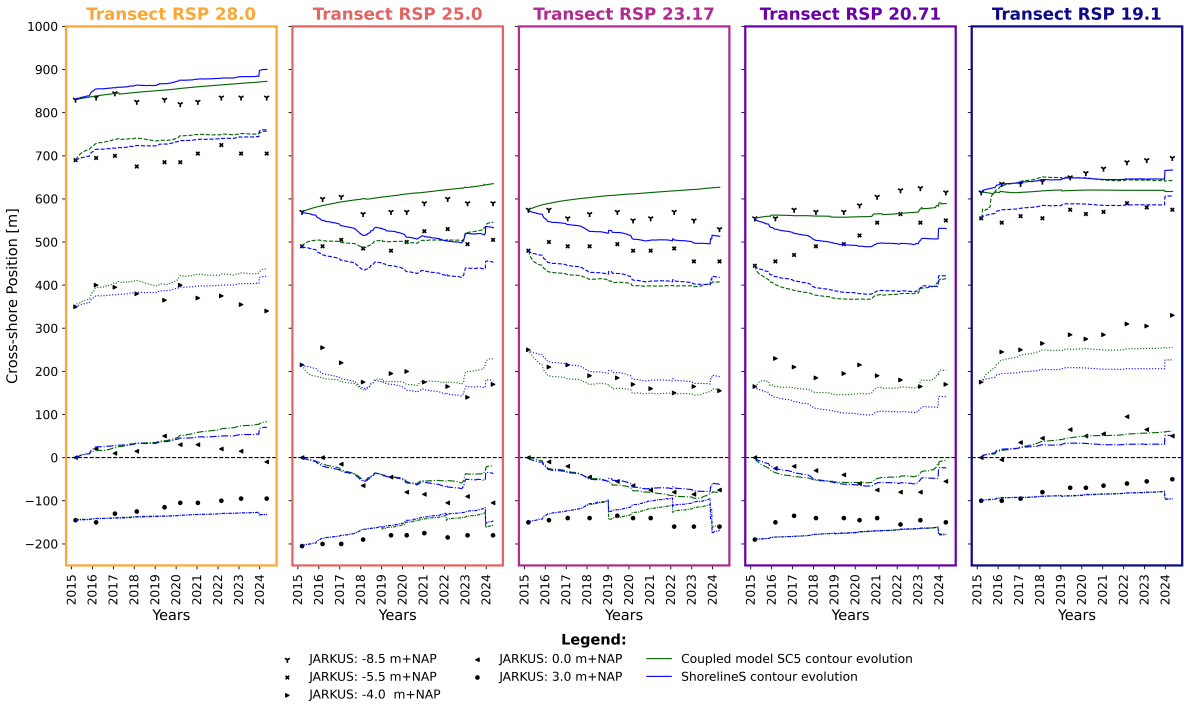

Figure 7.10: Corresponding depth contour development of the selected profiles; RSP 28.0, 25.0, 23.17, 20.71, 19.1.

7.3.2. Cross-shore Profile Development

The depth contour results depend on how the cross-shore profile evolves. To illustrate this, Figure 7.11 shows where volume changes occur in the profiles during simulations, how these influence depth contours, and how they compare to measured profiles.

Each row depicts one transect's evolution. The first column displays Jarkus profiles from 2015 to 2022, representing the stable phase of the SC5 simulation. The second column shows the coupled model's evolution over the same period, while the third shows ShorelineS results.

In the first column, profiles from 2015 (black), 2019 (purple), and 2022 (pink) reveal that transects 19.25 and 28.0 prograde seaward, while the central profiles retreat landward—consistent with coastal indicators.

The second column displays the evolution of the coupled model, from the starting year (shown in green) to 2022 (shown in pink). For reference, the initial and final Jarkus profiles are included as black and red dashed lines, respectively. Also here, a seaward progradation is observed for profiles 19.25 and 28.0, and a landward retreat for the central profiles. However, the most significant changes occur in the upper part of the profile (>-5.5 m+NAP), much of which lies above the shoreline.

The figure also shows that the shoreline is well reproduced by both the coupled model and ShorelineS. In the coupled model, this is achieved through substantial volume erosion above the waterline in the case of a retreating coast, and substantial accretion above the waterline for a prograding coast. This is because the coastal profile tends to adjust toward an equilibrium shape, which is steeper near the dunes and flatter at the beach. However, the simulated subaerial volume gains and losses appear much larger than the changes observed in the measurements.

Lower in the profile, around the shoreface, a progradational trend is visible for the transects in the central zone. Here, the shoreface simulated by the coupled model gains substantial volume, while in the JarKus data the shoreface remains relatively stable or even erodes. This distinction is also noticeable in Figure 7.4. Therefore, changes in the outer sandbar are not always accurately captured. Nevertheless, due to the alongshore-varying profile implemented in simulation SC5, a reasonably accurate fit is observed in the lower shoreface region (<-10 m+NAP), which is not the case for ShorelineS.

Because ShorelineS assumes an alongshore-uniform profile, at certain locations along the Hondsbossche Dunes, the lower shoreface (<-10 m+NAP) cannot be accurately reproduced. This is evident in transects 19.25 to 25.12, where a substantial mismatch occurs between 600 m and 1000 m offshore when compared to the Jarkus profiles, whereas transect 28.0 shows a good match. This emphasizes the strongly varying profile shapes at this site. Additionally, the volumes associated with shoreface changes do not always appear to be consistent. The shoreface does not simply scale with the position of the shoreline, but instead becomes steeper, flatter, higher, or lower, indicating a more complex adjustment than a simple translational movement.

Despite this, the growing and eroding patterns of the surf zone volumes in ShorelineS, as seen in Figure 7.4, show a similar shape to those in the Jarkus data. From Figure 7.11, it appears that in this zone, the Jarkus profiles indeed exhibit a largely translational movement over the years, directly proportional with the shifting shoreline. This pattern closely resembles the displacement applied in ShorelineS, resulting in a good match in this region.

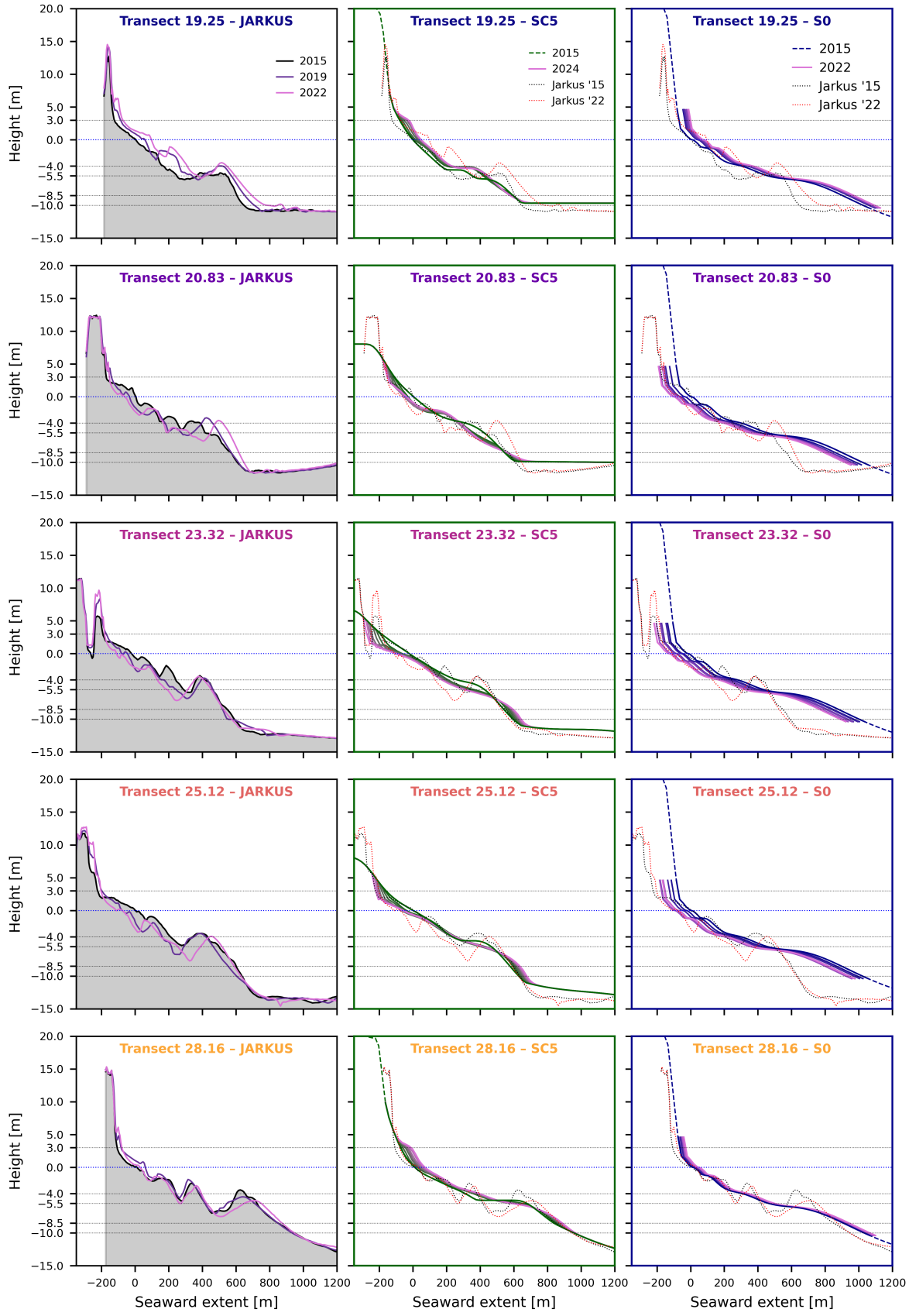

Figure 7.11: Profile development plot of the different transects (rows) for the JarKus data, coupled model and ShorelineS (columns.

8

Discussion

In this chapter, we discuss the performance, added value, and limitations of the ShorelineS and ShorelineS+Crocodile models. The focus is on evaluating ShorelineS and the coupled model, with special attention given to their behavior in the case study of the Hondsbossche Dunes. The results are interpreted in relation to the model setup, site-specific conditions, and the underlying model assumptions.

8.1. ShorelineS Performance and Limitations

ShorelineS Calibration and Shoreline Simulation

ShorelineS is a model that simulates the shoreline. The representation of the shoreline is very accurate, especially during the first 4 to 5 years. In 2019, the model had an average error of only 25 meters, compared to 40 meters for SC5. Although this shoreline is accurate, the ShorelineS model used a volume-based calibration approach with measurements up to 2020. This approach sustains a more robust model situation, as the shoreline might give an unrealistic image of the actual profile. Despite this volume calibration of ShorelineS, the total volume results of Figure 7.1 are not always very well represented, for example, from 2018 to 2020 (Figure 7.1). A reason for this might be that the volume definition used in the comparison with the coupled model (see Ch.4.2) is different from the definition used in the calibration.

For this study, the simulation period was extended by 4 years. In the years following 2020, the error increased to nearly 75 meters by 2024, which is three times as much than over the first 5 years in shoreline change error. A new calibration for the year 2024 would likely have improved the performance of the ShorelineS results on all coastal indicators.

During these remaining 4 years, four new maintenance nourishments were carried out in addition to the beach nourishment of 2018. This included two beach nourishments and two shoreface nourishments, see Table 5.1. In total, approximately 2.5 Mm^3 of sand were added to the coast. Such a sequence of maintenance interventions can also negatively affect the model results if successive nourishment activity are not accounted for in the calibration. In addition, the empirical formulation and underlying assumptions in the nourishment module are rather simplified, meaning that more nourishments induce higher uncertainty.

Previous research has shown that the inclusion of the dune module significantly improves the shoreline predictions [71]. This research demonstrates that the simulation of the dunefoot allows for a reliable global estimate of beach width. The results show that ShorelineS can simulate beach width over the first 7 years with a stable average error of around 50 meters.

ShorelineS Subaerial Simulation

For one-line models, volume estimates are entirely dependent on the shoreline development. Limitations become apparent when changes in shoreline position do not correspond proportionally to volume changes at certain depths, which becomes evident at the shoreface. The alongshore shoreline change shape (Figure 7.4 (right)) shows that up to 2018 there is little similarity to the shoreface evolution shape

of the JarKus data; the shoreface gradually erodes in similar magnitude and direction alongshore (between 0 and -250 m^3/m), but ShorelineS shows high alongshore variation at for example RSP 26.0 (erosion up to -500 m^3/m) and RSP 28.0 (accretion up to 250 m^3/m).

This also applies to evolution of shoreface contour lines in the erosive middle section. A mega-nourishment is often constructed with a steeper slope than its equilibrium state, which can cause sediment to move towards deeper waters in the initial years [10, 69]. This can result in an outbuilding trend. In line with the shoreline retreat at this section, one-line models will always show a landward trend here, leading to a consistent error between 30 and 80m for transects RSP 25.0, 23.27, and 20.71 in 2024 (Figure 7.10).

So further offshore, ShorelineS shows to be limited in representing coastal evolution at locations where morphological activity is lower; it has a deceased correlation to the shoreline evolution moving offshore (Ch.5.3).

8.2. Coupled Model Performance, Added Value and Limitations

8.2.1. Model Instabilities

Instabilities due to Horizontal Gradients

As mentioned in Ch.7.1.1, several Crocodile profiles at JarKus transects were deliberately left out of the coupled simulations in advance. Despite these precautionary measures, not all instabilities were solved. Several strategies have been implemented to overcome the instabilities. For example, halving the numerical timestep to 0.5 day, but it did not stabilize the simulation output. Similarly, adjustments to the grid smoothing coefficient did not reduce instability. Lower smoothing provides more detail in some locations but also leads to more extreme outliers in the results. Higher smoothing worsens performance without improving stability.

To investigate the cause of the instabilities in more depth, the drivers behind the profile changes were examined. Equation 3.2 contains several terms, each contributing differently to the profile adaptation. Figure 8.1 shows the temporal evolution of the diffusion term (b) (purple striped) and erosion term (c) (orange striped), who are the most important contributors. The diffusion term drives adaptation toward the equilibrium profile, and the erosion term accounts for the longshore transport. The diffusion term contains a gradient component, $\frac{d(Z-Z_{eq})}{dx}$, which represents the difference between the slope from two points in the cross-shore direction (dx) of the initial profile relative to the equilibrium profile (red).

The instability is likely related to a large difference in the slope between the initial profile (blue) and the equilibrium profile (black striped). The initial profile attempts to evolve toward the equilibrium profile, but if they cannot get to a similar slope due to large profile differences and activity restrictions by the depth-dependent diffusion coefficient (Figure 3.2), a persistent gradient arises that increases over time. This causes local amplifications in profile change, leading to the development of wiggles. These are then translated into larger gradient differences, which in turn exacerbate the instability and result in extreme values.

When such an unstable profile is compared to a transect location with a stable profile, it becomes visible that the equilibrium profile of the unstable case is not correctly configured; the equilibrium profile lies too low and becomes horizontal (-200m in Figure 8.1). This is likely due to the translation from the equilibrium grid to the dynamic equilibrium profile at a selected transect location during the simulation process. The reason for this is still unclear. This suggests that there is room for improvement to find the issue in the translational process to achieve more stable results.

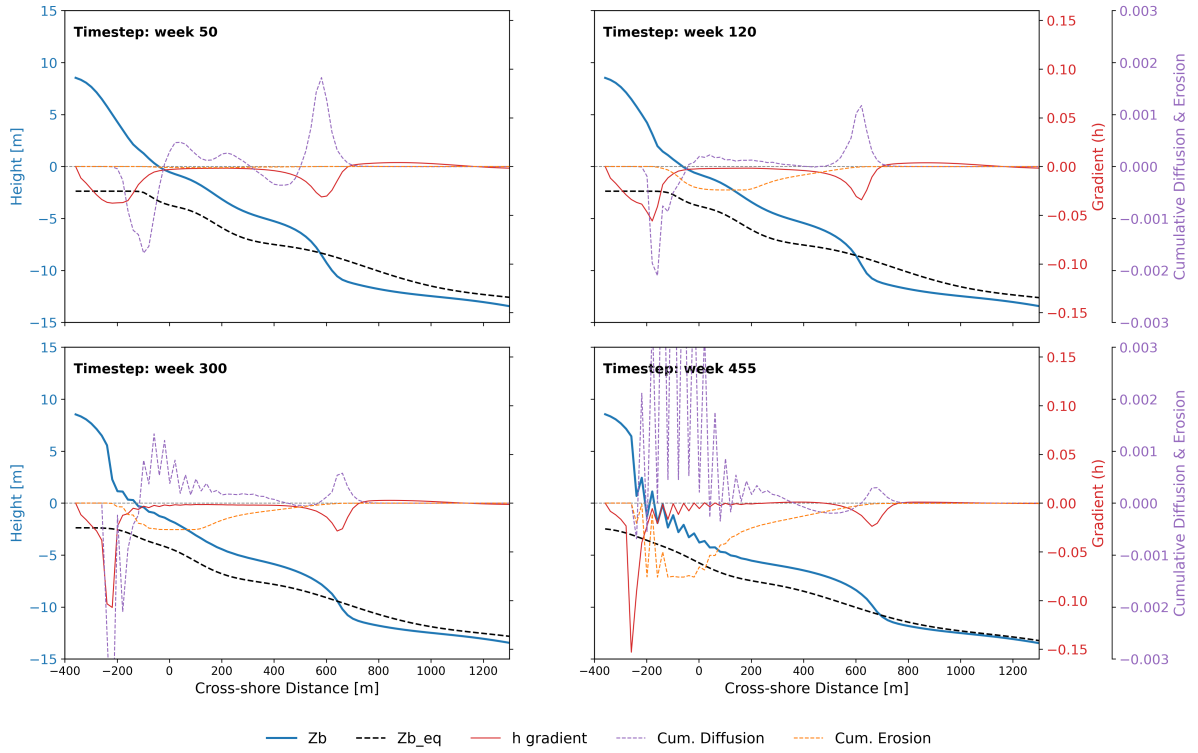

Figure 8.1: Error evolution of unstability at transect RSP 26.29. The plot shows the changing initial (blue) and equilibrium (black dashed) profile. The gradient (red) is the driver for the diffusion term (purple), and the momentary erosion term is shown in orange. At timestep 120weeks a concentration of diffusion is obtained near -200m. The beach get milder and the dune steeper, because beyond -200m the profile is not able to adapt to the equilibrium profile. This is due to the poorly defined equilibrium profile beyond -200m in combination with a height depended activity diffusion term.

Instabilities due to Model Set-up

Besides SC5, all other simulation runs that used different model inputs and configuration settings, encountered more severe instabilities. These showed to remain stable for a shorter period and generally yield less extreme results. The most stable simulation is SC5, which contains a curved equilibrium grid, an alongshore-varying equilibrium profile, and a dynamic equilibrium. For a given Crocodile profile in a simulation with all these added components, the equilibrium profile is situated closest to the initial profile. The horizontal distance between the initial and equilibrium profile decreases for every component taken into account for the simulation. This distance matters, as the initial profile aims to vertically match the slope of the equilibrium profile (Ch. 3.3). So, the larger the horizontal distance, the greater the slope difference, the greater and faster the profile adjustments become. Excessive slope differences may trigger instabilities by initiating extreme profile developments, as was already mentioned above. This again highlights the importance of the equilibrium profile, which derives from the equilibrium grid. Thus, it matters how the equilibrium grid set-up is defined for stability likelihood.

As mentioned, the first three years still showed stable model output for almost all simulations. Also, quite some transects of the SC5 run kept a stable simulation performance over the complete nine-years, like the profiles discussed in 7.3. However, some transect locations proved to be sensitive when a Crocodile profile was defined, also affecting nearby transects. As a precaution, no crocodile profile has been defined at these locations (see discontinuous lines in Figure 7.1). The shoreline displacement at these locations is based on linear interpolation of nearby grid points. Therefore, the discussion below will be based on the results of these stable time ranges and transects.

8.2.2. Model Performance

Performance of SC5 Simulation

In the stable areas, the coupled model SC5 does show improvements in the model performance relative to ShorelineS. The SC5 model configuration consists of a curved and alongshore varying equilibrium

grid, and a dynamic equilibrium grid. Its improved performance is mainly notable for the (total) volumetric evolution, subaqueous depth contours, and profile development for the first five stable years.

From the results in Chapter 7, it is mentioned that, in the erosive center zone (RSP 20.42-25.82), the SC5 simulation more than doubled the accuracy relative to the S0 simulation in 2019. Figure 7.2 then averaged the volumetric changes in groups for similar different coastal zones, and illustrated that its evolution over time indicates similar results. The SC5 simulation follows similar patterns to the JarKus data; for the center zones, a faster retreat in the initial years, but thereafter it stabilizes a bit more. S0 shows a faster retreat in the initial years; however, the S0 simulation, including the dunes and beach, has a similar erosion rate. This may support the idea from the Dean Ratio that, during the initial years, cross-shore dominance is not clearly present.

Also, the profile and offshore contour development show more realistic behavior with SC5. This mainly comes clear at depths where the morphological activity is lower, for example, near the shoreface, where at least an independent trend is shown from the shoreline movements.

Although some promising model output, the coupled model is not recalibrated for the inclusion of Crocodile. It just enhanced the calibrated model set-up of ShorelineS. This suggests that there might be some extra room for improvement. However, changing ShorelineS parameters like, for example, the q-scale parameter (Ch.3.2) only scales the longshore transport flux, but does not influence the evolution trend.

Comparison Definition of Models

Despite the apparent improvement in terms of volumetric change, it is important to add a critical note regarding the definition of the comparison as presented in the results.

The comparison of the simulations presents a complicated picture of reality. The shoreline change represented in ShorelineS primarily reflects underwater changes, since the volume calculation is based on shoreline position change multiplied by the Depth of Closure (DoC). In SC5 and the other coupled models, this is more complex. Changes can occur in the coastal profile between the DoC and +5 m above NAP, due to the diffusion coefficient in Crocodile, which governs the cross-shore redistribution of the longshore sediment flux and the adjustment of the profile toward its equilibrium.

In the results analysis, volume changes in the dune and beach were not included for either model. These would originate and calculated from dune interactions in the dune module—specifically, dune erosion (via wave run-up) and dune growth (via aeolian transport).

However, it is reasonable to assume that subaerial volume changes in SC5 would influence dune and beach erosion or growth. At this stage, the coupled model has not yet been developed to the extent that such feedback is integrated into the dune module functionality within ShorelineS. If additional beach and dune volume changes from the dune module had been included for both ShorelineS and the coupled model in the results analysis, this would have led to the coupled model accounting for multiple times the amount of subaerial change. This would provide a very unrealistic image of the subaerial dynamics.

This comparison would in any case result in a skewed comparison in the results analysis, at this stage. This highlights that the plots alone do not tell the full story. Nevertheless, they do indicate that in the ShorelineS configuration has a consistently too strong erosive behavior in the central sections (Figure 7.2). Here, at least interaction with the beach and dunes show that this overestimate is counteracted and show more realistic changes over time at some places. However, the influence of dune module also shows that it is not yet in the right portion. Further it can be concluded is that simulation SC5 provides a promising approach in reproducing the temporal distribution of coastal changes.

Performance Improvements

The simulation SC0 with a basic straight spatial varying equilibrium grid definition significantly overestimates shoreline retreat, with an average error of more than 100 meters after just three years. This highly erosive coastline results in a reduction in dry beach width, which impacts dune growth within the dune module. Since both the shoreline and dunefoot retreated, the beach width is still represented relatively well. This strong shoreline retreat erodes a significant amount of volume above the waterline. Meanwhile, the model seems to compensate for total volume balance by strongly underestimating

erosion in the surf zone and shoreface. In fact, the shoreface even shows accretion in these simulations. So, the total volume change of this simulation looks decent at first sight, but in reality, the volume change is unrealistically distributed over the profile. So it is necessary to analyse the building blocks of the coastal indicators.

The results demonstrate that by adapting the equilibrium coastline shape of the equilibrium grid from straight to a curved body, the performance is significantly improved. This improvement is visible in the shoreline and dunefoot representation, as well as in the various vertical volume layers. This improvement becomes especially evident in the central section of the HBD where the difference in horizontal distance between the initial and equilibrium profile of the straight grid (SC0 & SC1) and curved equilibrium grid (SC2 & SC3, SC4 & SC5) is the greatest (RSP 23.0, see Figure 6.5).

A further improvement is gained when the curved grid includes an alongshore-varying equilibrium profile (SC4 & SC5). Especially in the three central zones, these simulations show smaller error growth for all coastal indicators. Interestingly, in the southern part where the equilibrium profiles for both grids are equal, the results are similar. But once the equilibrium profile begins to vary alongshore (from RSP 26.0 northward), this new grid configuration performs better.

The same applies to the use of a dynamic equilibrium. In all simulations, the use of dynamic equilibrium improves results compared to the static case. Several elements were activated to define a dynamic equilibrium. It is expected that the most significant adjustments come from the seaward shift caused by the additional volume of the mega-nourishment placed on top of the static profile. This further reduces the horizontal distance between the equilibrium grid and the initial profile in the central part of the HBD. As a result, simulation SC5 shows a realistic shoreline evolution.

The results indicate that adding different equilibrium components can greatly improve the model output. The average profile error in shoreline position, for example, was reduced from 100 meters after the first three years (simulation SC0) to only 25 meters (simulation SC5). In addition to the inclusion of dynamic equilibrium and the alongshore varying profile, the definition of the equilibrium coastline shape itself turned out to be a key factor.

Interestingly, volume changes over the stable first three years are quite similar across all coupled model simulations. This is remarkable, considering the above-mentioned major differences in the other indicators: the shoreline position, shoreface volume, surfzone volume, and subaerial volume changes. The modeled output results of subaerial vertical volume layers (Figure 7.4) suggest that simulations with greater shoreline retreat lead to increasing errors between the modeled and observed volume changes in the surf zone and shoreface (<0 m+NAP). At the same time, greater shoreline retreat results in larger erosion above the waterline. These subaerial and subaqueous volume changes seem to balance each other, resulting in a relatively accurate total volume. Poorly represented volumes influence the performance of other indicators, like depth contours, with for example extreme accretion at the shoreface, while in reality, the shoreface is eroding.

It is also possible that the cross-shore diffusion coefficient of Crocodile distributes volume changes too far above the waterline. If the volume changes were more evenly distributed across the profile, changes below the waterline might become more realistic. Additionally, Crocodile only updates the shoreline but does not affect or use the dunefoot position as computed by ShorelineS. Since Crocodile is capable of simulating erosion and deposition above the waterline by run-up, it would be interesting if these volumes could be translated into changes into the dune module of ShorelineS. If the deposition and erosion above the waterline could be brought to realistic proportions, this could offer added value for the coupled model. Such as improving shoreline representation and allowing for good beach width results.

8.3. Modelling ShorelineS+Crocodile at the Hondsbossche Dunes

The Hondsbossche Dunes Case Study

The mega nourishment of the Hondsbossche Dunes was used as a case study, because an existing ShorelineS model was available. In addition, sufficient JarKus measurements were available to form a solid comparison for the simulations. The HBD also cover a large spatial scale, which makes it a good case for fast, equilibrium-based models to be applied effectively. Furthermore, it shows cross-shore

adaptation and volumetric trends that are not everywhere perfectly correlated with shoreline changes.

What makes this a challenging location for equilibrium models is its history with the old sea dike and the groynes on the northern side. The equilibrium profile south of the HBD is located at a more natural beach, where the coast can freely develop towards its equilibrium. Very different is the northern coast, where groynes constrain the cross-shore profile. Here, a nearshore shallow area exists, while in the south, the profile slopes more gradually into deeper water. The offshore bar dynamics are also behaving differently, north and south of the HBD. Before the construction of the HBD, these two coasts were separated by the presence of the old sea dike (see Chapter 5). Modelling this large project site brings together two very different coastal systems, which makes it complex to define a correct equilibrium grid. In addition, the combination of these contrasting systems and the significant change of the coastline position by the nourishment makes it even more complex to define a representative equilibrium grid.

What further complicates modelling the cross-shore contourlines and volumetric trends is the offshore sand bar evolution observed at the HBD. These bars have shown significant movement between 2015 and 2024 (Figure 5.2). The cross-shore sediment distribution in Crocodile does not capture the dynamics of such bar systems because this model operates on a long-term equilibrium basis. This makes predicting specific contour locations difficult in cross-shore areas with short morphodynamic timescales (e.g. surfzone). But even the movement of the more stable, outermost offshore bar shows complex behavior, as a result of which the shoreface contourlines are not always correctly captured by Crocodile (Figure 7.10). The movement of these offshore bars remains somewhat unpredictable and is also beyond the scope of this study, but still influences the model performance. However, what Crocodile does show well is that shoreface contour movement does not necessarily coincide with shoreline movement. Although Figure 7.10 shows that the shoreface contour evolution is not always accurate, its correlation with the shoreline change is lower than that of ShorelineS.

The results also show that the dune module overpredicts dune growth at the HBD. This is important, as it affects the representation of the beach width. A possible explanation is that the dune module only defines dune growth by seaward expansion, whereas in reality, dunes can also grow vertically. In Figure 7.10, it can be seen that in transects RSP 25.0 and 23.17 dune growth is overestimated, represented by dunefoot extension. But from Figure 7.11, it is clear from the JarKus data that in these locations the dunes mainly grow in height. This confirms a limitation of the current dune module.

In general, the coupled model distinguishes itself from a one-line model when significant profile redistribution is necessary to adhere to the equilibrium profile slope. As mentioned earlier in Chapter 5.3 and **??**, the significant cross-shore dominance in the initial years at the HBD has been less pronounced or has not been captured by the data. The slope steepness at the HBD quickly adjusted within a year to match that of the adjacent coasts. In this period, the coupled model could have been most meaningful. However, not enough data was available to model this period. In the following years, this may indicate a growing potential for applying one-line shoreline models at the HBD site. In the face of sea level rise, nourishment maintenance is required more often. This means that the coastal profile is brought out of its equilibrium more often. This favors the potential of the coupled model.

Alongshore Volumetric Asymmetry

From the JarKus data, it appears that the northern part of the Hondsbossche Dunes experienced more accretion than the southern part. Both models, ShorelineS and the coupled model, simulate a relatively equal distribution between north and south. As a result, they overestimate accretion in the south and underestimate it in the north. This becomes apparent at the results for the volumetric change. Several reasons could explain this mismatch with the data. First, as discussed before, the volume results of the simulations (especially ShorelineS) do not include volumetric changes composed by the dunemodule. However, Figure 5.4 of the Data Analysis shows that the dunegrowth is most significant in the north. This could partially solve this issue as Figure 7.2 illustrates that the inclusion of dune and beach volume in ShorelineS provides a quite precise hindcast in the north, but in other areas this accuracy is lacking.

Secondly, the effect of tidal currents is not included in the models, but only tidal water level variation is defined. Along the Dutch coast, the tidal wave moves northward. In relatively shallow water, such as the North Sea, a tidal wave can change shape, creating an unequal rise and fall in the tide. This leads to differences in the duration and strength of flood and ebb currents. This phenomenon of tidal asymmetry could, in the case of a flood-dominant current, lead to additional northward sediment transport.

ShorelineS has the option to include these tidal currents.

Furthermore, it is possible that due to the planform and bathymetric changes since the mega-nourishment implementation, the northern side has become more sheltered from wave energy. Although the wave climate is defined at many locations along the North Holland coast, the shallow zone in front of the northern HBD may have been less accurately captured in the model underlying the wave transformation table, which provided the input wave data for the simulations. Another possibility is the impact of shoreline curvature on longshore transport. The construction of the HBD introduced a significant change in the coastline, which was not included in the wave transformation model. The curvature of the coastline can locally affect the shoaling and refraction of the incoming waves. The angle at which a wave breaks at the shore determines the magnitude and direction of longshore transport.

Modelling Long-term Predictions

The simulations showcased at the HBD only ranged over a nine-year period. The models in this research, however, are intended to contribute to long-term predictions; the added value of these models lies in their ability to describe coastal evolution at a relatively low computational expense. To simulate long-term maintenance scenarios for different sea level rise scenarios, both models incorporated a sea level rise approach based on the principles of the Bruun coastal retreat rule [72]. Here, the equilibrium profile moves vertically due to the change in sea level, and is shifted landwards to balance the total volume. Crocodile is able to adjust the complete profile towards this changing equilibrium, but ShorelineS only indicates the shoreline retreat.

Long-term predictions involve several complications. One of these is the definition of the future wave climate. Since no measured wave data from the future exists, different approaches should be taken. For example, a wave climate can be constructed based on historical data, from which a randomly generated time series can be derived.

A second complication is how future nourishment projects will need to be defined. This is challenging, as nourishments implementations do not follow a fixed location or time interval. One possible approach is to study the average lifespan of nourishments along the North Holland coast and use this to define a fixed interval frequency. However, with rising sea levels, it is expected that nourishments will need to become more frequent and of larger volume [7], further complicating this approach. A more complex alternative could be to incorporate TKL assessment within the model. When the MKL drops below the critical coastal foundation level (BKL), a new nourishment is implemented. Its corresponding volume could, for example, increase or decrease based on a the interval of the previous nourishment.

A third complication for long-term studies involves the definition of the equilibrium profile and the model grid. In this study, equilibrium profiles are based on 50 years of historical data, but when making predictions over a 100-year timescale, this introduces growing uncertainty. However, before being able to make such future predictions, the stability of Crocodile as a module in ShorelineS should be fixed. Without improvements, the reliability of the results will be highly uncertain.

9

Conclusions and Recommendations

This chapter summarizes the research and presents the conclusions. First, the sub-questions are answered, followed by the main research question. The key findings of the study are then outlined, and the practical implications are discussed. The limitations encountered during the research are also addressed, leading to several recommendations for future research or development.

9.1. Answering Research Questions

9.1.1. Sub research questions

Question 1: *"How did the measured coastal state indicators evolve after the implementation of the mega-nourishment?"*

The coastal evolution at the HBD showed a clear structural spatial morphological trend. In the central zone, in front of the formal seadike, strong erosion trends were visible. The volume changed with an average loss of over 500 m^3/m over the nine-year period, with the strongest losses happening in the initial years. The shoreline retreated about 100m on average. At the same time, the northern and southern areas appeared to show accretion. The north gained significantly more volume (up to almost 2000 m^3/m) than the south, and also protruded forward. The south, however, started extending seaward, but eventually showed a coastline retreat relative to 2015. The dunes grow at an average steady rate between 20-50 $m^3/m/y$, independently of the shoreline and subaqueous volumetric changes.

Clear correlations were found between the shoreline change and the volumetric change, especially the surfzone scaled well with the shoreline ($r^2 = 0.90$). However, the shoreface and dune volume changes show a (much) smaller correlation to the shoreline ($r^2_{sf} = 0.65$ & $r^2_{dune} = 0.27$), highlighting the importance of cross-shore redistribution during the post-nourishment adaptation period.

Question 2: *"How well does ShorelineS simulate the evolution of the coastal state indicators at the Hondsbossche Dunes?"*

ShorelineS effectively simulates indicators of shoreline change and beach width during the first five years following the mega-nourishment implementation, achieving robust and efficient performance. In 2019, the average absolute shoreline error was only 25 meters. However, performance decreased in the following years, with errors reaching up to 75 meters by 2024. A new calibration including these years would have improved the performance.

This lack of performance over the four-year period could also have been influenced by a series of maintenance nourishments if it is not calibrated for. On the other hand, it is acceptable for a prediction model to yield less accurate results over a forecast period.

The model reproduces beach width with reasonable accuracy, as it simulates beach width over the first 7 years with a stable error of around 50 meters. This performance is partly due to the dune module's good representation of the dune foot. However, the dune module is limited to simulating horizontal dune growth and does not account for vertical growth. This limitation makes an impact particularly in

the central zone of the HBD, resulting in an overestimation of the dunefoot position and, consequently, a slight error in the beach width compared to the measurements for that area.

ShorelineS does not simulate depth-dependent processes. The model relies on a one-line formulation, which affects its ability to produce realistic results regarding morphological responses across various depths for both volumetric changes and contour lines. This limitation is especially apparent in the shoreface results. In the central zones of the HBD, sediment is redistributed to deeper areas that ShorelineS is unable to account for, especially in the initial years when the cross-shore profile is adapting towards an equilibrium slope. A significant improvement is gained when dune and beach volumes are added to the temporal evolution of the total volume definition for ShorelineS. However, the remaining gap also indicates that additional subaqueous depth-dependent processes are still missing.

Question 3: *"How well does the coupled model simulate the evolution of the coastal state indicators and cross-shore bathymetric change at the Hondsbossche Dunes?"*

The SC5 simulation is the best-performing simulation run of the coupled model. Despite that, it still contains instabilities at numerous transects. The instability stems from a growing gradient in the dispersion term in the Crocodile formulation, which is caused by a poorly translated equilibrium profile from the grid to the transect. Therefore, the model output is not entirely reliable and can be used only on a limited set of output results. The instabilities indicate that the coupled model is not yet a stable and robust solution for predicting future coastal evolution.

However, for the remaining results of the transects and periods that are stable, SC5 does show a very accurate representation of the volumetric changes, spatially and temporally. After 4 years, an error of less than 250 m/m^3 was present.

The model can also account for sediment deposition and erosion below and above the waterline due to its depth-dependent diffusion coefficient. In contrast to the precision of the total volume changes, this cross-shore redistribution seems to be disproportionate to the JarKus data. It underestimates subaqueous volumetric changes in erosive zones, particularly for simulations involving large coastal retreat. Additionally, the volumes above the waterline have not yet been translated into the dunefoot change, which limits the improvement of the beach width simulation.

The beach width is well represented in simulation SC5 with an error of less than 50 meters after 7 years. The coupled model underpredicts the absolute beach width slightly, primarily due to the small overprediction of shoreline retreat in the central section. However, in general, this shoreline evolution exhibits a consistent error.

The results also showed that the model can disconnect the shoreline progression from the evolution of other depth contours. Although the contour position is not always simulated correctly, for example, at the highly dynamic offshore sandbar system, the direction and magnitude of the development are often reasonable. Furthermore, the addition of Crocodile profiles provides valuable extra information on how the bathymetry evolves.

The SC5 simulation comprises a model configuration featuring elements of dynamic equilibrium, a curved equilibrium grid, and an alongshore varying equilibrium profile. With the addition of the mentioned elements, the simulation showed great improvements compared to the other runs.

The different simulation settings demonstrate that the distance between the initial profile and equilibrium is crucial. In simulations where a simple straight equilibrium profile was initially applied, shoreline retreat was significantly overestimated (errors exceeding 100 m after 3 years), resulting in unrealistic beach erosion and sediment accumulation below the shoreline. The error for the shoreline has been reduced from 100 meters in the first three years (SC0) to only 25 meters (SC5). Besides model improvement, the SC5 simulation also stayed stable for the longest period.

9.1.2. Main research Question

Main Research Question: *"To what extent does the coupling of ShorelineS with Crocodile improve the simulation of coastal state indicators' evolution at the Hondsbossche Dunes under present sea-level conditions, and provide additional information on bathymetric cross-shore evolution?"*

The coupling of ShorelineS with Crocodile has a good potential to improve the simulation of the evolution

of several coastal state indicators in the case of a dynamic equilibrium, and curved and alongshore varying profile. However, the stand-alone ShorelineS model yields better results on indicators such as shoreline position and beach width. Additionally, it demonstrates that at the moment, the ShorelineS model also provides a more robust and computationally efficient estimate of the coastal indicators in general, as the coupled model struggles with significant instabilities. These instabilities stem from the poor mapping of the equilibrium grid to individual transect levels, which affects the stability of the initial profile evolution through the gradient in the diffusion term.

In the parts where the SC5 model is stable, its performance stands out in terms of volumetric change and the evolution of shoreface contours. It also introduces a new feature that simulates an updated profile at every time step, formed by depth-dependent processes. Its volumetric improvements are most visible in the RMS error, which, after 3 years of simulation, halves the error obtained in the ShorelineS output.

The coupled model has been shown to be sensitive to the choice of equilibrium grids and settings. It suffers from increasing instabilities when using a static equilibrium or an insufficiently fitted alongshore equilibrium shoreline shape (simulation SC0). The inclusion of a dynamic equilibrium and an alongshore curved equilibrium grid demonstrates that great improvements are possible.

Its comparison to ShorelineS has turned out to be complicated, as the definition of the volume for ShorelineS and the coupled model is not directly similar. The coupled model is able to mimic the redistribution of sediment above the waterline as its depth-dependent diffusion coefficient accounts for wave influence in subaerial area. When the S0 simulation is plotted with the inclusion of beach and dune volume, the ShorelineS model shows its ability to follow the volume evolution of the measurements, which partly bridges the gap to SC5. From the analysis, it is also noted that the cross-shore dominance was limited in the initial years or not captured by the data, which reduces the benefit of the coupled model.

In conclusion, it is difficult to determine the extent to which SC5 has improved the simulation of coastal indicators. This is mainly because of the comparison definition issue mentioned earlier. However, the coupled model shows great potential in its volumetric evolution and offshore profile development. Despite the potential demonstrated, further model improvements and development are required to enhance spatial and temporal stability. This is necessary to make long-term predictions and contribute to future coastal maintenance strategies in the face of rising sea levels.

9.2. Key Findings

The key findings of this research are:

- ShorelineS is most accurate for reproducing shoreline evolution and beach width over a nine-year period at the Hondsbossche Dunes.
- The ShorelineS simulation has a good expression for the volume of the JarKus data when it includes beach and dune volume, but making a fair comparison with SC5 is difficult.
- The ShorelineS model simulation confirms findings from the data analyses that offshore contour behavior is not well-correlated with the shoreline evolution.
- Despite numerous improvements, the coupled model still experiences significant instabilities within the first five years of simulation, and permanently at certain transects.
- With the depth-dependent cross-shore diffusion coefficient, the Crocodile module adds a physically more realistic representation of coastal indicators and shows potential to simulate profile bathymetry development.
- Provided a proper model configuration (SC5), the coupled model can perform better and locally provide a more detailed representation of the total volumetric change than ShorelineS for at least the stable first 4 years. However, the magnitude of cross-shore redistribution still overpredicts both erosional and accretional interactions with subaerial areas at different transects.
- In two-dimensional equilibrium-based models, not only the cross-shore equilibrium profile but also the alongshore equilibrium shape plays a crucial role. The performance of the coupled model

is sensitive to the alongshore variation in the equilibrium profile, the initial deviation from this equilibrium, and the dynamic processes incorporated into the equilibrium definition.

9.3. Scientific and Practical Implications

The scientific implication from this research is that the cross-shore distribution technique shows promising results in better representing certain coastal indicators. It also offers insight into how coastal profiles move toward their equilibrium, while remaining relatively computationally efficient. The study also highlights areas where improvements are necessary.

Looking ahead, a more developed coupled model could support future coastal maintenance strategies by enabling the prediction of coastal behavior over decades and at larger spatial scales. However, first, complications in the model stability should be solved.

9.4. Limitations

The most important limitations to this research are:

- Tidal currents and asymmetry are not explicitly included, but have the potential to improve the northward transport influences.
- In the analysis of the results, the beach and dune volume are not assessed due to comparison complications with the cross-shore distribution of the coupled model to subaerial locations. This is then not included in the dunefoot development, making it difficult to compare one and another with ShorelineS subaerial volume changes.
- The dune module in ShorelineS does not account for vertical dune growth, possibly leading to overestimations in horizontal expansion.
- The models simulate nourishments by evenly distributing the added volume over the cross-shore profile, while in reality this is more location specific.
- The coupled model encounters model instabilities at some transects within five years of simulation. Also, at some locations, Crocodile profiles were deliberately not defined because their location has shown to be sensitive to instabilities as well. Therefore, not every year and transect of the HBD was assessed in the comparison study.
- In this study, only JarKus data is used. Therefore, insightful information in the initial year(s) is missing. In the first year, all profile slopes were adjusted to the adjacent coast. In this first period the coupled model was expected to distinguish itself the most from a one-line model.
- Before making long-term predictions, additional complications should be bridged related to future coastal condition settings. Examples of these limitations are timeseries of hydraulic conditions, an equilibrium profile definition, and a nourishment maintenance input list

9.5. Recommendations for Future Research

Based on the outcomes and limitations of this research, several recommendations are proposed for future studies.

First, further investigation into the instabilities of the cross-shore profile module is necessary, as mentioned in the discussion. Addressing these issues would not only improve the model's robustness but also enable reliable long-term simulations. This is crucial when assessing future coastal evolution scenarios.

Additionally, it might be beneficial to improve Crocodile's cross-shore diffusion formulation to more realistically distribute sediment for subaerial and subaqueous volume changes. In doing so, it is also worth considering how changes in upper beach volume could be added or translated into dunefoot dynamics. This could enhance the physical representation of the model.

When revisiting the Hondsbossche Dunes as a case study, it is recommended to develop a tidal current input file by calibrating the dominant tidal constituents using water level measurements. Incorporating tidal asymmetry may potentially enhance the accuracy of alongshore sediment distribution results in both models.

If a new study continues research at the HBD using a coupled model, it is recommended to acquire additional measurement datasets to fully leverage the model's strengths in the years following a nourishment, when increased cross-shore activity is expected. Furthermore, it might be useful to calibrate ShorelineS also on the last 4 years, as in this period four nourishments have been carried out. In the current calibration period of 5 years there was only a single additional nourishment. This makes the model more resilient to volumetric additions.

Another potential improvement lies in expanding the representation of dune dynamics. This could be achieved by integrating a new dune module that allows for vertical growth or by coupling existing modules with external aeolian transport models. Such additions would provide a more complete simulation of coastal evolution.

Furthermore, analyzing how the beach slope evolves over time could yield insights into the coastal system's response to large-scale sandy interventions. Comparing the evolving beach profile to adjacent, stable profiles may help determine whether the system is approaching an equilibrium state. Unlike one-line models, a coupled model can simulate such cross-shore developments. An interesting extension of Crocodile would be to ensure that it accurately simulates profile steepness as well. Although it might require some physical processes, it would provide new and helpful information for researchers.

Finally, regarding nourishment implementation in simulations, during this study, historical nourishments were incorporated into ShorelineS via simplified input files. These were modeled as uniformly distributed line segments across the profile, while in reality, nourishments are localized in the cross-shore direction. Research with the standalone Crocodile model offers a significant advantage in location-specific simulation of nourishments, even when subsequent nourishments have not yet fully adjusted to their equilibrium profiles. However, in the current coupled model, nourishments are still implemented through ShorelineS. Therefore, it is recommended to enable the direct implementation of nourishments through Crocodile within the coupled framework. Doing so would unlock the full potential of Crocodile and improve the physical nature of nourishment simulations.

References

[1] A. Luijendijk et al. “The State of the World’s Beaches”. In: *Scientific Reports* 8 (1 2018), pp. 2045–2322. DOI: https://doi.org/10.1038/s41598-018-24630-6. URL: https://www.nature.com/articles/s41598-018-24630-6#citeas.

[2] Joost Stronkhorst et al. “Sand nourishment strategies to mitigate coastal erosion and sea level rise at the coasts of Holland (The Netherlands) and Aveiro (Portugal) in the 21st century”. In: *Ocean and Coastal Management* 156 (2018). SI: MSforCEP, pp. 266–276. ISSN: 0964-5691. DOI: https://doi.org/10.1016/j.ocecoaman.2017.11.017. URL: https://www.sciencedirect.com/science/article/pii/S0964569117301576.

[3] J.P.M. Mulder et al. “Implementation of coastal erosion management in the Netherlands”. In: *Ocean and Coastal Management* 54.12 (2011). Erosion management implementations. URL: https://www.sciencedirect.com/science/article/pii/S0964569111000871?casa_token=M8KAIautuuIAAAAA:YC14UT_guRxyU4QK5D1i9mUymKQE7mYSqFT418BwXgp3C0-BENg2u1oRe8xIRN6NFkUIo1Q8684.

[4] I. Keizer et al. “The acceleration of sea-level rise along the coast of the Netherlands started in the 1960s”. In: *Ocean Science* 19.4 (2023), pp. 991–1007. DOI: 10.5194/os-19-991-2023. URL: https://os.copernicus.org/articles/19/991/2023/.

[5] R. Hillen et al. *DE BASISKUSTLIJN een technisch/morfologische uitwerking*. Rijkswaterstaat rapport GWWS-91.006. 1991. URL: https://www.deltaexpertise.nl/wiki/index.php/Dynamische_kustlijnhandhaving.

[6] Tosca Kettler et al. “Exploring decadal beach profile dynamics in response to nourishment strategies under accelerated sea level rise”. In: *Ocean and Coastal Management* 260 (2025), p. 107477. ISSN: 0964-5691. DOI: https://doi.org/10.1016/j.ocecoaman.2024.107477. URL: https://www.sciencedirect.com/science/article/pii/S0964569124004629.

[7] M Haasnoot et al. “Adaptation to uncertain sea-level rise; how uncertainty in Antarctic mass-loss impacts the coastal adaptation strategy of the Netherlands”. In: *Environmental Research Letters* 15.3 (Feb. 2020), p. 034007. DOI: 10.1088/1748-9326/ab666c. URL: https://dx.doi.org/10.1088/1748-9326/ab666c.

[8] Jos van Alphen et al. “Uncertain Accelerated Sea-Level Rise, Potential Consequences, and Adaptive Strategies in The Netherlands”. In: *Water* 14.10 (2022). ISSN: 2073-4441. DOI: 10.3390/w14101527. URL: https://www.mdpi.com/2073-4441/14/10/1527.

[9] M.J.F. Stive. “The sand engine: a solution for the Dutch Delta in the 21st century?” In: *Coastal Dynamics* (2013). Mega nourishment evaluatie Zandmotor, pp. 1537–1546. URL: https://southerncoastalgroup-scopac.org.uk/wp-content/uploads/2019/05/The-sand-engine-A-solution-for-vulnerable-deltas-in-the-21st-century-2013b.pdf.

[10] A. Kroon. “Subaqueous and Subaerial Beach Changes after Implementation of a Mega Nourishment in Front of a Sea Dike”. In: *Marine Science and Engineering* 10.8 (2022). Mega nourishment evaluatie Hondsbosscheduinen. URL: https://iopscience.iop.org/article/10.1088/1748-9326/9/11/115007.

[11] Matthieu Andréas de Schipper et al. “Morphological development of a mega-nourishment; first observations at the Sand Engine”. In: *Coastal Engineering Proceedings* 34 (2014), pp. 73–73.

[12] Matthieu A. de Schipper et al. “Beach nourishment has complex implications for the future of sandy shores”. English. In: *Nature Reviews Earth and Environment* 2.1 (2021). Accepted Author Manuscript, pp. 70–84. DOI: 10.1038/s43017-020-00109-9.

[13] Haye H. Geukes et al. “Sand nourishment for multifunctional coastal climate adaptation: three key implications for researchers”. In: *Nature-Based Solutions* 6 (2024). DOI: 10.1016/j.nbsj.2024.100191. URL: https://www.scopus.com/inward/record.uri?eid=2-s2.0-85214653693&doi=10.1016%2fj.nbsj.2024.100191&partnerID=40&md5=2ca85c9e004f0cc8af0e195f7356e463.

[14] Vincent Bax et al. “Beach user perspectives on the upscaling of sand nourishments in response to sea level rise – A discrete choice experiment”. In: *Ocean and Coastal Management* 253 (2024), p. 107139. ISSN: 0964-5691. DOI: https://doi.org/10.1016/j.ocecoaman.2024.107139. URL: https://www.sciencedirect.com/science/article/pii/S0964569124001248.

[15] Alessio Giardino et al. “Simulating Coastal Morphodynamics with Delft3D: case study Egmond aan Zee”. In: *Deltares* (Jan. 2010), p. 78. DOI: 10.13140/2.1.2596.9925.

[16] Arjen Luijendijk et al. “The initial morphological response of the Sand Engine: A process-based modelling study”. In: *Coastal Engineering* 119 (Jan. 2017), pp. 1–14. DOI: 10.1016/j.coastaleng.2016.09.005.

[17] M. Alvarez-Cuesta et al. “Modelling long-term shoreline evolution in highly anthropized coastal areas. Part 1: Model description and validation”. In: *Coastal Engineering* 169 (2021), p. 103960. ISSN: 0378-3839. DOI: https://doi.org/10.1016/j.coastaleng.2021.103960. URL: https://www.sciencedirect.com/science/article/pii/S0378383921001150.

[18] Andrew E. Whitley et al. “One-Line Modeling of Mega-Nourishment Evolution”. In: *Journal of Coastal Research* 37.6 (2021), pp. 1224–1234. DOI: 10.2112/JCOASTRES-D-20-00157.1. URL: https://doi.org/10.2112/JCOASTRES-D-20-00157.1.

[19] Mostafa Saleh. “The Application of Ensemble Kalman Filter - Data Assimilation in Simple One-line and Free-Form Coastline Evolution Models”. MA thesis. IHE Delft, 2021.

[20] P.G. Petrova. “Calibration of the ShorelineS model to predict the Hondsbossche Dunes dynamics with indication for the medium-term model uncertainty”. MA thesis. Utrecht University, 2022.

[21] D. Roelvink et al. “Efficient Modeling of Complex Sandy Coastal Evolution at Monthly to Century Time Scales”. In: *Frontiers in Marine Science* 7 (2020). ISSN: 2296-7745. DOI: 10.3389/fmars.2020.00535. URL: https://www.frontiersin.org/journals/marine-science/articles/10.3389/fmars.2020.00535.

[22] T. Kettler et al. “Simulating decadal cross-shore dynamics at nourished coasts with Crocodile”. In: *Coastal Engineering* 190 (2024), p. 104491. ISSN: 0378-3839. DOI: https://doi.org/10.1016/j.coastaleng.2024.104491. URL: https://www.sciencedirect.com/science/article/pii/S0378383924000395.

[23] S. Rudenko. *What is a hindcast in meteorology - and how to use it?* URL: https://www.infoplaza.com/en/blog/what-is-a-hindcast-in-meteorology-and-how-to-use-it. (accessed: 06.12.2024).

[24] SINAY. *What is Hindcast?* URL: https://sinay.ai/en/maritime-glossary/hindcast/. (accessed: 06.12.2024).

[25] L. Reimann. “Population development as a driver of coastal risk: Current trends and future pathways”. In: *Cambridge Prisms: Coastal Futures* 1.e14 (2023). Shows the coastal population and how it changes under the SSP scenario’s. URL: https://www.cambridge.org/core/journals/cambridge-prisms-coastal-futures/article/population-development-as-a-driver-of-coastal-risk-current-trends-and-future-pathways/8261D3B34F6114EA0999FAA597D5F2E2.

[26] K. Riahi. “The Shared Socioeconomic Pathways and their energy, land use, and greenhouse gas emissions implications: An overview”. In: *Global Environmental Change* (Jan. 2017), pp. 153–168. DOI: 10.1016/j.gloenvcha.2016.05.009.

[27] Plan Bureau Leefomgeving RWS. *Correctie formulering over overstromingsrisico Nederland in IPCC-rapport*. Plan Bureau Leefomgeving. URL: https://www.pbl.nl/correctie-formulering-over-overstromingsrisico-nederland-in-ipcc-rapport. (accessed: 02.12.2024).

[28] R. Hillen et al. “Dynamic preservation of the coastline in the Netherlands”. In: *Coastal conservation* 1.1 (1995). First review analysis after implementing the BKL, pp. 17–28. URL: https://www.scopus.com/record/display.uri?eid=2-s2.0-0029500138&origin=inward.

[29] RWS. *Kustverdediging na 1990, beleidskeuze voor de kustlijnzorg*. Beleid besluitvorming tweedekamer 1989-1990, Ministerie van Verkeer en Waterstaat Rijkswaterstaat en Dienst Weg- en Waterbouwkunde. 1990. URL: https://www.archieven.nl/nl/zoeken?mivast=0&mizig=383&miadt=236&miview=ldt&milang=nl&misort=last_mod%7C%7Casc&micode=3000&minr=4248575&miaet=14.

[30] Deltares. *Zeespiegelmonitor 2018*. De stand van zaken rond de zeespiegelstijging langs de Nederlandse kust. 2018. URL: https://publications.deltares.nl/11202193_000.pdf.

[31] Evelien Brand et al. "Dutch experience with sand nourishments for dynamic coastline conservation – An operational overview". In: *Ocean and Coastal Management* 217 (2022), p. 106008. ISSN: 0964-5691. DOI: https://doi.org/10.1016/j.ocecoaman.2021.106008. URL: https://www.sciencedirect.com/science/article/pii/S0964569121004919.

[32] Henk Jan Verhagen. *Basiskustlijn*. https://nl.wikipedia.org/w/index.php?title=Basiskustlijn&action=history [Accessed: 18-04-2025]. 2022.

[33] KNMI. *KNMI'23 klimaatscenario's voor Nederland*. Kerncijfers of regional climate change projections The Netherlands. 2023. URL: https://cdn.knmi.nl/system/ckeditor/attachment_files/data/000/000/357/original/KNMI23_klimaatscenarios_gebruikersrapport_23-03.pdf.

[34] M.J.F. Stive et al. "A new alternative to saving our beaches from sea-level rise: The sand engine". In: *Journal of Coastal Research* 29.5 (2013). Cited by: 259; All Open Access, Green Open Access, pp. 1001–1008. DOI: 10.2112/JCOASTRES-D-13-00070.1. URL: https://www.scopus.com/inward/record.uri?eid=2-s2.0-84884628623&doi=10.2112%2fJCOASTRES-D-13-00070.1&partnerID=40&md5=195120354331da5b9ffeeb3c36e4a4d1.

[35] Jaime Arriaga et al. "Modeling the long-term diffusion and feeding capability of a mega-nourishment". In: *Coastal Engineering* 121 (2017), pp. 1–13. ISSN: 0378-3839. DOI: https://doi.org/10.1016/j.coastaleng.2016.11.011. URL: https://www.sciencedirect.com/science/article/pii/S0378383916303659.

[36] Kathelijne M. Wijnberg et al. "Extracting decadal morphological behaviour from high-resolution, long-term bathymetric surveys along the Holland coast using eigenfunction analysis". In: *Marine Geology* 126.1 (1995), pp. 301–330. ISSN: 0025-3227. DOI: https://doi.org/10.1016/0025-3227(95)00084-C. URL: https://www.sciencedirect.com/science/article/pii/002532279500084C.

[37] Kathelijne M Wijnberg. "Environmental controls on decadal morphologic behaviour of the Holland coast". In: *Marine Geology* 189.3 (2002), pp. 227–247. ISSN: 0025-3227. DOI: https://doi.org/10.1016/S0025-3227(02)00480-2. URL: https://www.sciencedirect.com/science/article/pii/S0025322702004802.

[38] K. Horikawa. *Nearshore Dynamics and Coastal Processes: Theory, Measurement, and Predictive Models*. University of Tokyo Press, 1988. ISBN: 9784130681384. URL: https://books.google.nl/books?id=iuYHAQAAIAAJ.

[39] J Bosboom et al. *Coastal Dynamics*. English. Vol. Part 1. Lecture Notes CT4305. VSSD, 2010.

[40] M.J.F Stive et al. "Variability of shore and shoreline evolution". In: *Coastal Engineering* 47.2 (2002). Shore Nourishment in Europe, pp. 211–235. ISSN: 0378-3839. DOI: https://doi.org/10.1016/S0378-3839(02)00126-6. URL: https://www.sciencedirect.com/science/article/pii/S0378383902001266.

[41] B.J.A. Huisman et al. "Modelling of bed sediment composition changes at the lower shoreface of the Sand Motor". In: *Coastal Engineering* 132 (2018), pp. 33–49. ISSN: 0378-3839. DOI: https://doi.org/10.1016/j.coastaleng.2017.11.007. URL: https://www.sciencedirect.com/science/article/pii/S0378383917301011.

[42] Matthieu A. A. Luijendijk et al. "Morphodynamic Acceleration Techniques for Multi-Timescale Predictions of Complex Sandy Interventions". In: *Journal of Marine Science and Engineering* 7.3 (2019). ISSN: 2077-1312. DOI: 10.3390/jmse7030078. URL: https://www.mdpi.com/2077-1312/7/3/78.

[43] Bas Huisman. “On the redistribution and sorting of sand at nourishments”. Accessed: 2025-04-21. Ph.D. Dissertation. Mekelweg 5, 2628 CD Delft: Delft University of Technology, 2019. URL: https://doi.org/10.4233/uuid:a2bbb49d-8642-4a32-b479-4f0091f2d206.

[44] Roger Pelnard-Considère. “Essai de theorie de l’evolution des formes de rivage en plages de sable et de galets”. In: *Journées de L’hydraulique* 4.1 (1957), pp. 289–298.

[45] Hans Hanson. “GENESIS: a generalized shoreline change numerical model”. In: *Journal of Coastal research* (1989), pp. 1–27.

[46] DHI. *LITPACK: A software package for littoral processes and coastline kinetics*. Short description retrieved from https://www.dhigroup.com/upload/dhisoftwarearchive/shortdescriptions/marine/LITPACKShortDescription.pdf. DHI Water & Environment. Hørsholm, Denmark, 2003.

[47] Delft Hydraulics. “UNIBEST, A Software Suite for Simulation of Sediment Transport Processes and Related Morphodynamics of Beach Profiles and Coastline Evolution”. In: *Delft Hydraulics, 124p* (1994).

[48] Marek Szmytkiewicz et al. “Coastline changes nearby harbour structures: comparative analysis of one-line models versus field data”. In: *Coastal Engineering* 40.2 (2000), pp. 119–139. ISSN: 0378-3839. DOI: https://doi.org/10.1016/S0378-3839(00)00008-9. URL: https://www.sciencedirect.com/science/article/pii/S0378383900000089.

[49] Robert C. Thomas et al. *Shoreline Change Modeling Using OneLine Models: General Model Comparison and Literature Review*. Tech. rep. ERDC/CHL CHETN-II-55. Vicksburg, MS: U.S. Army Corps of Engineers, Coastal Engineering Research Center, 2013. URL: https://apps.dtic.mil/sti/tr/pdf/ADA591362.pdf.

[50] Robin G.D. Davidson-Arnott. “Conceptual model of the effects of sea level rise on sandy coasts”. In: *Journal of Coastal Research* 21 (6 2005), pp. 1166–1172. DOI: https://doi.org/10.2112/03-0051.1. URL: https://scholar.google.ca/citations?view_op=view_citation&hl=en&user=qzRCKKwAAAAJ&citation_for_view=qzRCKKwAAAAJ:zA6iFVUQeVQC.

[51] Per Bruun. *Coast erosion and the development of beach profiles*. Vol. 44. US Beach Erosion Board, 1954.

[52] Robert G Dean. *Equilibrium beach profiles: US Atlantic and Gulf coasts*. Vol. 12. Department of Civil Engineering, University of Delaware Newark, Delaware, 1977.

[53] Sean Vitousek et al. “A model integrating longshore and cross-shore processes for predicting long-term shoreline response to climate change”. In: *Journal of Geophysical Research: Earth Surface* 122.4 (2017), pp. 782–806.

[54] Arthur Robinet et al. “A reduced-complexity shoreline change model combining longshore and cross-shore processes: The LX-Shore model”. In: *Environmental modelling & software* 109 (2018), pp. 1–16.

[55] José AA Antolínez et al. “Predicting climate-driven coastlines with a simple and efficient multiscale model”. In: *Journal of Geophysical Research: Earth Surface* 124.6 (2019), pp. 1596–1624.

[56] Jaime Palalane et al. “A long-term coastal evolution model with longshore and cross-shore transport”. In: *Journal of Coastal Research* 36.2 (2020), pp. 411–423.

[57] Yen Hai Tran et al. “Combined longshore and cross-shore shoreline model for closed embayed beaches”. In: *Coastal Engineering* 158 (2020), p. 103692.

[58] Shore Protection Manual. “CERC, Waterways Experiment Station”. In: *Vicksburg, USA* (1984).

[59] Andrew D Ashton et al. “High-angle wave instability and emergent shoreline shapes: 1. Modeling of sand waves, flying spits, and capes”. In: *Journal of Geophysical Research: Earth Surface* 111.F4 (2006).

[60] J William Kamphuis. “Alongshore sediment transport rate”. In: *Journal of Waterway, Port, Coastal, and Ocean Engineering* 117.6 (1991), pp. 624–640.

[61] João Mil-Homens et al. “Re-evaluation and improvement of three commonly used bulk longshore sediment transport formulas”. In: *Coastal Engineering* 75 (2013), pp. 29–39.

[62] Magnus Larson et al. “Simulating cross-shore material exchange at decadal scale. Theory and model component validation”. In: *Coastal Engineering* 116 (2016), pp. 57–66. ISSN: 0378-3839. DOI: https://doi.org/10.1016/j.coastaleng.2016.05.009. URL: https://www.sciencedirect.com/science/article/pii/S0378383916300850.

[63] J.B. Van der Waal. “Understanding the behaviour of maintenance nourishments and the implications of maintenance strategies”. MA thesis. Utrecht University, 2024.

[64] S. de Vries et al. “Dune behavior and aeolian transport on decadal timescales”. In: *Coastal Engineering* 67 (2012), pp. 41–53. ISSN: 0378-3839. DOI: https://doi.org/10.1016/j.coastaleng.2012.04.002. URL: https://www.sciencedirect.com/science/article/pii/S0378383912000725.

[65] AD Fockert et al. “Wave look-up table Building with Nature”. In: *Delft, The Netherlands: Deltares, Technical Note, Ref* (2011), pp. 1002337–002.

[66] Gerben Ruessink et al. “A Multi-Year Data Set of Beach-Foredune Topography and Environmental Forcing Conditions at Egmond aan Zee, The Netherlands”. In: *Data* 4.2 (2019). ISSN: 2306-5729. DOI: 10.3390/data4020073. URL: https://www.mdpi.com/2306-5729/4/2/73.

[67] Kathelijne M Wijnberg. “Environmental controls on decadal morphologic behaviour of the Holland coast”. In: *Marine Geology* 189.3 (2002), pp. 227–247. ISSN: 0025-3227. DOI: https://doi.org/10.1016/S0025-3227(02)00480-2. URL: https://www.sciencedirect.com/science/article/pii/S0025322702004802.

[68] Robert G Dean. *Beach nourishment: theory and practice*. Vol. 18. World scientific publishing company, 2003.

[69] Matthieu A. de Schipper et al. “Initial spreading of a mega feeder nourishment: Observations of the Sand Engine pilot project”. In: *Coastal Engineering* 111 (2016), pp. 23–38. ISSN: 0378-3839. DOI: https://doi.org/10.1016/j.coastaleng.2015.10.011. URL: https://www.sciencedirect.com/science/article/pii/S037838391500188X.

[70] Nicole A. Elko et al. “Immediate profile and planform evolution of a beach nourishment project with hurricane influences”. In: *Coastal Engineering* 54.1 (2007), pp. 49–66. ISSN: 0378-3839. DOI: https://doi.org/10.1016/j.coastaleng.2006.08.001. URL: https://www.sciencedirect.com/science/article/pii/S037838390600113X.

[71] Anna Kroon et al. *Evaluating beach-dune evolution at the Hondsbossche Dunes*. Tech. rep. Rotterdam, NL: Svasek Hydraulics, 2024.

[72] Per Bruun. “Sea-level rise as a cause of shore erosion”. In: *Journal of the Waterways and Harbors division* 88.1 (1962), pp. 117–130.

A

Appendix A: Coastal Indicator Plots

This appendix shows the figures following the model results in their completeness for the years 2015 to 2024, for all simulations: S0, SC1, SC2, SC3, SC4, SC5.

A.1. Total Volume Change

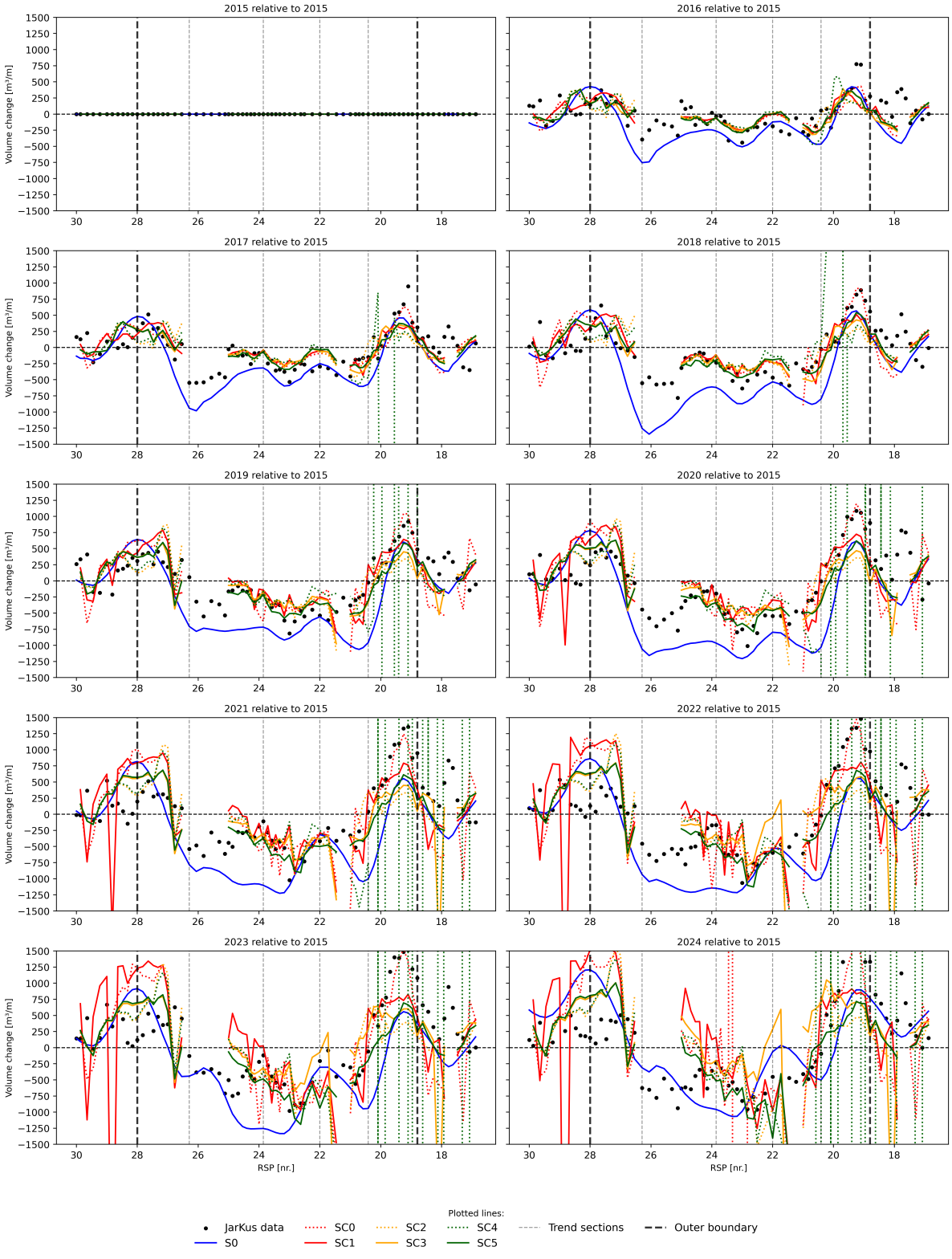

Figure A.1: Model output results of volumetric change over the period 2015-2024, for simulations S0, SC1, SC2, SC3, SC4, SC5.

A.2. Surfzone Volume Change

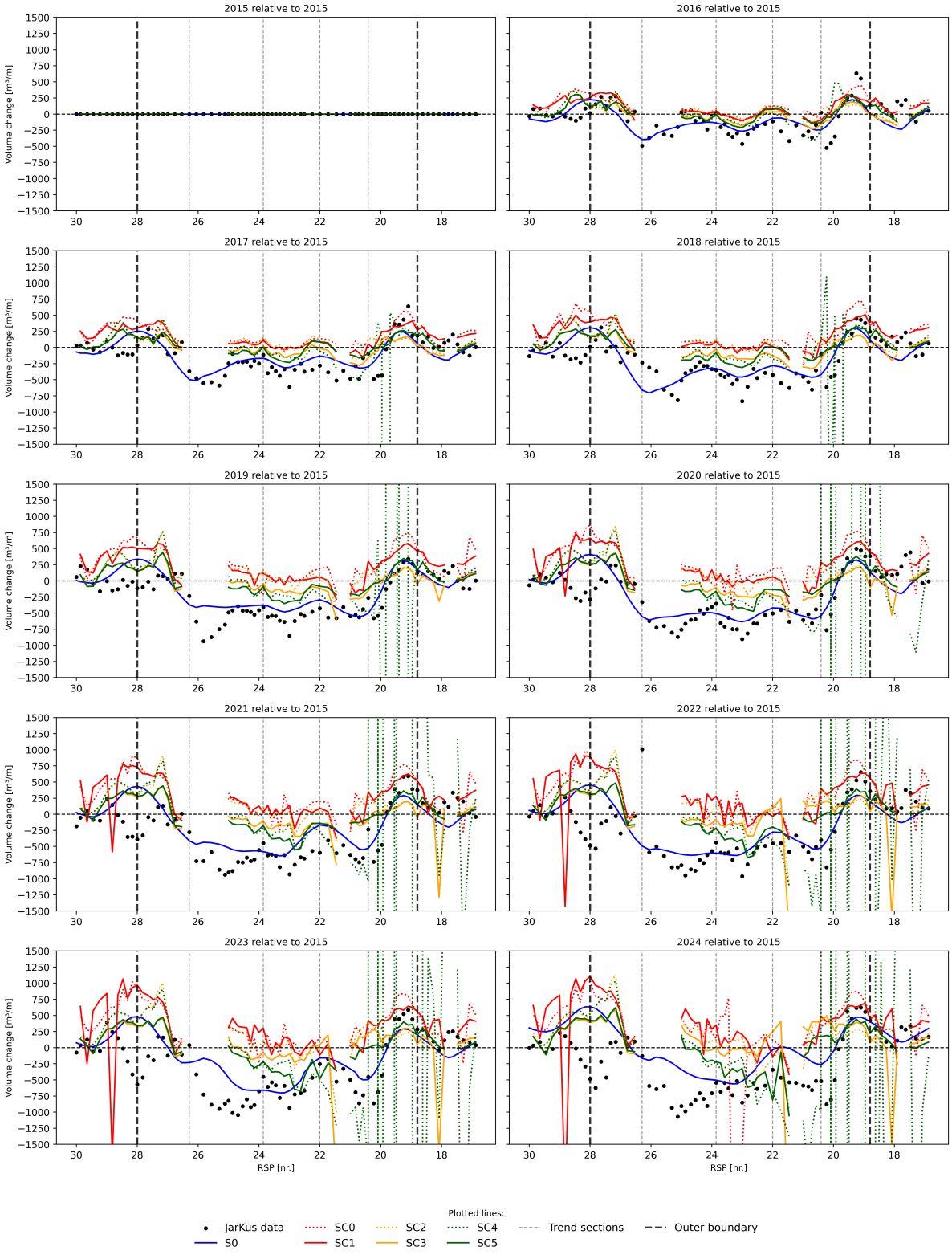

Figure A.2: Model output results of volumetric change in the surfzone over the period 2015-2024, for simulations S0, SC1, SC2, SC3, SC4, SC5.

A.3. Shoreface Volume Change

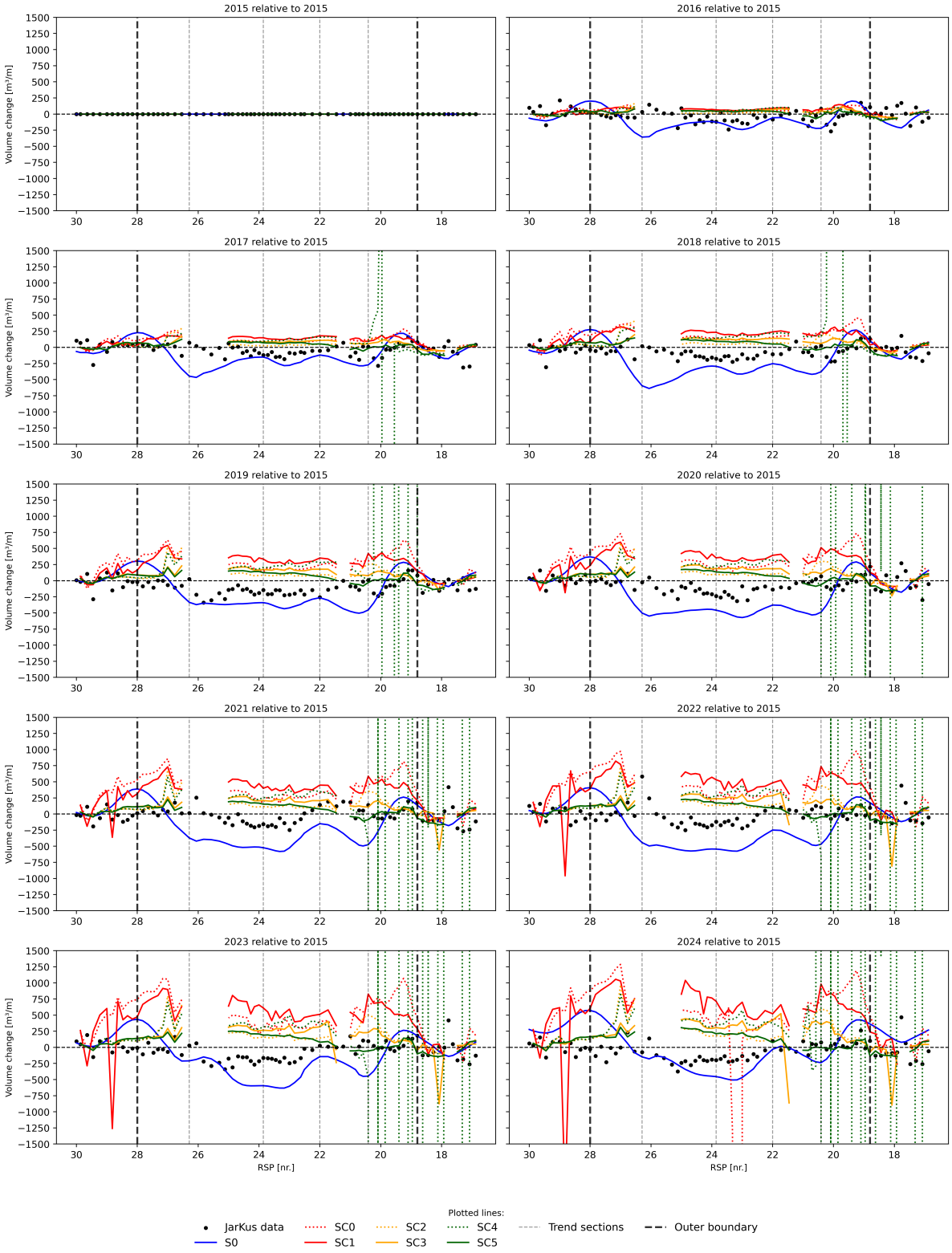

Figure A.3: Model output results of volumetric change in the shoreface over the period 2015-2024, for simulations S0, SC1, SC2, SC3, SC4, SC5.

A.4. Shoreline Change

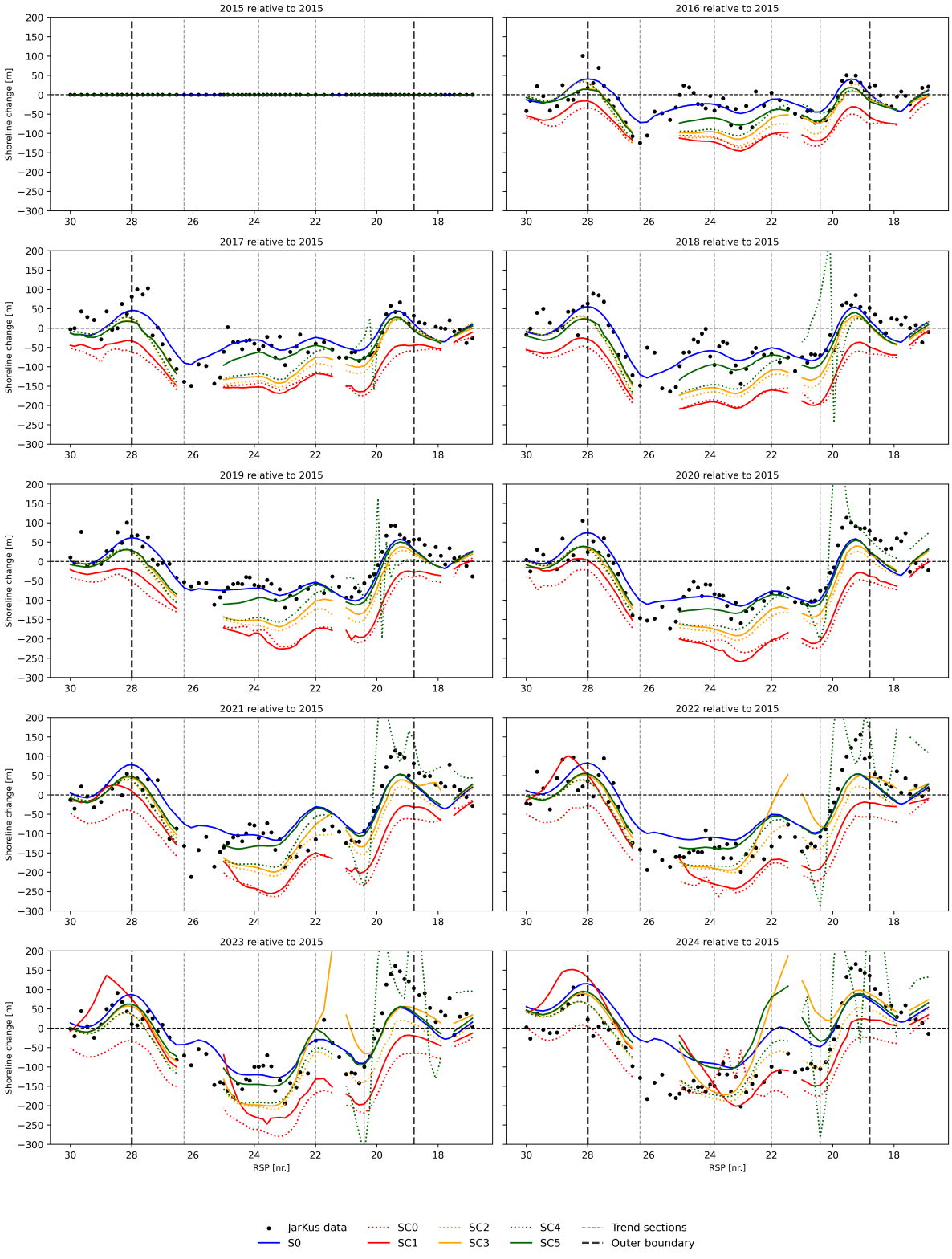

Figure A.4: Model output results of shoreline position change over the period 2015-2024, for simulations S0, SC1, SC2, SC3, SC4, SC5.

A.5. Dunefoot Change

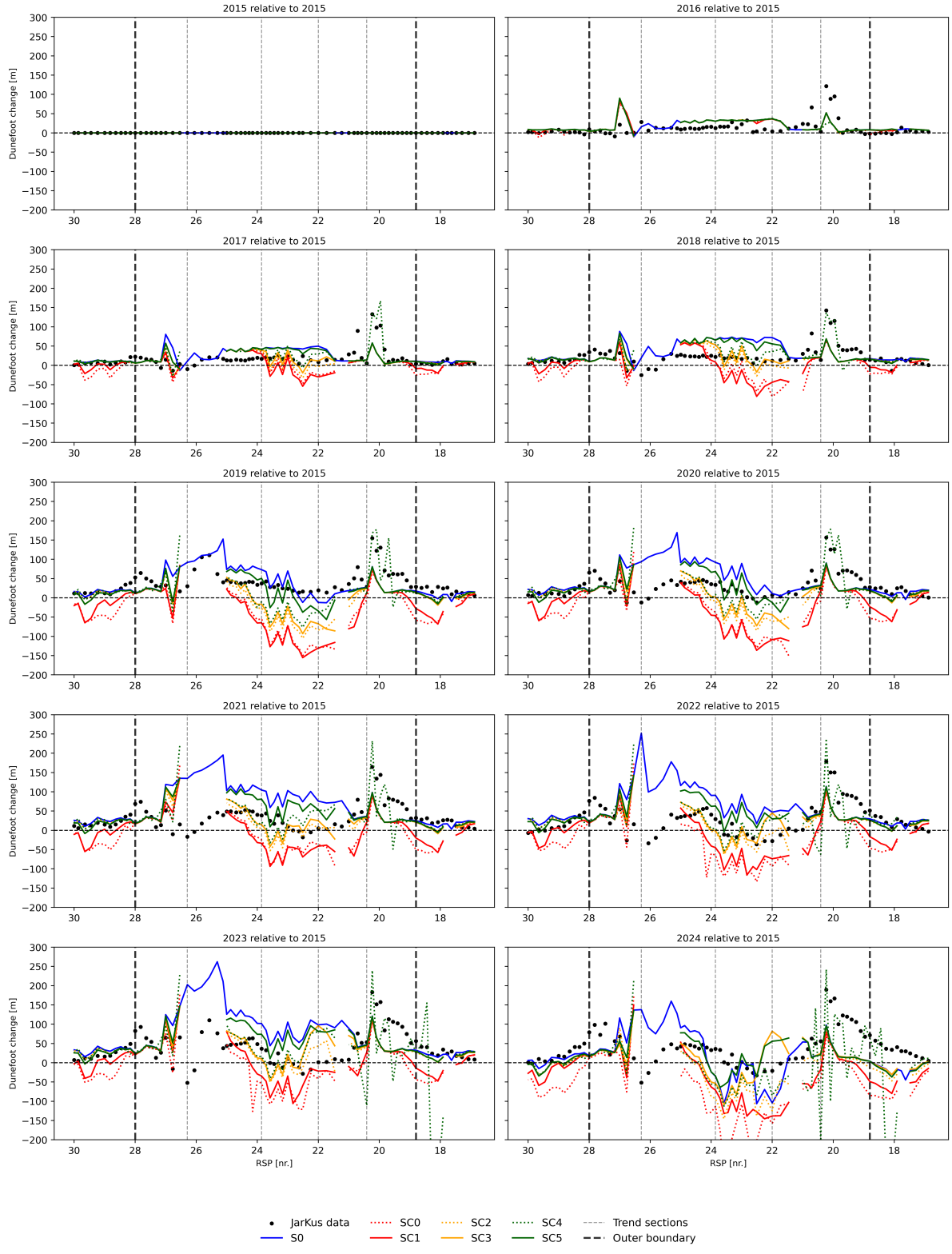

Figure A.5: Model output results of dunefoot position change over the period 2015-2024, for simulations S0, SC1, SC2, SC3, SC4, SC5.

A.6. Beach width Change

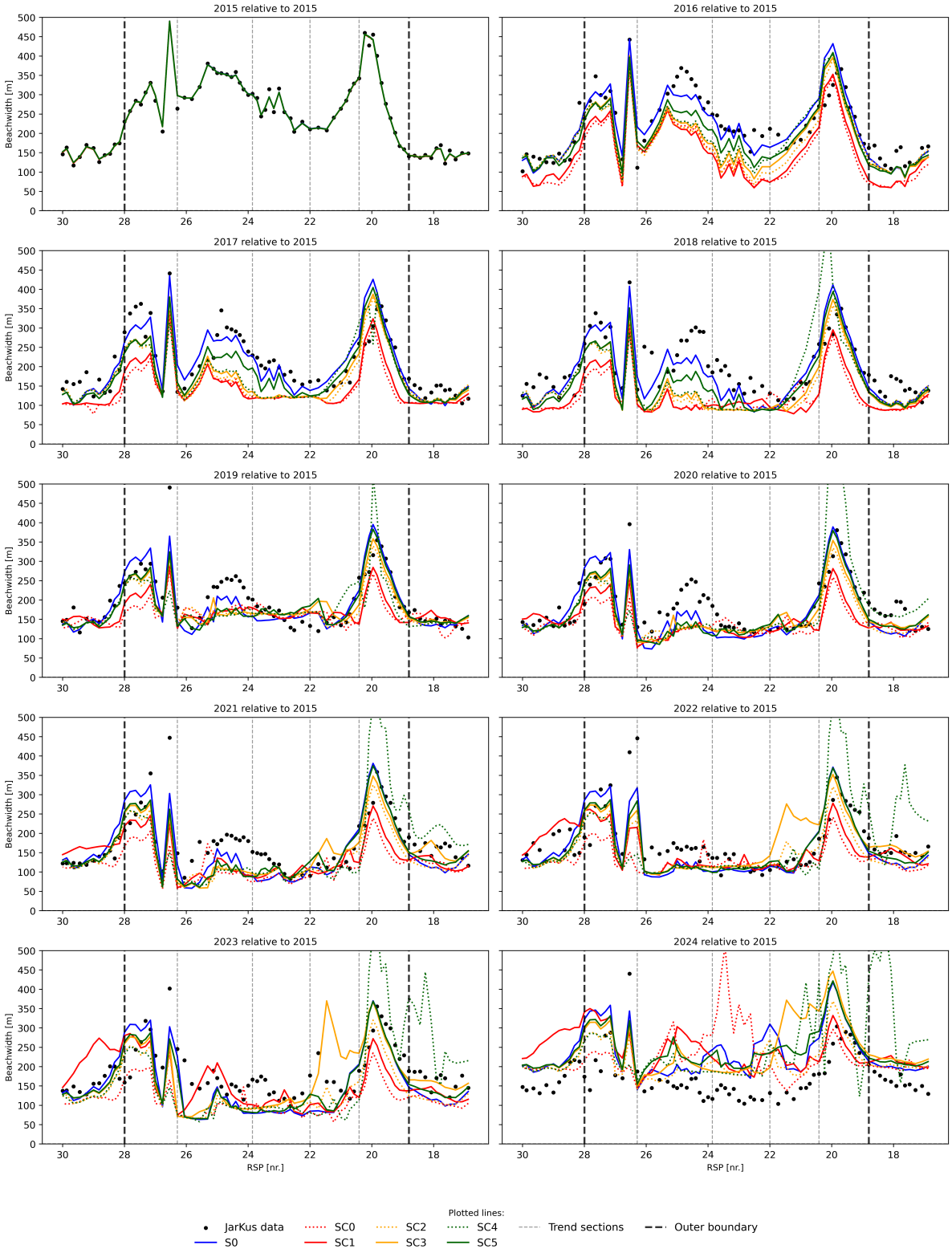

Figure A.6: Model output results of beach width over the period 2015-2024, for simulations S0, SC1, SC2, SC3, SC4, SC5.

A.7. Additional: Cross-shore Activity (Dean Ratio)

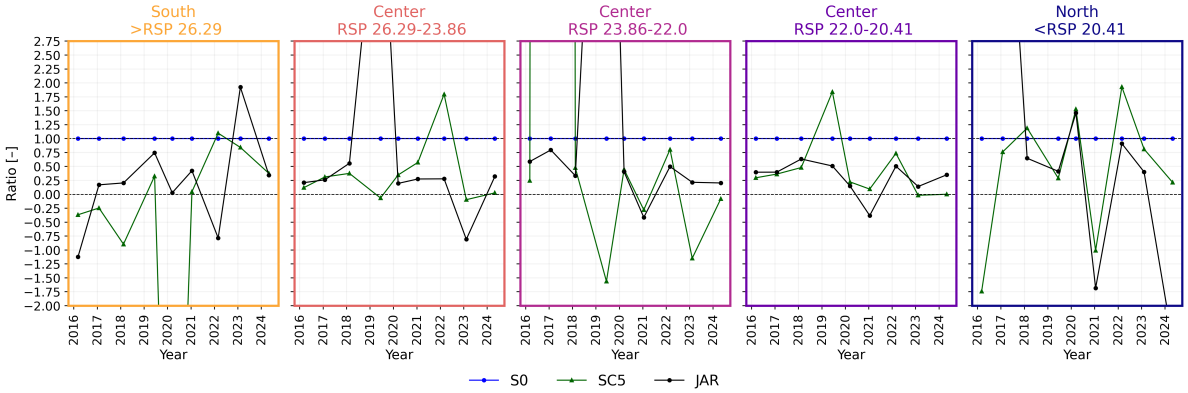

Figure A.7: Model output results are reworked to demonstrate the ratio of nourished profile volume change against the planform retreat (one-line principle). The five subplots indicate the different coastal zones. Simulation SC5 shows a relatively similar trend as the JarKus data. Shorelines S0 remains constant at y=1, as was expected since its volume change is similar to the planform retreat definition (shoreline change times active height).